Fakultät für Medizin

Modulation of cardiac L-type calcium channels
by genetic modification

Montatip Poomvanicha

Vollständiger Abdruck der von der Fakultät für Medizin

der Technischen Universität München zur Erlangung des akademischen Grades eines

Doktors der Naturwissenschaften

genehmigten Dissertation.

Contents

List of Figures

List of Tables

Abbreviations

AC	Adenylyl cyclase
AKAP	A-kinase-anchoring protein
Ala	Alanine
C- subunit	Catalytic subunit
Ca^{2+}	calcium
CaM	calmodulin
CaMKII	Ca^{2+}/calmodulin-dependent kinase II
cAMP	Adenosine-3′,5′-cyclic monophosphate
CDF	calcium-dependent facilitation
CDI	Ca^{2+}-dependent inactivation
DHPs	1,4-dihydropyridines
DNA	Deoxyribonucleic acid
EC	excitation-contraction
F2	filial generation 2 mice
HEK293	Human Embryonic Kidney 293 cell line
HVA channel	high- voltage-activated channel
i.p	intraperitoneal
I_{Ca}	Ca^{2+} current through L-type Ca^{2+} channels
IGF-1	insulin-like growth factor
Ile	Isoleucine
LTCC	L-type Ca^{2+} channels
PCR	Polymerase Chain Reaction

PI3K	Phosphoinositide 3-Kinase
PIP2	Phosphatidylinositol 4,5-bisphosphate
PIP3	Phosphatidylinositol 3,4,5-trisphosphate
PKA	Protein kinase A
PKB	Protein kinase B
Ser	Serine
SR	sarcoplasmic reticulum
VDF	voltage-dependent facilitation
VDI	voltage-dependent inactivation
VGCCs	voltage-gated L-type Ca^{2+} channels
β-AR	β-adrenergic receptor

1. Introduction

The influx of calcium (Ca^{2+}) ions through voltage-gated L-type Ca^{2+} channels (VGCCs) plays a critical role for the initiation and regulation of excitation-contraction (EC) coupling in cardiac muscle (Zhou and January, 1998). The rapid influx of Ca^{2+} through these channels triggers the release of intracellular Ca^{2+} from the sarcoplasmic reticulum (SR) stores and consequential cardiac contraction (Fabiato, 1983). L-type Ca^{2+} channels (LTCC) can also impact on other cellular processes modulated by intracellular Ca^{2+} such as gene activation, neurotransmitter and hormone release. Loss of function or mutation in L-type Ca^{2+} channels can lead to a variety of cardiovascular diseases such as cardiac arrhythmia, heart failure and congenital heart disease (Antzelevitch, 2003; Splawski et al., 2004).

Cardiac L-type Ca^{2+} channels are regulated by the membrane potential and other factors that include protein kinases, phosphatases, and Ca^{2+} binding proteins. One of them is the regulation by the β-adrenergic receptor. Increased activity of L-type Ca^{2+} channels due to activation of β-adrenergic receptors and phosphorylation by Adenosine-3′,5′-cyclic monophosphate (cAMP)-dependent protein kinase A (PKA) contributes to the increase in beating rate and contractile force upon activation of the sympathetic nervous system (Brodde, 1991; McDevitt, 1989). Other signaling pathways have also been suggested to regulate the channel by phosphorylation, for example activation of protein kinase B (Akt/PKB) (Catalucci et al., 2009), Ca^{2+}/calmodulin-dependent kinase II (CaMKII) (Maier, 2009).

Another intrinsic process that regulates L-type Ca^{2+} channels is the regulation by calmodulin (CaM). The interactions between CaM and the IQ-motif in the C-terminal cytoplasmic tail of voltage-gated calcium channels are involved in two opposing mechanisms to control the calcium influx: calcium-dependent inactivation (CDI) and calcium-dependent facilitation (CDF) (Zuhlke et al., 1999). Over the past years, complexes of Ca^{2+}-CaM with the IQ-motif of L-type Ca^{2+} channels have been studied by high-resolution structures (Findeisen and Minor, 2010). These techniques have provided structure-based insight into mechanisms but have also raised some new questions.

1.1 Calcium channel

There are two main types of calcium channels: voltage-gated calcium channels, which open in response to changes in membrane potential and ligand-gated calcium channels, which are activated by ligand binding, such as IP_3 receptors, store operated calcium channels and ryanodine receptors.

Voltage-gated calcium channels are large transmembrane proteins that regulate the intracellular concentration of calcium ions. According to the electrophysiological properties, VGCCs were divided into two major classes: low-voltage-activated (LVA) channels need only a small depolarization to be activated (voltage positive to -70 mV) and high-voltage-activated (HVA) channels require a relatively high step in membrane voltage to open (voltages positive to -20 mV) (Hagiwara et al., 1975; Llinas and Yarom, 1981). Based on amino acid sequence similarity, pharmacological and biophysical properties, VGCCs are divided into three subfamilies: Ca_V1, Ca_V2 and Ca_V3 (Budde et al., 2002).

The Ca_V1s subfamily includes channels that conduct L-type Ca^{2+} currents. These channels are sensitive to various 1,4-dihydropyridines (DHPs) such as the inhibitors nifedipine, nisoldipine, isradipine and the activator Bay K 8444 (Nilius et al., 1986; Nowycky et al., 1985). L stands for large conductance and long-lasting length of activation.

The Ca_V2 subfamily includes channels that conduct N-, P/Q-, and R-type Ca^{2+} currents. N-type channels are blocked by ω-conotoxin GVIA (N for neuronal). P/Q-type channels are blocked by ω-agatoxins (P for Purkinje cells). R-type channels, sometimes also called intermediate voltage-activated Ca^{2+} channels, are blocked by SNX-482 (R stands for resistant to the other blockers).

The Ca_V3 subfamily includes channels that conduct T-type Ca^{2+} currents (T for transient, referring to the length of activation) (Lee et al., 1999). Family of VGCCs and specific blocker are shown in Table 1.

In cardiac myocytes, Ca^{2+} current through L-type Ca^{2+} channels (I_{Ca}) is the main way for Ca^{2+} influx from extracellular space into cytoplasm; I_{Ca} triggers the contraction of heart muscle and regulates the force of contraction (Bers, 2002).

Table 1: Family of VGCCs and specific blocker

	Ca^{2+} current types	Ca^{2+} channels	Gene names	Specific Blocker
HVA channels	L-type	$Ca_V1.1$ (α_{1S})	*CACNA1S*	1,4-Dihydropyridine (DHPs) Phenylalkylamine (PAA) Benzothiazepine (BTZ)
		$Ca_V1.2$ (α_{1C})	*CACNA1C*	
		$Ca_V1.3$ (α_{1D})	*CACNA1D*	
		$Ca_V1.4$ (α_{1F})	*CACNA1F*	
	PQ type	$Ca_V2.1$ (α_{1A})	*CACNA1A*	ω-Agatoxin IVA
	N type	$Ca_V2.2$ (α_{1B})	*CACNA1B*	ω-Conotoxin GVIA
	R type	$Ca_V2.3$ (α_{1E})	*CACNA1E*	SNX-482
LVA channels	T type	$Ca_V3.1$ (α_{1G})	*CACNA1G*	Ethosuximide
		$Ca_V3.2$ (α_{1H})	*CACNA1H*	Mibefradil
		$Ca_V3.3$ (α_{1I})	*CACNA1I*	Kurtoxin

L-type Calcium channel

The L-type calcium channel family has currently four known members (Table 1) belonging to the $\alpha_1 1$ subfamily. The skeletal muscle $Ca_V1.1$ channel consists of five proteins, the principal $\alpha_1 1.1$ (α_{1S}) and auxiliary β_1, $\alpha_2\delta$ and γ subunits. Subunit composition of another three L-type channels, $Ca_V1.2$, $Ca_V1.3$ and $Ca_V1.4$ is less certain. The $Ca_V1.2$ channel is assembled from three tissue-specific isoforms of $\alpha_1 1.2$ (α_{1C}), $\alpha_2\delta$, and β (largely the β_2 and β_3 isoforms) with no evidence as yet for a cardiac γ polypeptide (Mikami et al., 1989). The neuroendocrine tissue $Ca_V1.3$ channel was not investigated systematically, but coexpression studies confirmed regulation of the channel by the $\alpha_1 1.3$ (α_{1D}), β_2, β_3 and $\alpha_2\delta$ subunits. (Williams et al., 1992). $Ca_V1.4$ consists of a complex of α_1, $\alpha_2\delta$, β, and γ subunits, however little is known about the detailed biophysical and pharmacological properties of $Ca_V1.4$ channels (Doering et al., 2005).

To date, at least 10 different α_1 subunit genes have been identified, but only α_{1C} ($Ca_V1.2$) isoform is expressed at high levels in cardiac muscle with possible contribution by α_{1D} ($Ca_V1.3$).
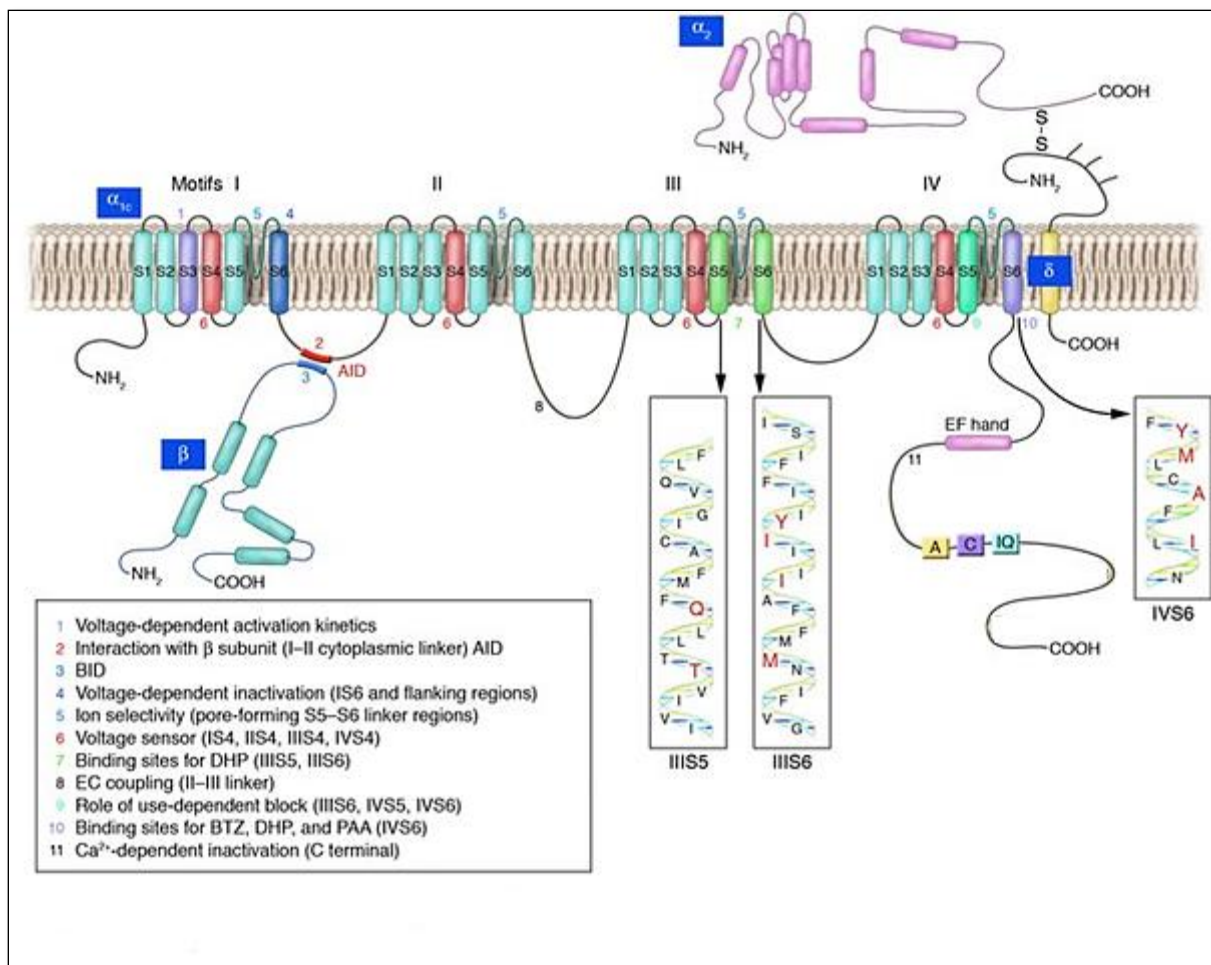
Figure 1. General structure of the Ca$_V$1.2 channel (modified from Bodi et al., 2005). Topology of the pore-forming α1 subunit is composed of 4 homologous repeating domains (I–IV), each of which consists of 6 transmembrane segments (S1–S6). The β$_2$ subunit is entirely intracellular and interacts with its high-affinity binding site on the I-II intracellular loop known as α interaction domain (AID). The numbers are highlighting areas found to be important for specific channel functions. At least 5 consensus sites for phosphorylation by cAMP-dependent PKA have been discovered within the C terminal tail of α$_{1C}$ (Bodi et al., 2005).

L-type calcium channel subunits

The α_1 subunit is the main functional component of the channel complex. It is a 190-250-kDa protein (1600-2400 amino acids) consisting of 4 homologous repeats (domains I–IV). Each domain is composed of 6 transmembrane segments (S1–S6) (Tanabe et al., 1987), as schematically shown in Figure 1. The P-loop between S5 and S6 forms the ion-selectivity filter. S6 segments line the inner pore. Positively charged arginine and lysine residues in the S4 segments form part of the voltage sensor. It is responsible for voltage-dependent Ca^{2+} channel opening. Moreover, the α_1 subunit has specific binding sites for Ca^{2+} channel blockers (1, 4-dihydropyridines, Phenylalkylamine, Benzothiazepine). Intracellular loops bridge the four repeats and serve as docking sites for auxiliary subunits and regulatory molecules that control channel activity (Catterall, 2000; Hofmann et al., 1994; Moosmang et al., 2007). The Ca_V α_1 C-terminal cytoplasmic tail bears an isoleucine-glutamine domain (IQ) domain, the main site of Ca^{2+}/CaM binding (Zuhlke et al., 1999). In addition to the IQ domain, biochemical studies have indicated that the $Ca_V1.2$ C-terminal tail contains other CaM-binding sites generally known as the A-region and C-region (Fig. 1) which are located between the EF-hand motif and the IQ motif (Findeisen and Minor, 2010).

The expression studies suggested that the α_1 subunit can also be a phosphorylation target for PKA (Kamp and Hell, 2000), CaMKII (Lee et al., 2006), PKG (Yang et al., 2007), Akt/PKB (Sun et al., 2006), and by PKC (Singer-Lahat et al., 1992).

The $\alpha_2\delta$ subunits are created from a precursor protein, which is encoded by a single mRNA and is post-translationally cleaved by proteolytic cleavage. Both fragments remain linked via a disulfide bridge. This subunit has also been implicated in modifying the gating properties of the channel as well as the expression level of the channel complex (Davies et al., 2010).

The β subunits are peripheral membrane proteins with an apparent molecular weight of ~55-60 kDa (Glossmann et al., 1987). They are important for trafficking of the channel complex to the surface membrane as well as for modifying its gating properties. Four different β subunit isoforms (β_1- β_4) from 4 distinct genes, *Cacnb1-4*, have been described by now. They all have 14 exons except *Cacnb3,* which has 13 (Buraei and Yang, 2010). The β_2 isoform is the predominant isoform in the heart. The $Ca_V\beta_2$ cDNA was detected by two groups that screened heart and brain libraries but identified two different splice variants; both were called $Ca_V\beta_{2a}$. To prevent further confusion on the used $Ca_V\beta_2$ subunit, Hofmann (Hofmann et al., 2014) suggested renaming the $Ca_V\beta_2$ subunits according to the expressed

NH$_2$ terminus. The major splice variant expressed in adult heart call „Ca$_V$β$_2$-N4" and in brain call „Ca$_V$β$_2$-N3" (for review, see Hofmann et al., 2014).

A recent report describing the targeted mutagenesis of mouse β$_2$ indicated that homozygous loss of this gene (β$_2^{-/-}$) diminished L-type Ca^{2+} currents in cardiomyocytes of embryonic day 9.5 (E9.5). This led to a functionally compromised heart, causing defective remodeling of intra- and extra-embryonic blood vessels and embryonic death following E10.5, significantly earlier than the α$_{1C}$-deficient mouse (Weissgerber et al., 2006). Besides these well know functions, trafficking and gating modulation of the pore channel, β-subunits are also known to contain the phosphorylation sites for PKA at Ser$^{479/480}$ (Bunemann et al., 1999), CaMKII at Thr^{498} (Grueter et al., 2006), and Akt/PKB at Ser^{574} (Sun et al., 2006). We believe that Ca$_V$β$_2$-N4-C terminus contains the relevant phosphorylation sites for the protein kinases described above.
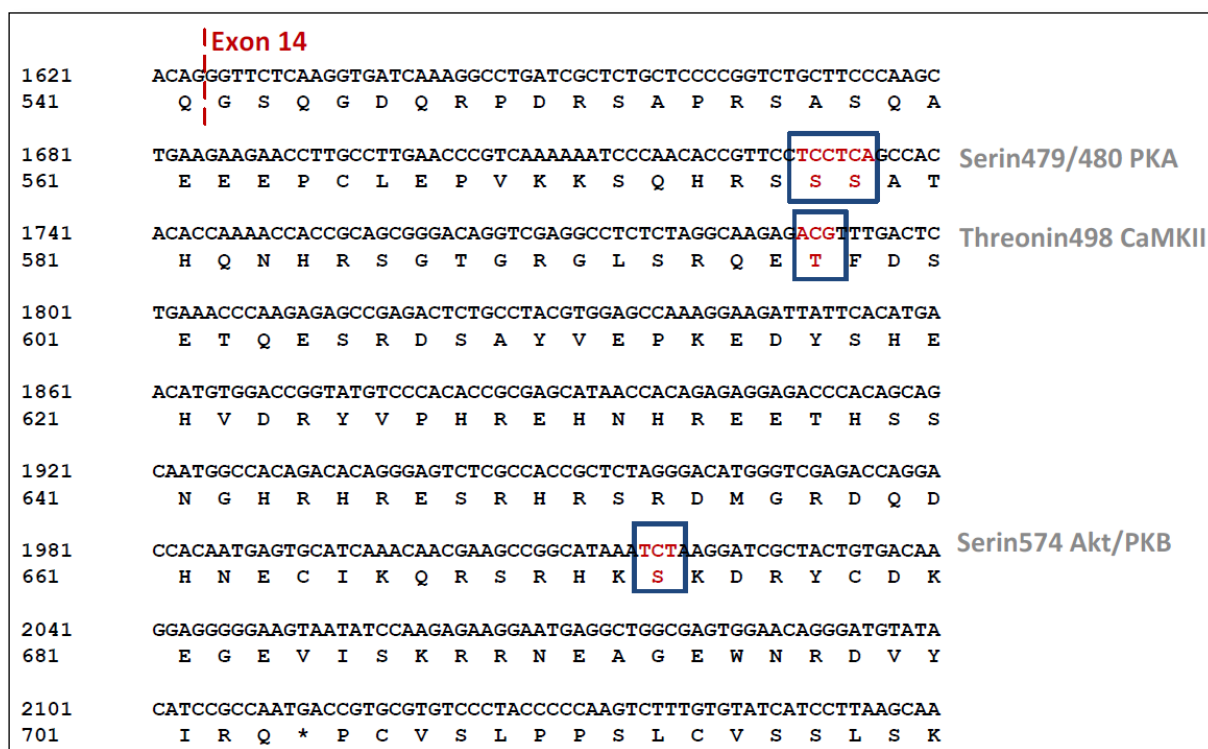
Figure 2. Location of potential PKA, CaMKII and Akt/PKB phosphorylation sites in exon 14 of the murine Ca$_V$β$_2$-N4 protein (modified from Brandmayr et al. 2012). The amino acid sequence is according to *M. musculus CACNB2* sequence (GenBank accession number Q8CC27), and the nucleotide sequence is according to *M. musculus CACNB2* sequence (GenBank accession number NM_023116.4). The phosphorylation sites (*right*) are those of the mouse amino acid sequence (Brandmayr et al., 2012).

1.2 Regulation of calcium channel

Calcium influx into cardiac myocytes via voltage-gated Ca^{2+} channels is a key step in initiating the contractile response. During prolonged depolarizations, toxic Ca^{2+} overload is prevented by channel inactivation occurring through two distinct inactivation processes: voltage-dependent inactivation (VDI) and calcium-dependent inactivation (CDI).

Voltage-dependent inactivation (VDI)

VDI has been considered to play a minor role in the decay of L-type Ca^{2+} channel currents in cardiac myocytes (Bodi et al., 2005). The molecular determinants of VDI are complex and still not fully understood. Different parts of the channel, including $Ca_V\beta$ subunit (Findeisen and Minor, 2010), Ca_V α_1 transmembrane segment IS6 (Raybaud et al., 2006), $Ca_V\alpha_1$ intracellular I-II loop (Berrou et al., 2001; Geib et al., 2002), the cytoplasmic N-terminal domain (Kanevsky and Dascal, 2006; Kobrinsky et al., 2005) and the carboxyl terminus (Bernatchez et al., 1998) seem to be involved. The domain I-II linker may act as the inactivation lid that may dock to the S6 segments to prevent current flow through the channel (Stotz and Zamponi, 2001).

To differentiate VDI from CDI, several studies have used Ba^{2+} as charge carrier via LTCC (I_{Ba}) instead of Ca^{2+} (I_{Ca}) (Peterson et al., 2000). As Ba^{2+} is typically less effective than Ca^{2+} at inactivating the channels, the use of Ba^{2+} as the principal charge carrier results in a reduction in the rate of inactivation and a decrease in the inactivation ratio. CDI can also be retarded by increasing the Ca^{2+} buffering capacity of the cytoplasm through the introduction of exogenous calcium chelators. BAPTA is believed to buffer Ca^{2+} effectively within a distance as small as 30 nm from the mouth of the inner channel, while EGTA is observed with a distance of 100 nm or more from the channel protein (Budde et al., 2002).

Ca^{2+}-dependent inactivation (CDI)

Calcium dependent inactivation can be observed predominantly with L-type channels. It is characterized by a decrease in the channel opening probability during prolonged depolarization that is only seen when Ca^{2+} is the charge carrier (Pietrobon and Hess, 1990). The mechanism of CDI focused recently on the association between the Ca^{2+}-binding protein CaM and the IQ motif.

Calmodulin (CaM) is a 16.7-kDa calcium binding protein. It contains two pairs (N-lobe and C-lobe) of independently folded domains that each contains two Ca^{2+} binding motifs

known as EF hands, each of which can bind a single Ca^{2+} ion (Gifford et al., 2007). Both lobes wrap around a helix formed by the $Ca_V1.2$ IQ domain.

       The IQ motif, named for the isoleucine-glutamine (IQ) pair, is approximately 25 amino acids in length. The motif conforms to the consensus sequence [I,L,V]QxxxRGxxx[R,K], which forms a seven-turn α-helix (Terrak et al., 2003). $Ca_V1.2$ has an IQ motif located in the C-terminal cytoplasmic tail around 150–180 residues C-terminal to the last transmembrane segment (IVS6) (Fig. 3). Short amino-acid segments which locate at the amino terminus of the IQ domain have been found to interact with CaM in cardiac myocytes and heterologous expression systems at low levels of Ca^{2+}. One of these regions is the CB domain (Fig. 3, blue circle). The other region upstream of the CB domain is the 1-8-14 calmodulin-binding motif. At resting Ca^{2+} levels, the N-lobe of CaM binds to the 1-8-14-binding motif, whereas both the N-lobe and the C-lobes bind to the CB region (Fig. 3). When the channel opens, Ca^{2+} reaches CaM and binds to its C- lobe, causing a conformational change in the individual lobes that allows Ca^{2+}/CaM to interact with the IQ motifs and consequently changes conformation of the C terminus, which leads to blockage of α_{1C} pore.
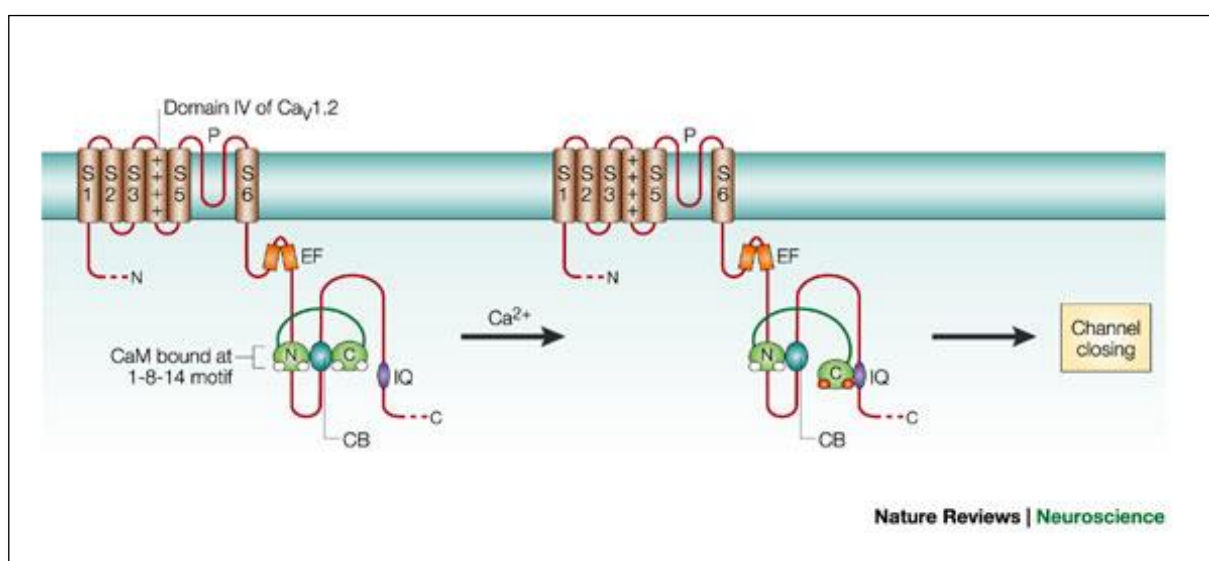
Figure 3. Calcium dependent inactivation (CDI) is modulated by Ca^{2+}/calmodulin (modified from Budde et al., 2002). The EF hands of CaM (white circles) were proposed to be calcium sensor for CDI. When Ca^{2+} binds these four sites, Ca^{2+} activated CaM reorients its attachments and causes a conformational change of the α_1 C-terminus structure, and therefore drives CDI (Budde et al., 2002).

Ca^{2+} -dependent facilitation (CDF)

In contrast to inactivation, facilitation is the process whereby Ca^{2+} influx through Ca$_V$1.2 channels is increased upon repeated stimulation, which contributes to increased force-frequency relationship of the heart muscle during exercise. Recent studies have implicated Ca^{2+} dependent binding of CaM to the carboxy terminus of the L-type Ca^{2+} channel α$_{1C}$ subunit as an essential element in the modulation of CDF. However, several studies have also shown that CaM is not sufficient to stimulate facilitation (Dzhura et al., 2000; Zamponi, 2005). It is possible that binding of CaM to the C terminus of the L-type Ca^{2+} channel probably has a facilitatory role, by anchoring CaM at a site that supports Ca^{2+}/calmodulin-dependent kinase (CaMK) mediated phosphorylation or by producing a conformational change in the L-type Ca^{2+} channel that allows CaMK-mediated phosphorylation (Dzhura et al., 2000). It is not clear how CaMK might interact with CaM binding to the IQ domain in promoting CDF, the molecular mechanism still needs to be elucidated.

CaM binds to the IQ motif located at amino acids 1624-1635 of the Ca$_V$1.2 carboxyl terminus (Halling et al., 2005; Zuhlke et al., 1999). Isoleucine-1624 is essential for CaM binding. The mutation Ile1624 to glutamate decreases the affinity of the IQ sequence for CaM by around 100-fold and abrogated CDF and CDI in *Xenopus oocytes* (Zuhlke et al., 1999; Zuhlke et al., 2000). It is unclear if the binding of CaM to the Ca$_V$1.2 channel is relevant for the function of the cardiac calcium channel in the behaving mouse.

Regulation of L-type Ca^{2+} channel by protein kinase A

β-adrenergic receptor (AR)–mediated stimulation of cardiac L-type Ca^{2+} channels is due to phosphorylation of the channel by cAMP-dependent protein kinase A. β-adrenergic receptors are coupled to heterotrimeric G proteins, which either stimulate (G$_s$) or inhibit (G$_i$) adenylyl cyclase (AC). An increase in AC activity leads to increased production of cAMP. cAMP binds to the regulatory subunits of PKA (PKA consists of two catalytic subunits and two regulatory subunits). PKA is activated, followed by release of the catalytic (C) subunits. The released active C-subunit phosphorylates serine and threonine residues of the target protein (Fig. 4). Phosphorylation of L-type Ca^{2+} channels by PKA increases the probability and duration of the open state of the channels and thereby causes an increase in cardiac contractility (McDonald et al., 1994; Osterrieder et al., 1982; Reuter, 1974)

Both the α$_{1C}$ and β$_2$ subunits of LTCC have been demonstrated to be direct targets of PKA-mediated phosphorylation (De Jongh et al., 1996). The phosphorylation of α$_{1C}$ by PKA is critically dependent on close localization of PKA and L-type Ca^{2+} channel, whereas

phosphorylation of the β subunit by PKA does not require such a close PKA dislocation (Gao et al., 1997). PKA is anchored near its targets through association with an A-kinase-anchoring protein (AKAP). When the association of an AKAP with PKA is interrupted, PKA dependent phosphorylation of skeletal and cardiac LTCC is not observed (Treinys and Jurevicius, 2008).

A PKA phosphorylation site on the α_1 subunit (Ser^{1928}) has been proposed to mediate the β adrenergic response (Hulme et al., 2006). Ser^{1928} is located in the C-terminal portion that is reported to be cleaved off the full-length form (Kamp and Hell, 2000). Biochemical studies showed that the cleaved α_1 subunit lacking its distal C-terminal tail is not a substrate for phosphorylation by PKA (Yoshida et al., 1992), whereas the full-length α subunit was readily phosphorylated on Ser^{1928} in the distal C-terminal domain (Mitterdorfer et al., 1996; Yoshida et al., 1992). However, recent studies using the $Ca_V1.2$ (S1928A) knock-in mice show that basal L-type currents and the upregulation of L-type currents by PKA and β-adrenergic receptor stimulation are unchanged (Ganesan et al., 2006; Lemke et al., 2008), indicating that PKA phosphorylation of Ser^{1928} is not the underlying cause for L-type current upregulation.

Phosphorylation by PKA is not detectable in the α_2-δ subunit of the Ca^{2+} channel (Davare et al., 1999; Hell et al., 1993), but β subunits serve as substrates for these kinases in vitro and in intact cells. It has been shown *in vitro* that PKA phosphorylates three sites on β_{2a}: Ser^{459}, Ser^{478}, and Ser^{479}. Mutation of Ser^{459} to Alanine results in a reduced rate and degree of phosphorylation of the β_{2a} subunit by PKA. Mutation of Ser^{478} and Ser^{479} to Alanine completely abolishes the PKA-induced phosphorylation (Gerhardstein et al., 1999). Bunemann (Bunemann et al., 1999) showed that coexpression of β_{2a} with a C-terminally truncated version of α_{1C} lacking Ser^{1928} caused an increase in channel activity by PKA. These results indicate that phosphorylation of either Ser^{478}, Ser^{479}, or both on the β subunit contributes to channel regulation by PKA at least in the presence of C-terminally truncated α_{1C}.
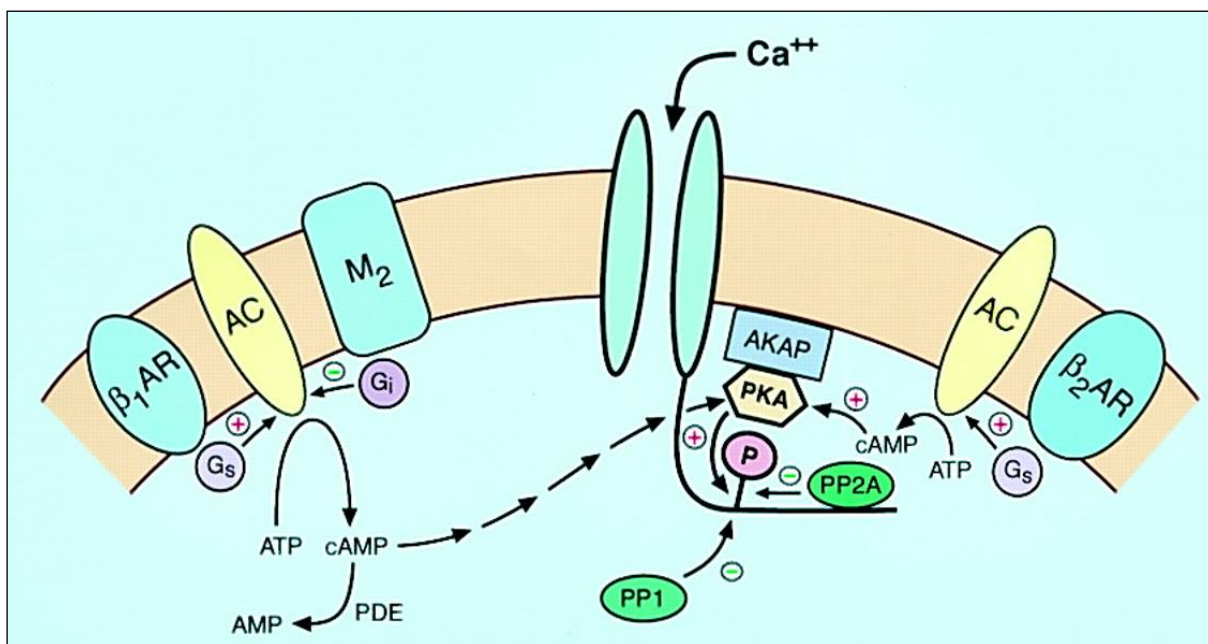
Figure 4. Scheme of the cAMP/PKA cascade regulating L-type channels (modified from Kamp and Hell, 2000).

Regulation of the L-type Ca^{2+} channel by Phosphoinositide 3-Kinase (PI3K) and Protein Kinase B/Akt

The Protein kinase B (also called Akt) family of Ser/Thr kinases consists of three isoforms (Akt-1, -2, and -3). They are activated by IGF-1 (insulin-like growth factor) and PI3K, which is a member of the lipid kinase family (Sun et al., 2006). In the heart, the IGF-1 – PI3K – Akt pathway is involved in the regulation of contractile function, and impairment of this signaling pathway is considered an important determinant of cardiac function (McMullen et al., 2004; Sun et al., 2006). Akt activation upregulates L-type Ca^{2+} current and this current is decreased by Akt inhibition (Catalucci and Condorelli, 2006; Viard et al., 2004), suggesting a pivotal role of Akt in regulating LTCC function. This mechanism likely involves PI3K activation and subsequent production of phosphatidylinositol 4,5-bisphosphate (PIP2) and phosphatidylinositol 3,4,5-trisphosphate (PIP3). Increased PIP3 levels recruit PKB to the membrane, which can phosphorylate β_{2a} at Ser^{574}. This results in an increase of channel surface expression. L-type Ca^{2+} channel surface expression is greatly reduced in cardiac-specific knockout mice that lack active PKB, causing severe cardiomyopathy (Catalucci et al., 2009).

Regulation of the L-type Ca^{2+} channel by CaMKII

CaMKII is a key downstream effector of LTCC signals. In myocytes, CaMKII is required for normal excitation contraction coupling (Couchonnal and Anderson, 2008) and transcription (Bossuyt et al., 2008). CaMKII also works as a feedback regulator of LTCCs (Xiao et al., 1994). CaMKII participates in several forms of facilitation of calcium channel, including voltage-dependent facilitation (VDF), Ca^{2+}dependent facilitation, and an increase in channel open probability (Dzhura et al., 2000; Lee et al., 2006).

Studies in heterologous cells using β$_{2a}$-N3 subunit demonstrate that CaMKII binds to the COOH terminus of β$_{2a}$-N3 and phosphorylates it at Thr^{498}, which leads to an upregulation of L-type currents (Abiria and Colbran, 2010; Grueter et al., 2006) This upregulation is not observed in the absence of β$_{2a}$-N3 or when a non-phosphorylatable β$_{2a}$-N3 mutant, β$_{2a}$-N3 T498A, is coexpressed in tsA201 cells. This mutant can also act as a dominant negative β$_{2a}$-N3, preventing CaMKII-mediated facilitation of endogenous Ca^{2+} currents. However, the significance of these phosphorylation sites for voltage-dependent facilitation in vivo has remained unclear. The β$_{2a}$-N3 subunit has not been found in the murine heart (Link et al., 2009; Qin et al., 1998).

Recent studies also show that CaMKII can interact directly with the α$_1$-subunit of high- voltage-activated (HVA) Ca^{2+} channels and support the facilitation properties of the channel (Lee et al., 2006). Hudmon (Hudmon et al., 2005) reported that CaMKII is tethered to the C terminus in close proximity to the IQ motif, and CDF was abolished by mutating the putative interaction site. CaMKII was reported by our group (Blaich et al., 2010) to phosphorylate Ser^{1512} and Ser^{1570}. The influence of CaMKII was examined using knock-in mutation of the CaMKII phosphorylation sites S1512/S1570 in a mouse model. Mutation of the two serines showed a negative shift in voltage-dependent inactivation, a slowed recovery from inactivation and a decreased VDF as reported previously (Guo and Duff, 2003, 2006; Hashambhoy et al., 2009). These results support the notion that CaMKII-dependent phosphorylation at Ser^{1512} and Ser^{1570} mediates facilitation in cardiomyocytes.

1.3. Objective of this work

1. To investigate the physiological significance of the I/E mutation in vivo.

Although much is known about the CaM binding site of the IQ motif however, most data are based on in vitro experiments in multiple cell lines. Strong evidence exists that CaM binds to the IQ motif of the Ca$_V$1.2 channel that is located at amino acids 1624-1635 of Ca$_V$1.2 C-terminus. Especially Ile1624 determines the amount of CaM binding. In addition, the I/E

mutation abrogates CDF and CDI of LTCC expressed in xenopus oocytes. It is unclear whether binding of CaM to the $Ca_V1.2$ channel is relevant for the function of the cardiac calcium channel in the behaving mouse. To develop a better understanding, animal-based in vivo studies should be perform.

2. To assess the role of phosphorylation sites on exon 14 of *CACNB2* gene in vivo.

The $Ca_V\beta_2$-N4 protein carries three putative phosphorylation sites, which are located in very short distance on the carboxyl-terminal exon 14 of the gene *CACNB2*. It involves PKA ($Ser^{479/480}$), CaMKII (Thr^{498}) and Akt/PKB (Ser^{574}) phosphorylation sites. Due to truncation of the carboxy terminus in the $Ca_V\beta_2$-N4 of βStop mouse line, these phosphorylation sites were removed in vivo which should lead to a decrease in β-adrenergic response ($Ser^{479/480}$), facilitation of I_{Ca} (Thr^{498}) and I_{Ca} density (Ser^{574})

3. To examine collaboration between two PKA phosphorylation sites; Ser^{1928} on α_1-subunit and $Ser^{479/480}$ on β subunit.

Studies by Bünemann (Bunemann et al., 1999) demonstrate that PKA can phosphorylate $Ser^{479/480}$ of the $Ca_V\beta_2$-N4 subunit as well as Ser^{1928} of the α_{1C} subunit. Previously, Lemke (Lemke et al., 2008) also reported that mutation of Ser^{1928} to Ala did not affect β-adrenergic regulation of the cardiac I_{Ca} in vivo. This data raise the possibility that phosphorylation of the $Ca_V\beta_2$-N4 subunit by PKA might be the requested regulatory step.

4. To examine collaboration between two CaMKII phosphorylation sites; Ser^{1512}/Ser^{1570} on α_1 subunit and Thr^{500} on β subunit.

Blaich (Blaich et al., 2010) investigated the functional significance of CaMKII dependent phosphorylation of Ser^{1512}/Ser^{1570} for CDF of cardiac LTCC. They reported that mutation of these Ser to Ala affected facilitation in vitro and in vivo. The question was raised whether CaMKII phosphorylation site Thr^{500} on β subunit work together with S1512/S1570 to synergistic effect on CDF.

2. MATERIALS AND METHODS

2.1. Preparation, Solution and Substance

2.1.1 HEK293T cell culture

HEK 293T is an HEK (Human Embryonic Kidney) 293 derived cell line that expresses the activating protein, SV40 large T-antigen. The cell were plated into 50 ml flask, added with pre-warmed Quantum 286 medium and incubated at 37 ^{o}C with 5% CO_2. For general maintenance, HEK 293T cells were passaged at 80% confluency. The growth medium was carefully aspirated from the cells. The cells were washed gently with PBS and were trypsinized with 2 ml of 0.05% trypsin-EDTA. Culture medium (10 ml) was added to resuspend cells and inactivate trypsin. The cells were pipetted up and down to get a single cell suspension, and then cells were plated in new sterile flask containing culture medium and were incubated at 37°C with 5% CO_2.

Lipofectamine transfection

The day before transfection, HEK293T cells were trypsinized and plated on poly-L-lysine coated glass coverslip in 0.5 ml serum-reduced Opti-MEM medium per well. The day of transfection, a solution A (0.15 µg of $Ca_V\alpha_{1a}$, $Ca_V\beta_{2a}$-N4 and $Ca_V\alpha_2\delta$ DNA in 50 µl of Opti-MEM) was mixed with a solution B (0.5 µl of Lipofectamine in 50 µl of Opti-MEM) by gentle pipetting. After 20 min at room temperature, DNA-Lipofectamine reagent complexes were added to each well containing cells and mix gently by rocking the plate back and forth. Cells were incubated for 18-24 hours. The solution of DNA/Lipofectamine complexes was then aspirated and replaced with 500 µl of Quantum medium.

2.1.2. Mouse ventricular cardiomyocyte preparation

Generation of Mice with the I1624E Mutation

This part was performed by Stefanie Fischer. Our group has created a mouse line in which Ile1624 was mutated to Glu ($Ca_V1.2^{I1624E}$). Homozygous $Ca_V1.2^{I1624E}$ mice were not viable. To overcome this problem, we generated mice with a conditional heart-specific I/E mutation in the $Ca_V1.2$ channel gene. Therefore, we inactivated the floxed $Ca_V1.2$ gene of heterozygous $Ca_V1.2^{I1624E}$ mice by the inducible α-myosin heavy chain-MerCreMer system

(Blaich et al., 2012). The resulting $Ca_V1.2^{I1624E}$ mice were studied after treatment with tamoxifen.

To construct the targeting vector, a 8.0-kb fragment containing exons 39-44 of *CACNA1C* was isolated from 129/Svj mouse genomic DNA. The targeting vector was composed of a 1.1-kb short 5´-arm, a 4.5-kb fragment containing the *neo-tk* an *loxP* sequences, a 743-base fragment including the I/E mutation at position 1624, and a 5.5-kb long 3´-arm. All mutation procedures were carried out by site-directed PCR mutagenesis (Stratagene). The targeting construct was electroporated into R1 embryonic stem cells (129/Sv×129/Sv-CP F1) (Nagy et al., 1993). Positive clones were identified by PCR and confirmed by Southern blotting. The *neo-tk* cassette was removed from the germ line through *cre/loxP-* mediated excision in a second targeting step. A positive embryonic stem cell clone was injected into C57BL/6 blastocysts, and chimeras were crossed with C57BL/6 mice. After confirmation of successful targeting by polymerase chain reaction (PCR) and Southern blot analysis, heterozygous mice were bred with mice, which carry a mutant estrogen receptor ligand binding domain fusion protein-Cre (MerCreMer) under control of the α-myosin heavy chain gene promoter, thus conferring tamoxifen-inducible Cre activity in the heart and with floxed $Ca_V1.2$ L2 mice (Seisenberger et al., 2000) to produce inducible adult mice bearing the I1624 E mutation (Fig. 5). The intercross of the three mouse lines resulted in production of $Ca_V1.2^{I1624E/L2}$ ×MerCreMer (identified as I/E) and $Ca_V1.2^{L2/+}$ × MerCreMer (Ctr) offspring at the expected Mendelian ratio.

Tamoxifen injection

Tamoxifen base in Mygliol (20 mg/ml) was prepared by sonication (suspending 100 mg Tamoxifen in 5 ml Mygliol). The aliquots were frozen and stored at -20°C for up to 4 weeks and were thawed at 37 °C before use. MerCreMer crossover mice were i.p injected with 100 µl of tamoxifen stock solution at 24 hours interval for 4 consecutive days. Experiments were performed 10 days after the first tamoxifen injection.
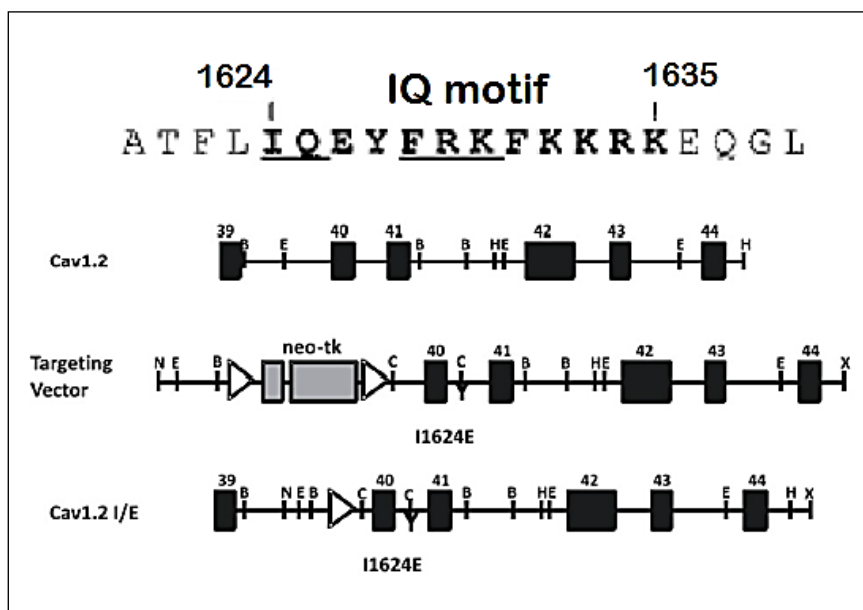
Figure 5. Generation of I/E mice. *First row*, sequence around the IQ motif of *CACNA1C*. *Second row*, genomic DNA structure of *CACNA1C*, boxes represent exons 39-44 encoding part of the C terminus of $Ca_V1.2$. *Third row*, targeting vector. *Neo*, neomycin resistance gene; *tk*, thymidine kinase gene with loxP sequence (triangles) at both sides. The I1624E substitution is shown. *Fourth row*, knock-in locus after homologous recombination and Cre-mediated deletion of resistance markers (modified from Poomvanicha et al., 2011)

Generation of Mice Lacking the C Terminus of $Ca_V\beta_2$ (βStop)

This part was performed by Julia Brandmayr (Brandmayr et al., 2012). The βStop mouse is the knock-in mouse line with targeted mutation of the $Ca_V\beta_2$-N4 gene by insertion of a stop codon after proline 501 in exon 14.

To construct the targeting vector, a 7.3-kb fragment containing exons 13-14 of *CACNB2* was isolated from 129/Sv mouse genomic DNA. The targeting vector included a 1.6-kb short arm and 5.7-kb long arm with *PGK-neo* and the thymidine kinase gene (*tk*) flanked by two loxP sites. The 3´-side long arm contained exon 14 with the stop codon TGA in frame after Pro501 and the phosphorylation sites $Ser^{529/530}$ (corresponding to $Ser^{479/480}$ rbs), Ser^{545} (corresponding to Ser^{496} rbs), Thr^{549} (corresponding to Thr^{498} rbs), and Ser^{625} (corresponding to Ser^{574} rbs) behind the stop codon. All mutation procedures were carried out by QuikChange II site directed mutagenesis (Stratagene). The targeting construct was electroporated into R1 ES cells (129/Sv x 129/Sv-CP F1). Positive clones were identified by

PCR and confirmed by Southern blotting using a probe on the *neo* gene. One positive clone was detected and injected in C57BL/6 blastocysts. Chimeras were crossed to C57BL/6 mice. By crossing with a Cre-recombinase expressing transgenic B6.C-Tg (CMV-cre) 1Cgn/J mouse strain, the neo tk marker genes were excised. Heterozygous mice were bred to produce homozygotes. The intercross of heterozygotes resulted in production of wild-type, heterozygous, and homozygous offspring at almost the expected Mendelian ratio (75:131:64). For all analyses, filial generation 2 (F2) mice with 129/Sv and C57BL/6 hybrid genetic background were used. All procedures relating to animal care and treatment were authorized by the "Regierung von Oberbayern" and conformed to the institutional, governmental, Directive 2010/63/EU of the European Parliament guidelines and to the Care and Use of Laboratory Animals published by the US National Institutes of Health.

Figure 6. Generation of βStop mice. *First row*, genomic DNA structure of *CACNB2* with the relevant restriction enzyme sites; *boxes* represent exons 13 and 14 encoding the C terminus of Ca$_V$β$_2$-N4. *Second row*, targeting vector. *Neo*, neomycin-resistance gene; *TK*, thymidine kinase gene with loxP sequence (triangles) at both sides. The insertion of the stop codon after proline 501 is shown. *Third row*, knock-in locus after homologous recombination and Cre-mediated deletion of resistance markers (Brandmayr et al., 2012).

Generation of Mice Lacking the C Terminus of Ca$_V$β$_2$-N4 and Ser1928 Phosphorylation Site on Cav1.2 (SAβStop mouse)

The βStop line was cross-bred with Ca$_V$1.2^{SA} line. The Ca$_V$1.2^{SA} mouse line expresses a Ca$_V$1.2 channel containing the mutation S1928A. Ca$_V$1.2^{SA} line was created by Toni Lemke (Lemke et al., 2008).

To construct the targeting vector, a 7.4-kb fragment containing exons 44–47 of *CACNA1C* was isolated from 129/Sv mouse genomic DNA. The targeting vector included a 1.2-kb short arm and 6.2-kb long arm with PGK-neo and the thymidine kinase gene (tk) flanked by two loxP sites. The 3` -side long arm contained exon 45 with the phosphorylation site, Ser1928, mutated to alanine. All mutation procedures were carried out same as describe above.
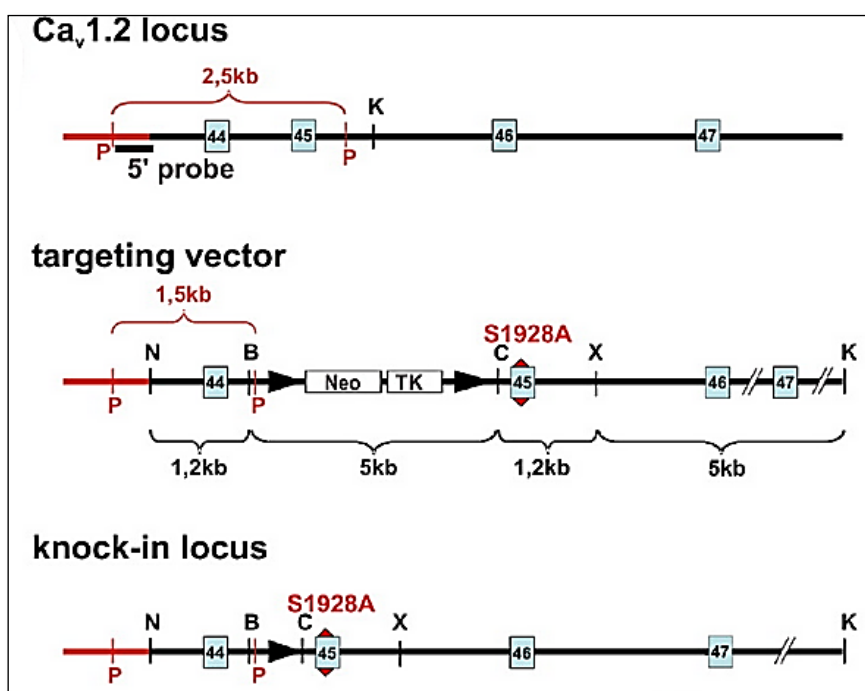
Figure 7. Generation of Ca$_V$1.2 S1928A mutant mice. *First row,* genomic DNA structure of *CACNA1C* with the relevant restriction enzyme sites; *boxes* represent exons $44 - 47$ encoding the C terminus of Ca$_V$1.2. *Second row,* targeting vector. *Neo*, neomycin resistance gene; *TK*, thymidine kinase gene with loxP sequence (*triangles*) at both sides. The S1928A alanine substitution for serine is shown. *Third row,* knock-in locus after homologous recombination and Cre-mediated deletion of resistance markers. (Lemke et al., 2008).
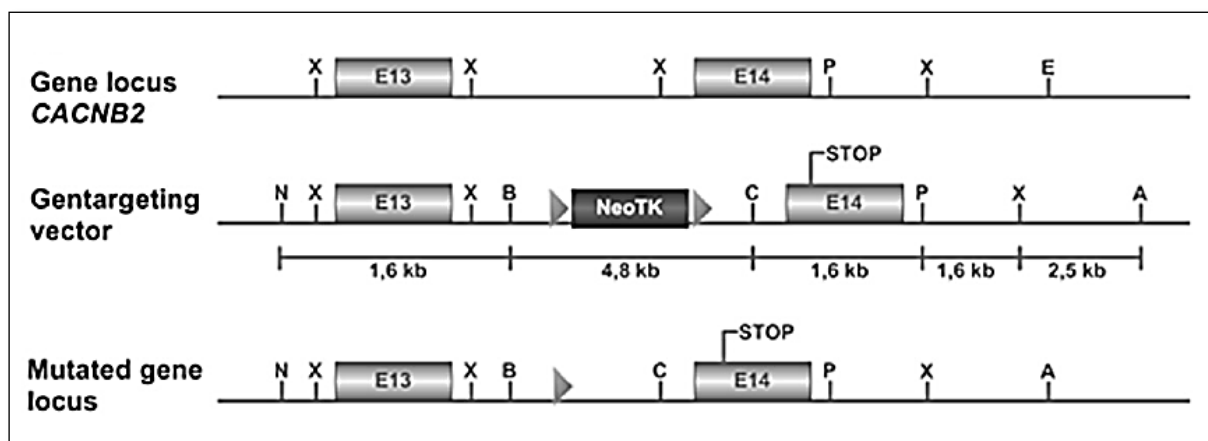
Generation of Mice Lacking the C Terminus of Ca$_V$β$_2$-N4 and Ser1512/1570 Phosphorylation Site on Ca$_V$1.2 (SFβStop mouse)

The βStop line was cross-bred with Ca$_V$1.2^{SF} line. The Ca$_V$1.2^{SF} mouse line expresses a Ca$_V$1.2 channel containing the double mutation S1512A and S1570A. Ca$_V$1.2^{SF} line was created by Stefanie Fischer. To construct the targeting vector, a 8.5 kb Not I-Kpn fragment containing exons 35 -38 of CACNA1C was isolated from 129/Svj mouse genomic DNA. The targeting vector was comprised of a 1.2 kb short arm and 6.7 kb long arm with PGK-neo and the thymidine kinase gene flanked by two lox-P sites. The 3′-side long arm contained exons 36 and 38 with the two phosphorylation sites, Ser1512 and Ser1570, mutated to Ala. All mutation procedures were carried out in the same way as described above (Blaich et al., 2010).
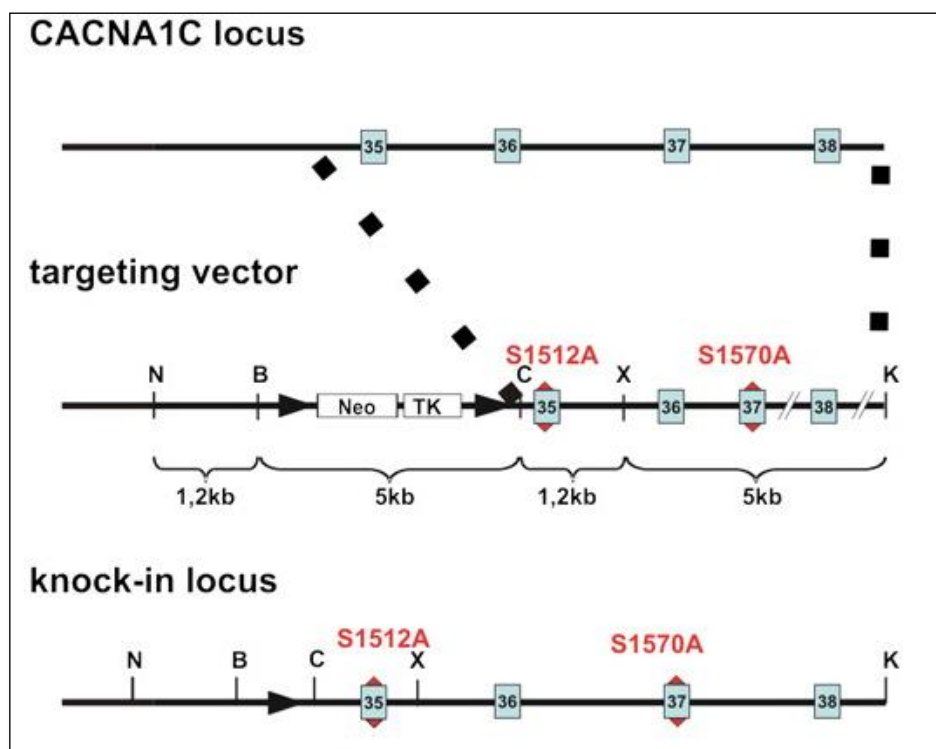
Figure 8. Generation of Ca$_V$1.2 S1512A/S1570A mutant mice. *First row*, genomic DNA structure of *CACNA1C*. Boxes represent exons 35 − 38 encoding part of the carboxy-terminus of Ca$_V$1.2. *Second row,* Targeting vector. Neo, neomycin-resistance gene; TK, thymidine kinase gene with loxP sequence (triangles) at both sides. S1512A/S1570A, alanine substitutions for serines are shown. *Third row*, Knock-in locus after homologous recombination and Cre-mediated deletion of resistance markers. (Blaich et al., 2010)

All animals were maintained and bred in the animal facility of the Institut für Pharmakologie und Toxikologie, Technische Universität München, and had access to water and standard chow *ad libitum*. Experiments were performed with male or female mice aged 8 – 12 weeks (weighing 25 - 35 g). They were housed in a temperature-controlled room with 12h:12h light-dark cycle. All procedures relating to animal care and treatment were authorized by the ´Regierung von Oberbayern´ and conformed to the institutional and governmental guidelines.

Cardiomyocyte isolation

Ventricular myocytes were isolated using a procedure from Alliance for Cellular Signaling (AfCS) (PP00000125). Male and female mice (8 – 12 weeks old) were first injected intraperitoneally with 0.5 ml of heparin diluted in normal saline to 100 IU/ml followed by anesthesia with 100 mg/ml ketamine, 2% xylazine (Rompun®), 1% acepromazin (Vetranquil ®) in normal saline. After wiping the chest with 70% ethanol, the chest was opened to expose the lungs and heart. The heart was rapidly excised and canulated by tying the aorta to the cannula, then perfused the heart with a Ca^{2+}-free perfusion buffer (Table 5) for 4 minutes at a speed of 3 ml/min at 37°C. Then, enzymatic digestion was performed for 15 min using digestion buffer (Table 6). After enzyme digestion of the heart was complete (heart appeared swollen, pale and flaccid). The heart was then cut from the cannula. The atrium was excised. The ventricle was placed in a dish with enzyme buffer, minced into small pieces and gently dissociated for several minutes until large pieces of heart tissue were dispersed into the cell suspension. Stop1 buffer (Table 7, left panel) was added into the cell suspension. Cells were allowed to sediment by gravity for 10 minutes followed by centrifugation at 1000 rpm for 1 minute. Cells were resuspended again in stop2 buffer (Table 7, right panel). External Ca^{2+} was added to the solution with a final concentration of 1 mM.

Single cells were plated on to glass coverslips pre-coated with laminin (sigma-aldrich) in plating medium (Table 8). The cells were incubated for 1 hour at 37°C and 2%CO_2 in humidified to allow myocyte attachment. After 1 hour, plating medium was aspirated with a sterile pasteur pipette to remove unattached myocytes and debris. Culture medium (Table 9), which has been equilibrated at 37°C in a 2%CO_2 incubator for at least 2-3 hours, was added to the cells and myocytes were immediately returned to the incubator until used. The experiment was performed on the same day as isolation. Only rod shaped cells with clear striations were selected for current recordings.

2.1.3. Chemicals and consumables

The reagents were obtained from Sigma-Aldrich, Carl Roth, Sarstedt, Biochrom and Merck unless stated otherwise. For making all solutions and media, deionized water was used. All substances used were of the highest purity available.

Table 2.

Reagent	Source
Agarose	Biozym
Bovine serum albumin	Gibco-BRL
Collagenase Type II	Worthington
DMEM	Invitrogen
Fetal calf serum	Gibco
Heparin 10000 I.E	Braun
Lipofectamine^{TM} 2000	Invitrogen
OptiMEM	Gibco
Penicillin-Streptomycin 100x	Gibco
Proteinase K	Roche Applied Science
Quantum 286 Medium	PAA
Standard marker DNA-Extension-ladder	Gibco
Standard marker Precision Blue Protein	Gibco
Trypsin-EDTA 10x	Gibco

2.1.4. Devices

Table 3.

Devices	Manufacture
4°C Refrigerator	Liebherr
-20°C Freezer	AEG
Agarosegel chamber	MWG Biotech
Apx-60 Balance	Denver instrument
Biological Safety Cabinets	NuAire
Camera AxioCam MRc 5	Zeiss
Dark Hood DH-40/50	biostep
Digidata 1332A digitizer	Molecular Devices
DMZ-Universal Puller	Dagan
Eppendorf Centrifuge 5804R	Eppendorf
Eppendorf Centrifuge 5417R	Eppendorf
Eppendorf Centrifuge 5415C	Eppendorf
Haake coolness Thermostate D8	Haake
Incubator Binder CB53	Binder
Microscope Stemi SV6	Zeiss
Microscope Axioscope	Zeiss
Micro Forge MF-830	Narishige
Multiclamp 700A	Molecular Device
Oven 37°C	Memmert
PCR-Machine Biometra T Gradient	Biometra
pH-Meter 766 Calimatic	Knick
Pump head Minipuls 2	Abimed
Standard Power Pack P25	Biometra
Tabletop centrifuge	Neolab
Thermomixer Compact	Eppendorf
Vortex-Mixer	Neolab
Waterbath MT/2	Mgw Lauda

2.1.5. Solution

Table 4. Solutions for electrophysiology recording

Substance (mM)	HEK293T Cell		Cardiomyocyte		Cardiomyocyte (for facilitation recording)	
	External saline	Internal saline	External saline	Internal saline	External saline	Internal saline
NaCl	82	-	137	-	137	-
KCl	-	-	5.4	-	-	-
TEA-Cl	20	10	-	10	-	10
CaCl$_2$ or BaCl$_2$	30	-	1.8	-	1.8	-
CsCl	5.4	102	-	102	25	120
MgCl$_2$	1	1	1	1	0.5	-
Glucose	10	-	5.6	-	10	-
Hepes	5	5	10	5	10	10
EGTA or BAPTA	0.1	10	-	10	-	1
MgATP	-	-	-	-	-	1
Na$_2$ATP	-	3	-	3	-	1
GTPNa$_2$	-	0.1	-	0.1	-	-
Phosphocreatine	-	-	-	-	-	5
Adjust pH to	7.4	7.4	7.4	7.2	7.4	7.2

The internal solution was filtered through a 0.20-µm syringe filter (Carl Roth, Germany) before use. The pH of saline was adjusted with NaOH for external solution and with CsOH for internal solution.

Table 5. Myocyte perfusion buffer

Final concentration (mM)	Reagent
113	NaCl
4.7	KCl
0.6	KH_2PO_4
0.6	Na2HPO$_4$
1.2	$MgSO_4-7H_2O$
0.032	Phenol red
12	$NaHCO_3$
10	$KHCO_3$
10	HEPES
30	Taurine
10	2,3-Butanedione monoxime
5.5	Glucose

Table 6. Myocyte digestion buffer

Final concentration	Reagent
1×	Perfusion buffer
0.25 mg/ml	Collagenase Type II
0.14 mg/ml	Trypsin
12.5 μM	$CaCl_2$

Table 7. Myocyte stopping buffer

Stopping buffer 1		Stopping buffer 2	
1×	Perfusion buffer	1×	Perfusion buffer
10%	Bovine calf serum	5%	Bovine calf serum
12.5μM	$CaCl_2$	12.5 μM	$CaCl_2$

Table 8. Myocyte plating medium (50 ml)

	Reagent
45.5 ml	MEM medium
2.5 ml	Fetal calf serum
1 ml	2,3-Butanedione monoxime
500 µl	Penicillin
500 µl	L-glutamine

Table 9. Myocyte culture medium (50 ml)

	Reagent
49 ml	MEM medium
50 µl	Bovine serum albumin
500 µl	Penicillin
500 µl	L-glutamine

2.2 Experimental setup

2.2.1. Telemetric Electrocardiogram (ECG) Recordings

This part was performed by Katrin Domes and Anne Blaich. Radiotelemetric ECG transmitters (ETA-F20; DSI, St. Paul, MN) were implanted into the peritoneal cavity under general anesthesia with isoflurane/O_2. The ECG leads were sutured subcutaneously onto the upper right chest muscle and the upper left abdominal wall muscle. The animals were allowed to recover for 2 weeks before the experiments. Isoproterenol (0.1 mg/kg mouse) or phenylephrine (3 mg/kg mouse) was dissolved in 0.9% NaCl. After 15 min of base-line recording, the mice were injected intraperitoneally with the drugs. The ECGs were recorded for 45 min thereafter. The animals were allowed to recover for at least 48 h between experiments. Data were acquired using the DSI acquisition system.

2.2.2. Echocardiography

This part was performed by Katrin Domes and Anne Blaich. Images were obtained using a Vevo 770 Visual Sonics scanner equipped with a 30-MHz probe (Visual Sonics Inc., Toronto, ON, Canada). The mice were lightly anesthetized (1.5% isoflurane) and anchored to a warming platform in dorsal position, and ECG limb electrodes were placed. The chests were shaved and cleaned to minimize ultrasound attenuation. Fractional shortening (FS, the diameter at the end of systole minus the diameter at the end of diastole divided by the diameter at the end-diastole) was assessed from the M mode of the parasternal short axis view. Control and mice carrying the various mutations were studied before and after administration of isoproterenol (0.1 mg/kg mouse intraperitoneally).

2.2.3. Principle of patch clamp technique and Instrument

To study biophysical properties of L-type calcium channel current, voltage clamp experiments were performed. Whole-cell configuration of the patch clamp technique was used for the electrophysiological study.

All experiments were done under a 400-fold magnification of an inverted microscope (Axiovert 200, Carl Zeiss, Germany) with a recording chamber which was connected to a gravity-driven flow system. Vibration was reduced by an anti-vibration table (TMC vibration control, USA). A Faraday cage was used to shield the work station from electromagnetic interference. All voltage clamp protocols and data collection were

accomplished with the use of an Multiclamp 700A amplifier/Digidata 1322A interface (Axon Instruments, USA). pCLAMP 9 software (Axon Instruments) was used to control stimulating pulses, data collection and processing.

The electrical signals from a cell were collected through an electrolyte-filled glass micropipette containing a Ag/AgCl recording electrode (a chlorinated silver wire) immersed in the pipette solution. This electrode was held by a pipette holder, which was connected to the recording headstage (a current-to-voltage converter, CV 7B, Axon Instruments). The headstage was in turn mounted on a micromanipulator (Display SM-5, Luigs & Neumann, Germany), which gave control and stability, permitting very fine control of axial excursions of the pipette. The bath solution was grounded through the bath electrode connected to the signal ground from the headstage.

The collected electrical signals from the cell were processed in the headstage and then sent to the patch clamp amplifier. Recorded currents were filtered at 5 kHz with a low-pass Bessel filter in the patch-clamp amplifier. Analog signals were digitized at a sampling rate of 4 kHz by the analog-to-digital converter (Digidata 1322A) before being analyzed on a personal computer, using pCLAMP9 software. Stored records were used for measuring current amplitudes, plotting the current traces, constructing current-voltage curve and fitting exponential time course, before being sent to a personal computer to display and store for later analyses.

Establishing whole-cell configuration

Experiments were performed within 1-2 days of cell preparation. By the 3rd day, the cell membranes were usually frail and cells were detached from coverslips. At the time of a patch clamp experiment, cover slip fragment with attached isolated cells was transferred out of the culture medium to the recording chamber smoothly perfused with control external solution at room temperature.

An internal solution-filled glass microelectrode was first immersed in the bath solution while a positive pressure was maintained within the pipette, to chase away dusts that may be present at the fluid surface, and to prevent mixing of external and internal solutions. Microelectrode resistance in the bath solution was determined and the junction potential (pipette offset) was compensated. Then the microelectrode was moved, by controlling the micromanipulator, to approach a chosen cell. Gentle suction was applied when the tip of the microelectrode touched the cell membrane, until a Gigaohm (GΩ) resistance seal was formed between the tip of the pipette and the cell membrane (cell-attached configuration). After the

gigaseal formation, the patch of membrane underneath the pipette was ruptured with a transient suction to obtain whole-cell configuration, where the pipette solution and the cell interior became contiguous.

After the whole-cell configuration was made, preset voltage pulses (see Voltage protocol) were applied through the Clampex program of pClamp 9. If the gigaseal was still stable, the bath solution was changed to a test solution. The current was recorded in the control solution before and after applying the test solutions (control and washout traces). Currents showing any notable run-down before drug (or test voltage pulses) application were discarded from analysis.

2.2.4. HEK current voltage protocol

To evoke whole-cell barium current in HEK293T cells, the membrane potential was clamped at the holding potential of -80 mV, which is the resting membrane potential. Then, cells were depolarized with 400 ms command pulses from -80 to voltages between -40 and $+60$ mV in 10 mV increments. The pulse intervals were 1 s each. A diagram representing the set of voltage pulses is shown in Fig. 9.
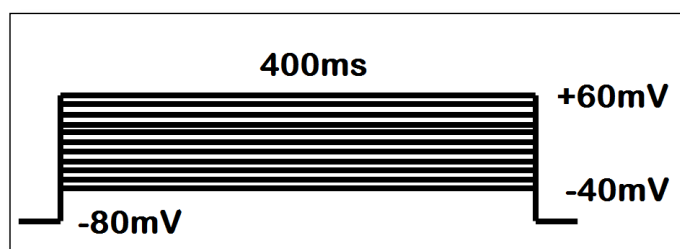
Figure 9. Voltage protocol for I_{Ca} recording in HEK293.

2.2.5. Cardiomyocyte current voltage protocol

I_{Ca} from CMs was stimulated by the voltage protocol in Figure 10. The cardiomyocytes were held at -80 mV to ensure complete recovery from inactivation of I_{Ca}. A prepulse was then applied to -40 mV to voltage inactivate Na^+ and any T-type Ca^{2+} channels that might be present. This was followed by a 200 ms long test pulse to between -40 and $+60$ mV in 10 mV increments to activate I_{Ca}. I_{Ca} was measured as the difference between the peak inward current and the current at the end of a 200 ms test pulse.
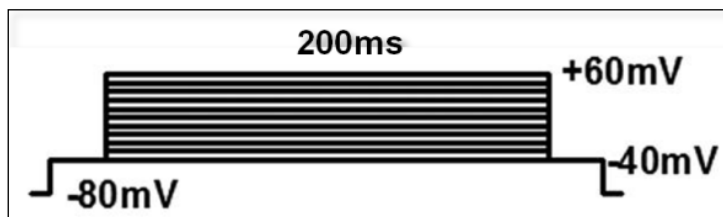
Figure 10. Votage protocol for I_{Ca} recording in CMs

Facilitation of I_{Ca} was measured during a triple pulse protocol with a 200 ms control pulse to 0 mV (I_1) followed by a 200 ms prepulse to +80 mV followed by a 200 ms test pulse to 0 mV (I_2) (Fig. 11). The extent of facilitation was calculated as the ratio of the peak current during I_2 and I_1 (I_2/I_1).
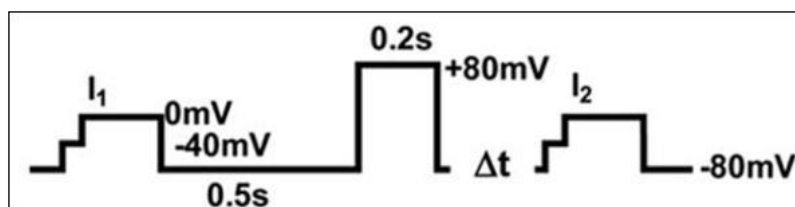
Figure 11. Voltage protocol for I_{Ca} facilitation recording

For measuring ***steady- state inactivation,*** CMs were stimulated by a twin pulse protocol (Fig. 12). A brief (30 ms) pulse to −40 mV preceding the test to 0 mV was used to inactivate the fast sodium current. The steady state inactivation was assessed using test depolarizations to 0 mV preceded by a set of prepulses clamped to various voltages between -70 and +10 mV for 2s. For analysis, fractions of current (I_2/I_1) were plotted against the prepulse voltage. $E_{0.5}$ was calculated after fitting the data sets with a Boltzmann equation.
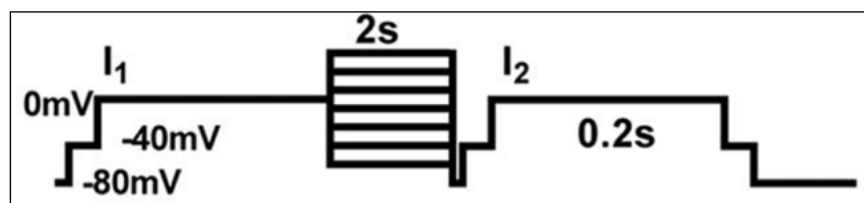
Figure 12. Voltage protocol for steady-state inactivation recording

Time course of ***recovery from inactivation*** of I_{Ca}, measured using twin-pulse protocol. Two rectangular depolarizing voltage pulses (I_1 and I_2) were delivered to 0 mV from the holding potential of -80 mV. A brief (30 ms) pulse to -40 mV preceding the test to 0 mV was used to inactivate the fast sodium current The duration of both pulse (I_1 and I_2) were 200 ms. The interpulse interval was gradually increased up to 100 ms. The peak current measured during the second pulse was normalized to that measured during the first one and these current ratios were plotted against the interpulse interval.
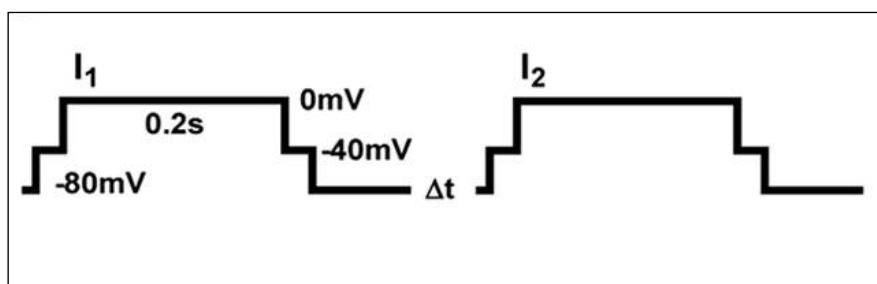
Figure 13. Voltage protocol for recovery from inactivation of I_{Ca}

Calcium-dependent inactivation was measured using the IV protocol (Fig. 10). After adjusting the baseline, peak amplitude was normalized. Time constant was calculated after fitting the data sets with 2 exponential functions.

Data plotting and statistical analysis was carried out using GraphPadPRISM 5.0 (GraphPad Software, Inc., La Jolla, USA).

2.3. Data analysis

Analysis of membrane currents was performed only in cells whose pipette seal resistance could be maintained at more than 1 GΩ throughout the recording. In addition, cells with excessive noise in the current traces and cells with rapid rundown were discarded.

Stored current traces were initially processed by the pCLAMP 9 program. First, the baseline current (during holding potential, before a pulse) was set at 0 pA. Current density was calculated by dividing the peak membrane currents by the cell capacitance, which is proportional to the cell membrane area, and reported in pA/pF. Data from each cell were used

to construct a current-voltage (I-V) curve by plotting current density (pA/pF) on the Y- axis against applied voltage (mV) on the X-axis, using Microsoft Excel or GraphPad Prism.

To compare the control and test conditions (i.e stimulation of I_{Ca} by isoproterenol), I_{Ca} was measured at a membrane potential of 0 mV (peak current amplitude) and is given as percentage of control (= 100%) before superfusion with isoproterenol. The percentage change of amplitude was calculated.

Time constants of I_{Ca} inactivation were obtained by a fit from the peak current to the current value at the end of the voltage pulse by a two-exponential function. All fits showed a correlation coefficient >0.98.

The relation between I_{Ba} and I_{Ca} current fraction remaining 100 ms after depolarization ($f100$) was calculated by the following equation:

$$f100 = \left(\frac{r100Ba}{r100Ca}\right) - 1$$

$f100$	=	the fractional current after 100 ms
$r100Ba$	=	the remaining I_{Ba} after 100 ms
$r100Ca$	=	the remaining I_{Ca} after 100 ms

The calculation and display of current traces, current amplitude and density conformed to the usual convention, i.e. inward currents are negative, outward currents are positive. The null hypothesis was rejected if p was < 0.05.

3. Results

3.1. $Ca_V1.2^{I1624E}$ channel mutation

It has been demonstated that CaM binding to the IQ motif of the $Ca_V1.2$ channel is necessary for CDI and CDF. The mutation of I1624 to Ala in the IQ motif resulted in ablation of CDI and a significant reduction of apoCaM binding to $Ca_V1.2$ in *Xenopus oocytes* (Zuhlke et al., 1999; Zuhlke et al., 2000). Whether I1624 residual also plays a prominent role in $Ca_V1.2$ regulation in whole, living organism remain to be determined. In this present work, we have tested this idea further in vivo.

First, we examined the effect of the I1624E mutation in HEK293T cells. α_1 subunits (WT or I1624E mutation) of $Ca_V1.2$ channels were co-expressed with β_2-N4 and $\alpha_2\delta$ subunits in HEK293T cells. Current were measured by stepwise depolarizing pulses in 10 mV intervals between -60 mV and +60 mV from a holding potential of -80 mV. Ba^{2+} was used as a charge carrier to enhance currents through Ca^{2+} channels as illustrated in Fig. 14A (WT) and Fig. 14B (I/E). The current density of I_{Ba} did not significantly differ between WT and I/E (Fig. 14C and D). However, the decay of I_{Ba} through WT was slower than that of I/E (Fig. 14A and B). Currents carried by Ba^{2+} and Ca^{2+} ions were recorded in the same HEK 293T cell to assess the effects of Ca^{2+} entry on the decline of current during a standard depolarizing pulse to +20 mV. Fig.14E and F compares the Ca^{2+} dependence of current decay in I/E mutation with that found in WT channels. The difference between Ca^{2+} and Ba^{2+} as charge carrier was prominent with the WT channel but was barely detectable with I/E.
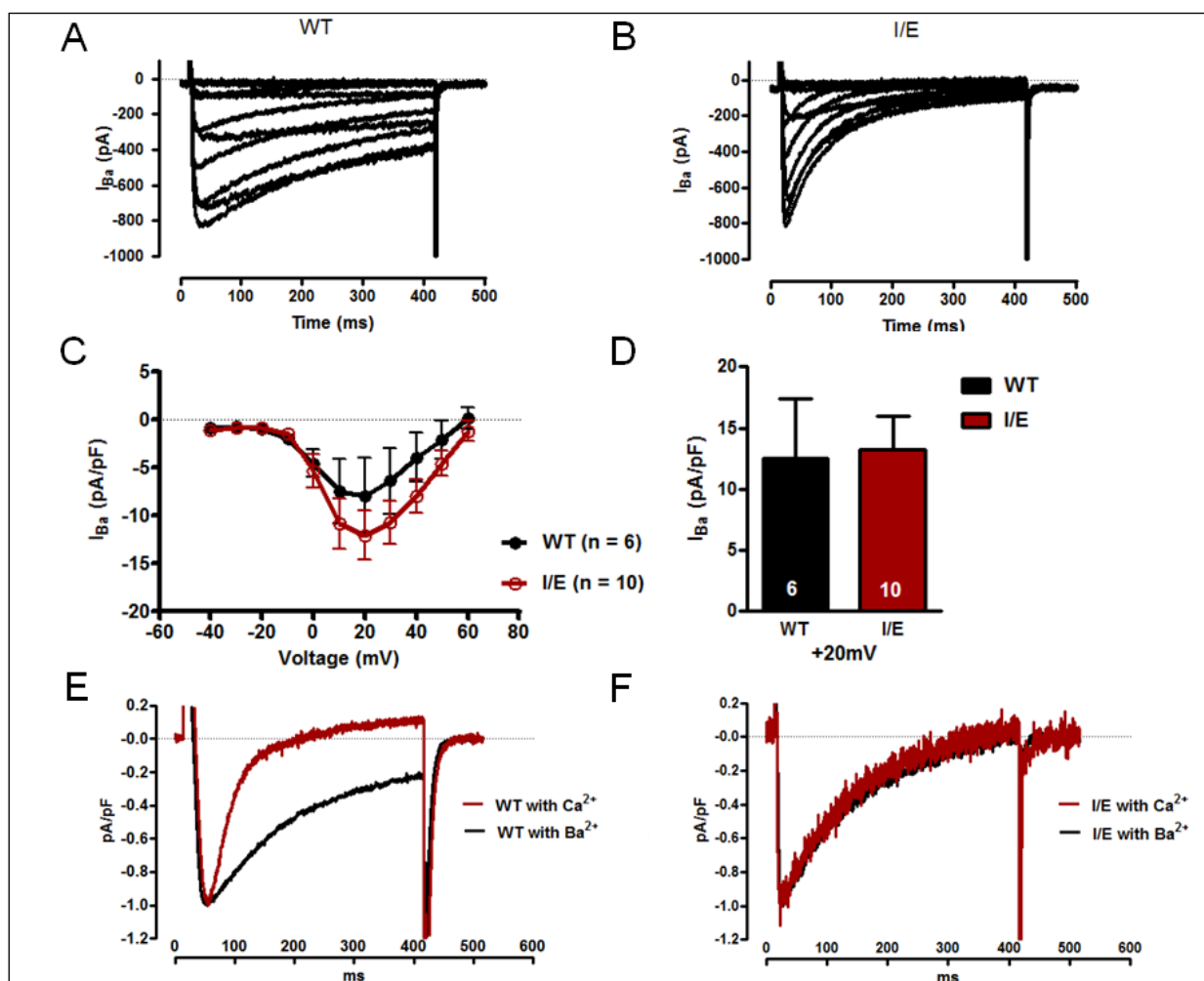
Figure 14. $Ca_V1.2^{I1624E}$ mutation in HEK 293 cells affects inactivation. A and B, representative examples for I_{Ba} of WT (A) and I/E mutation (B). C, normalized current-voltage (I-V) curve for WT (black) or I/E (red) are not significantly different. D, current density of I_{Ba} elicited at +20 mV. E and F, representative currents recorded from WT (E) and I/E (F) during test pulses of holding potential from -80 to +20 mV. I_{Ca} was scaled to peak I_{Ba}. (modified from Poomvanicha et al., 2011)

Further investigation was made in vivo using transgenic gene knock-in techniques. This knock-in mouse line has a mutation that changes Isoleucine at position 1624 of the *CACNA1C* gene to glutamate. The resulting homozygous mice (genotype $Ca_V1.2^{I1624E}$ on both alleles) were not viable. Therefore, we crossbred heterozygous $Ca_V1.2^{+/I1624E}$ mice with mice that expressed the floxed $Ca_V1.2$ gene and Cre recombinase under the α-myosin heavy chain promoter (MerCreMer), allowing tissue-and time-dependent inactivation of the $Ca_V1.2$ gene by tamoxifen induced Cre recombinase. The mutation in the resulting I/E mice (genotype $Ca_V1.2^{-/I1624E}$) was confirmed by genomic sequencing (Fig. 15A). I/E mice had a reduced life span and died within 3 weeks after treatment with tamoxifen (Fig. 15B). Western blot analysis of cardiac muscle using anti-$Ca_V1.2$ antibody detected reduced protein levels in the ventricles of I/E mice compared with littermatched Ctr mice (genotype $Ca_V1.2^{-/+}$) at day 10 after tamoxifen injection (Fig. 15C).
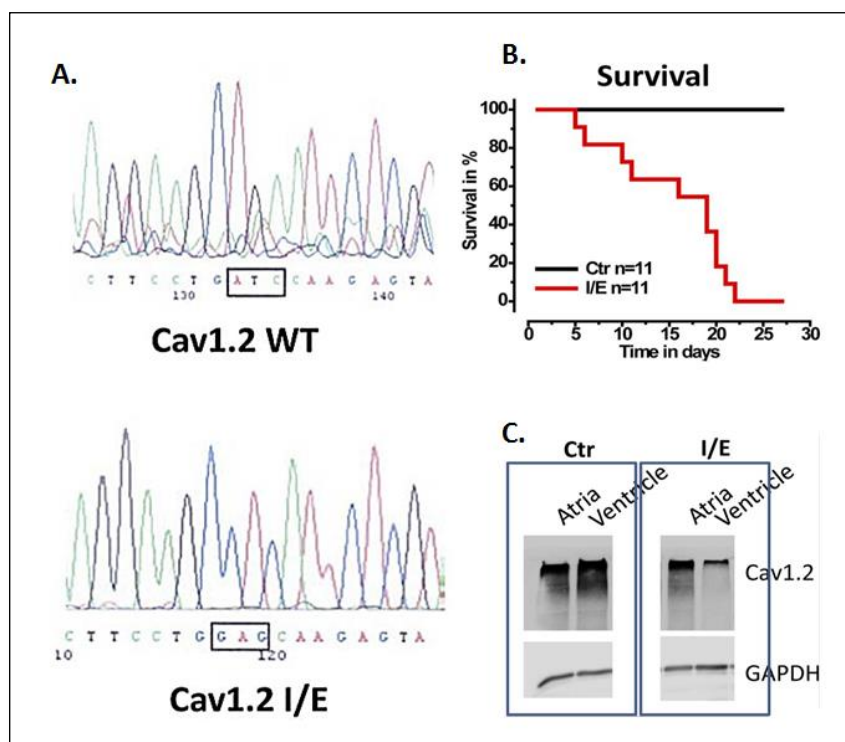
Figure 15. Mutation of Isoleucine 1624 to Glutamine. A, sequence analysis of genomic DNA in the region coding for Ile-1624 from one WT $Ca_V1.2$ and one $Ca_V1.2^{I1624E}$ mouse. B, survival curve of $Ca_V1.2^{I1624E}$ mouse and littermatched Ctr mice. $t = 0$ represents the start of the treatment of the mice with tamoxifen. C, immunoblot of cardiac membrane preparations. This experiments were performed by Anne Blaich (modified from Poomvanicha et al., 2011)

To test the physiological significance of the mutation of Ile to Glu in the cardiac $Ca_V1.2$ channel, cardiomyocytes (CMs) were isolated 5 days after the final tamoxifen injection following a modified AfCS protocol PP00000125. Fig. 16 shows representative photographs of mouse ventricular cardiomyocytes. Features typical of acutely isolated (Day0) cells were the rod shape with rectangular "stepped" ends and clear cross-striations (Fig. 16; red arrow). After 1 day, the cells were still rod-shaped with clear cross-striations; however, the ends of the cells started to become slightly rounded in appearance (Fig. 16; blue arrow) and progressively more rounded over subsequent days of culture. Rounding at the cell ends may be due to ultrastructural reorganisation (Mitcheson et al., 1998). Current measurements were only performed on Ca^{2+} tolerant rod-shaped, rectangular ends with clear cross striations myocytes (Day 0 – Day 1) (Fig. 16; red arrow)
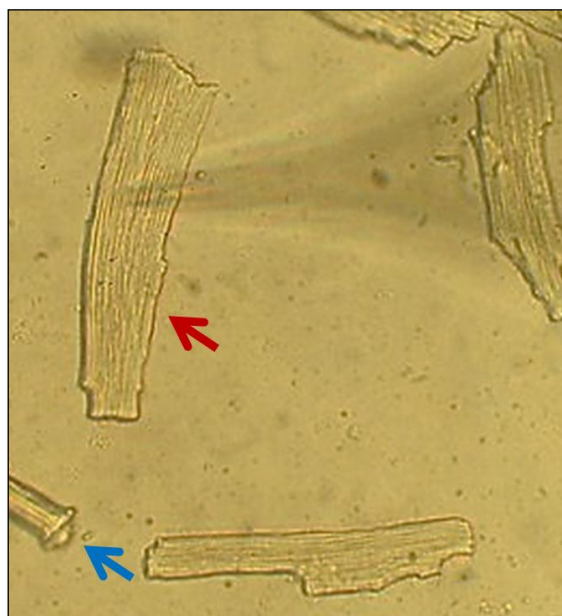
Figure 16. Adult mouse ventricular myocytes. Myocytes were photographed under an inverted microscope (40×) after 24 hours in culture.

I_{Ca} was recorded in isolated ventricular CMs from Ctr and I/E mice using the patch-clamp technique (Fig. 17A and B). Cell capacitance was similar in CMs from I/E and Ctr mice (221 ± 14 pF, n = 52 and 213 ± 10 pF, n = 60 respectively) (Fig. 17E). The current density of I_{Ca} was significantly reduced in CMs from I/E mice versus CMs from Ctr mice (Fig. 17D). These findings indicate expression of $Ca_V1.2^{I1624E}$ channels in the membrane of CMs from I/E mice and an even functional availability of these channels.
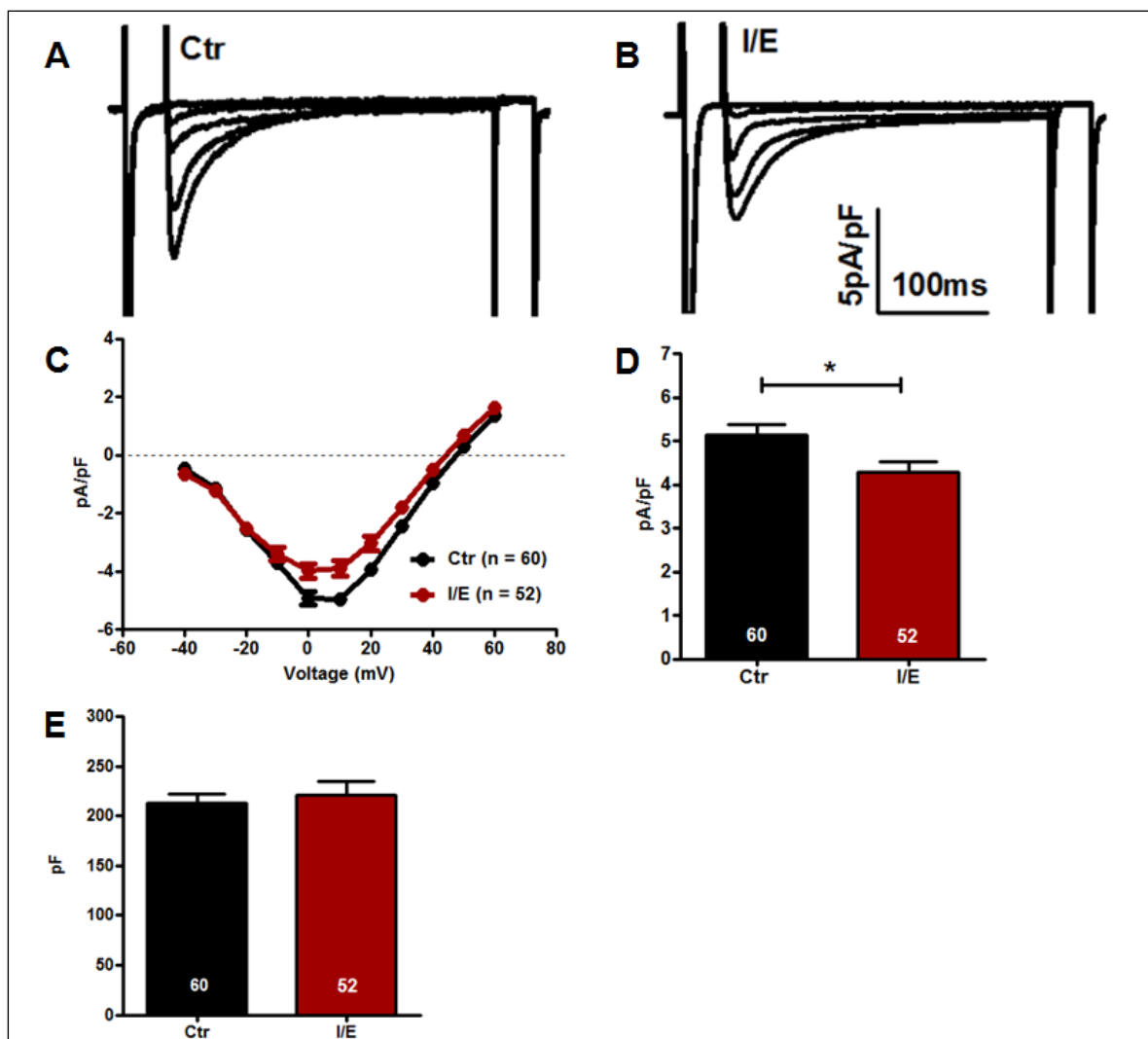
Figure 17. I_{Ca} in ventricular CMs from I/E mice. A and B, original recordings of I_{Ca} in a CM from a Ctr mouse (A) and from an I/E mouse 10 days after tamoxifen injection (B). Traces are corrected for cell capacitance. C, current-voltage relation of I_{Ca}. Peak current density is plotted against the voltage pulse. D, The bar graph summarizes current densities for Ctr and I/E. E, The bar graph summarizes CM size (pF). Data points represent means ± S.E.M. Data sets from Ctr and I/E mice were statistically different as revealed by two-way analysis of variance, *, $p < 0.05$. (modified from Poomvanicha et al., 2011)

CaM regulates CDF and CDI of $Ca_V1.2$. Facilitation is mainly due to activation of multifunctional CaMKII (Anderson et al., 1994; Yuan and Bers, 1994). Inhibition of CaMKII has been shown to influence recovery from inactivation and steady-state inactivation of I_{Ca}. In accordance with these studies, recovery from inactivation of I_{Ca} was slowed down in CMs from I/E mice compared with CMs from Ctr mice (Fig. 18A). Fits of the recovery from inactivation by one-exponential functions revealed time constants of 54 ms (Ctr) and 72 ms (I/E). Likewise, the steady-state inactivation curve of I_{Ca} was shifted to the left in CMs from I/E mice compared with CMs from Ctr mice (Fig. 18B). Using the Boltzmann equation, the voltage for half-maximal inactivation was calculated to be -16 mV (Ctr) and -27 mV (I/E). KN-93, a CaMKII inhibitor, (1 μM) did not influence recovery from inactivation and steady-state inactivation in CMs from I/E mice. These results indicate that the I/E mutation in the $Ca_V1.2$ channel mimics the effects of CaMKII inhibitors on $Ca_V1.2$ channel properties.
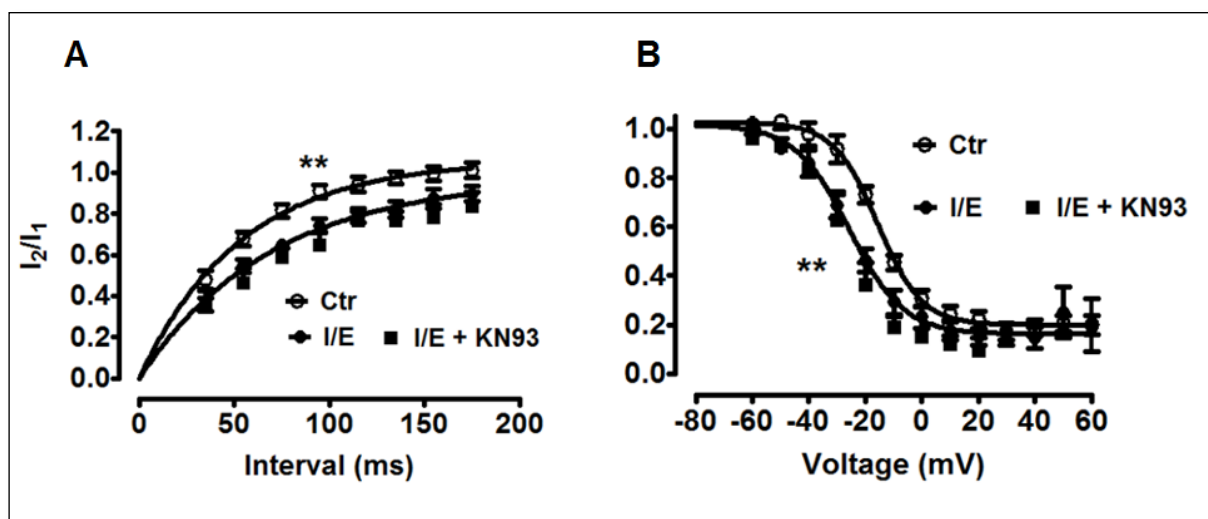
Figure 18. Analysis of I_{Ca} in ventricular CMs from I/E mice. A, recovery from inactivation of I_{Ca}. Data points represent means ± S.E.M with n = 13 for Ctr, n = 14 for I/E mice, and n = 3 for I/E mice with KN-93 (1 μM). Data sets from Ctr and I/E mice were statistically different as revealed by two-way analysis of variance. B, steady-state inactivation of I_{Ca}. Data points represent means ± S.E.M. $E_{0.5}$ was calculated to be -16 ± 1 mV (n = 11) for Ctr mice and -27 ± 4 mV (n = 17) for I/E mice after fitting the data sets with a Boltzmann equation. Some data points from I/E mice (n = 3) were obtained in the presence of KN-93 (1 μM). Data sets from Ctr and I/E mice were statistically different as revealed by two-way analysis of variance, **, $p < 0.01$. (modified from Poomvanicha et al., 2011)

Several studies have shown that facilitation of $Ca_V1.2$ currents depends on CaM/CaMKII (Hudmon et al., 2005; Lee et al., 2006). Facilitation of I_{Ca} was almost abolished in CMs from I/E mice (Fig. 19A and B). As suggested previously (Blaich et al., 2010) facilitation depended on CaMKII. Inhibition of CaMKII activity by KN-93 (1 μM) abolished facilitation in CMs from Ctr mice but had no effect in CMs from I/E mice, supporting a specific effect of KN-93 in Ctr CMs (Fig. 19C). Taken together, these results support the notion that the I/E mutation of the $Ca_V1.2$ channel abolishes CaM/CaMKII-mediated effects on facilitation.
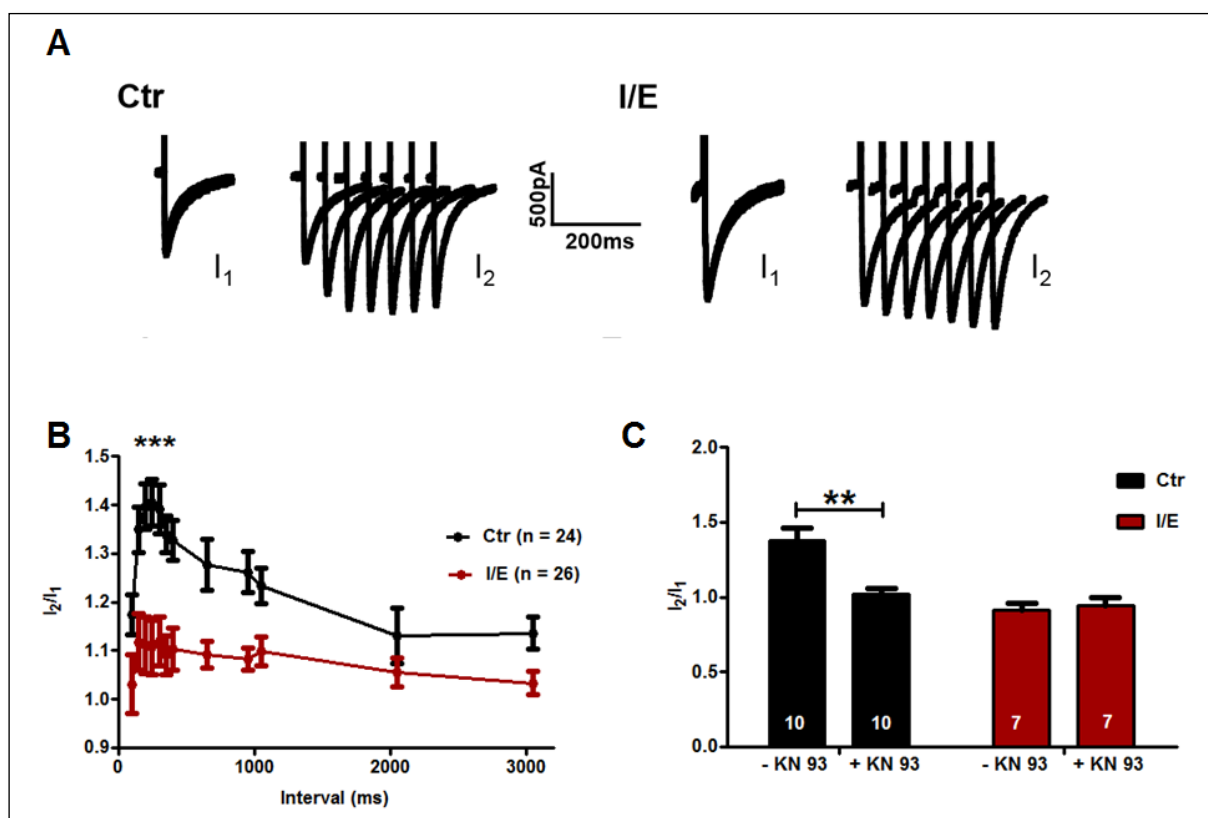
Figure 19. Facilitation of I_{Ca} in ventricular CMs from I/E mice. A, original recordings of I_{Ca} in a CM from a Ctr mouse (left panel) and from an I/E mouse (right panel). B, Facilitation of I_{Ca}. Fractions of current (I_2/I_1) are plotted against the interval duration (Δt). Data points represent means ± S.E.M. with n = 24 for Ctr and n = 26 for I/E mice. Data sets from Ctr and I/E mice were statistically different as revealed by two-way analysis of variance, ***$p<0.001$. C, effect of KN-93 (1 μM) on peak facilitation of I_{Ca} in CMs from Ctr and I/E mice. Error bars represent means ± S.E.M. Numbers indicate the number of experiments. Each experiment was performed with and without KN-93. **, $p < 0.01$ (modified from Poomvanicha et al., 2011)

In general, CDI of I_{Ca} is attenuated by the use of Ba^{2+} as charge carrier or by high concentrations of intracellular Ca^{2+} buffers. Consequently, we recorded current through L-type Ca^{2+} channels in the same CMs using Ca^{2+} and Ba^{2+} as the charge carrier. As expected, the fast component of inactivation observed with Ca^{2+} was slowed down with Ba^{2+} as the charge carrier, resulting in poorly inactivating curents in CMs from Ctr mice (Fig. 20A and B). In contrast, a fast component of inactivation was still present in CMs from I/E mice with both Ca^{2+} and Ba^{2+} as the charge carrier (Fig. 20B and C).
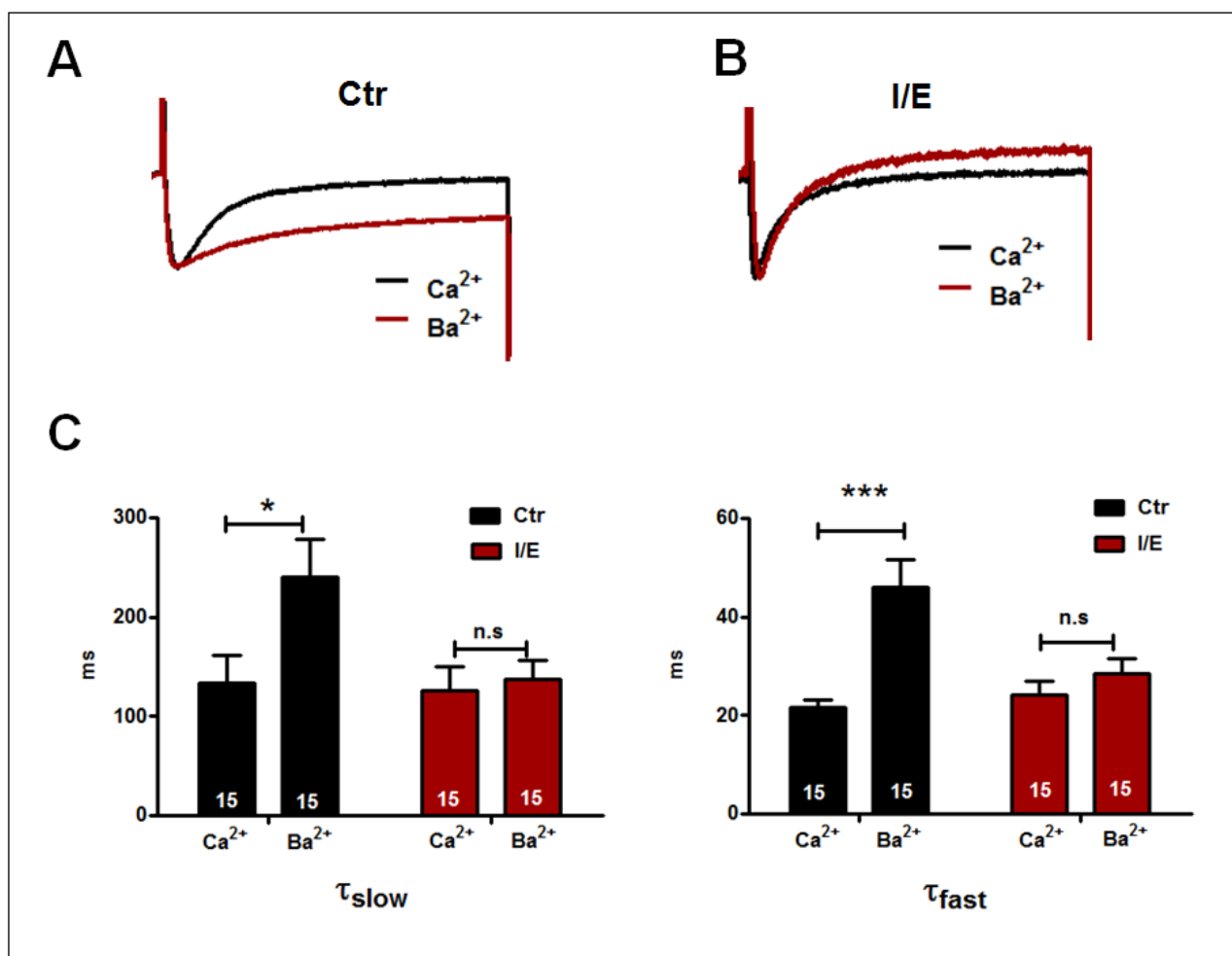
Figure 20. Inactivation of I_{Ca} in ventricular CMs from I/E mice. A and B, original recordings of I_{Ca} and I_{Ba} in a CM from a Ctr mouse (A) and from an I/E mouse (B), activated by a voltage pulse to 0 mV. Currents were normalized to the maximal inward current. Both displayed recordings were obtained from the same CM. C, time constants of current inactivation (slow component in left panel and fast component in right panel). Error bars represent means ± S.E.M. *, $p < 0.05$, *** $p < 0.001$ (modified from Poomvanicha et al., 2011)

To assess the effect of Ca^{2+} dependent inactivation in a more quantitative fashion, we measured residual Ca^{2+} and Ba^{2+} currents at 100 ms, expressed them as a fraction of peak I_{Ca} and I_{Ba}, and calculated the ratio as the Ca^{2+} dependent fraction, the f_{100} value. The change in kinetics is also observed by the f_{100} value. The f_{100} value decreased significantly ($p < 0.003$) from 1.65 ± 0.38 (n = 9) in Ctr CMs to 0.53 ± 0.14 (n = 16) in I/E CMs (Fig. 21) and indicated that, in the presence of Ba^{2+}, inactivation of the $Ca_V1.2^{I1624E}$ channel was as fast as that in the presence of Ca^{2+}. These results confirm that the $Ca_V1.2^{I1624E}$ channel always has the "CDI kinetics" regardless of the permeating ion.
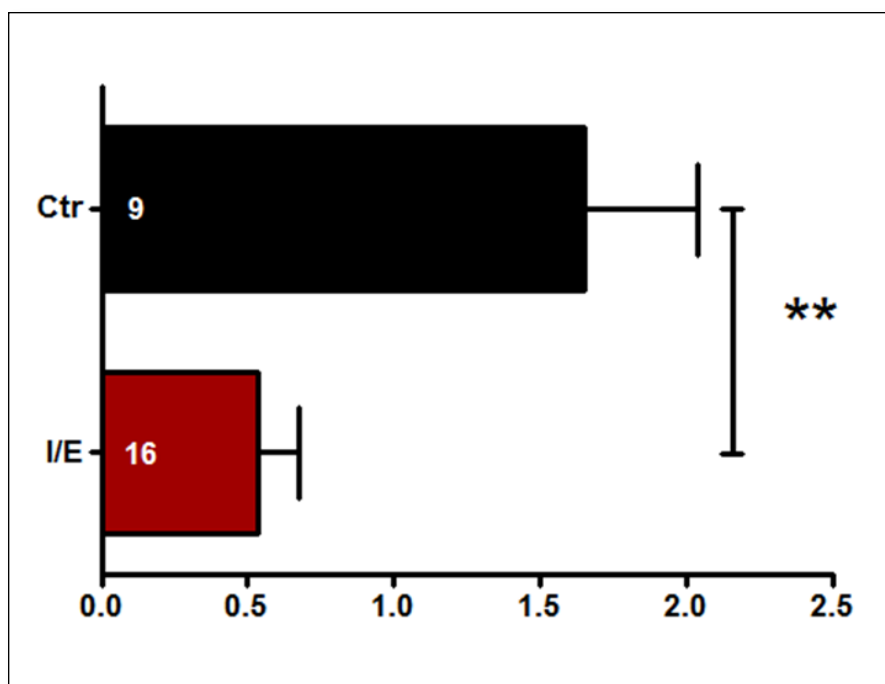
Figure 21. Inactivation of I_{Ca} in ventricular CMs from I/E mice. f_{100} values for I_{Ba} / I_{Ca} in Ctr and I/E CMs. f_{100} is the fraction of current remaining 100 ms after depolarization calculated by the ratio of I_{Ba} / I_{Ca} present at 100 ms after depolarization. Error bars represent means $\pm$ S.E.M. **, $p < 0.003$ (modified from Blaich et al., 2012)

Next, we compared the effects of buffering intracellular Ca^{2+} by the Ca^{2+} chelators EGTA and BAPTA. BAPTA has been shown to bind Ca^{2+} more efficiently than EGTA, thus attenuating CDI of I_{Ca}. Indeed, inactivation of I_{Ca} was slowed down in BAPTA- versus EGTA-dialyzed CMs from Ctr mice (Fig. 22A and C). However, inactivation of I_{Ca} was not slowed down in BAPTA- versus EGTA-dialyzed CMs from I/E mice (Fig. 22B and C), in which the fast component of inactivation was even faster in BAPTA-versus EGTA-dialyzed CMs. Slow components of inactivation were not different in CMs from Ctr and I/E mice (Fig. 22C, right panel). These results suggest that the mutation of Ile to Glu at position 1624 of the $Ca_V1.2$ channel abolishes the effects of Ca^{2+} on inactivation of I_{Ca}, most likely because the channel has already been transformed to a phenotype mimicking CDI.
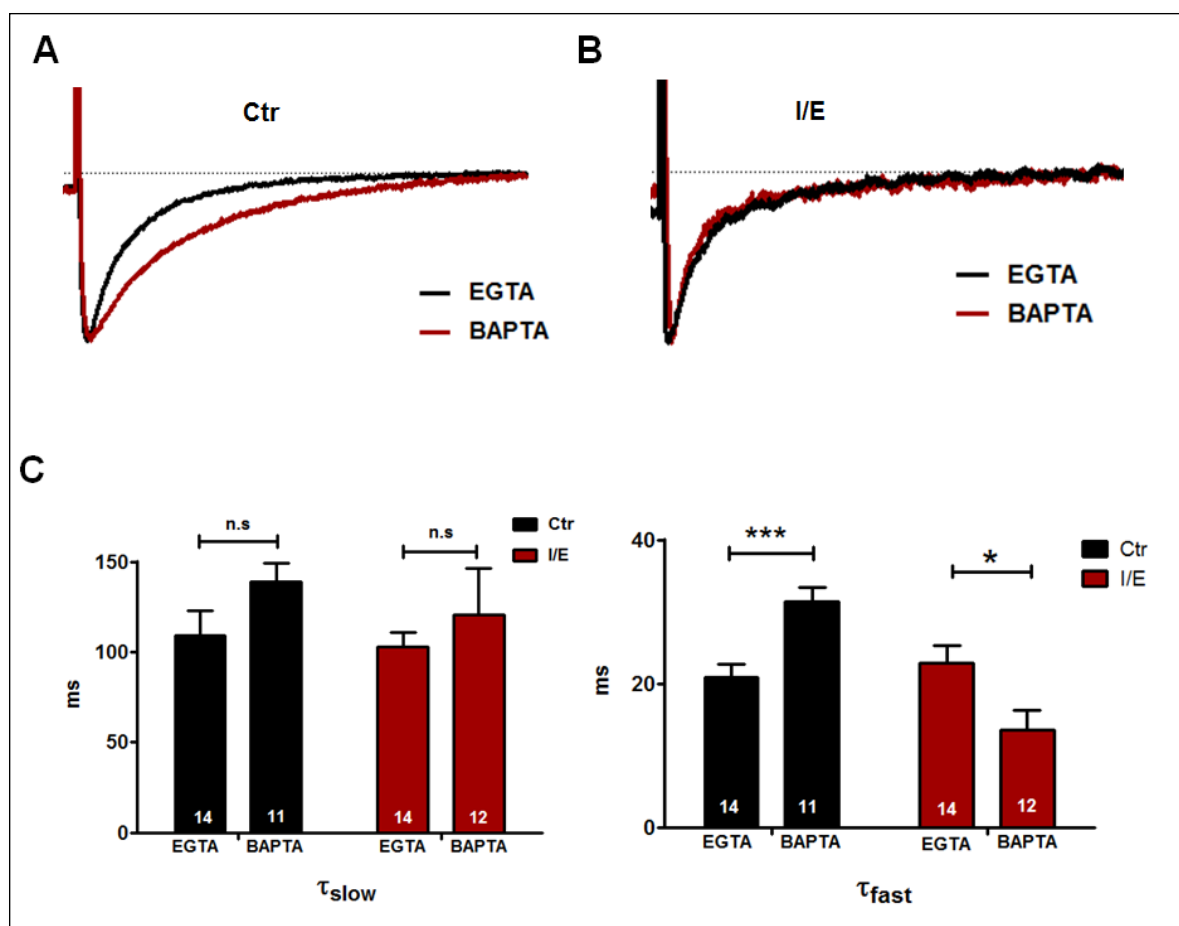
Figure 22. Inactivation of I_{Ca} in ventricular CMs from I/E mice. A and B, original recordings of I_{Ca} in CMs from Ctr mice and from I/E mice, respectively, activated by a voltage pulse to 0 mV. Currents were normalized to the maximal inward current. Cells were dialyzed with 10 mM BAPTA or 10 mM EGTA. C, time constants of current inactivation (slow component in left panel and fast component in right panel). Error bars represent means ± S.E.M. *, $p < 0.05$, ***, $p < 0.001$ (modified from Poomvanicha et al., 2011)

3.2. $Ca_V\beta_2$-N4 mutation

Phosphorylation of the cardiac β subunit ($Ca_V\beta_2$-N4) of the $Ca_V1.2$ L-type Ca^{2+} channel complex has been proposed as a mechanism for regulation of L-type Ca^{2+} channels by various protein kinases including PKA, CaMKII, Akt/PKB and PKG. To test this hypothesis directly *in vivo*, we generated a knock-in mouse line with targeted mutation of the $Ca_V\beta_2$-N4 by insertion of a stop codon after proline 501 in exon 14 (mouse sequence *Cacnb2*; βStop mouse). This mutation prevented translation of the $Ca_V\beta_2$-N4 C terminus that contains the relevant phosphorylation sites for the above protein kinases. The mutation in βStop mice was confirmed by Southern blotting and genomic sequencing (Fig. 23A). βStop mice were viable, fertile, and reproduced in a 1:2:1 Mendelian ratio. Western blot analysis of heart and brain membrane fraction showed no alteration in $Ca_V1.2$ expression. The expression of the C-terminal truncated $Ca_V\beta_2$-N4 protein was confirmed by the C-terminal binding $Ca_V\beta_{2v2}$ antibody and the N-terminal binding antibody $Ca_V\beta_2$-N4/1195. The C-terminal binding $Ca_V\beta_{2v2}$ antibody detected the 75-kDa WT $Ca_V\beta_2$-N4 protein, but not the truncated $Ca_V\beta_2$-N4 protein (Fig. 23B), whereas the N-terminal binding $Ca_V\beta_2$-N4/1195 antibody detected both the truncated $Ca_V\beta_2$-N4 protein (58 kDa) and the WT protein (75kDa) (Fig. 23C). The results show that the βStop mouse expressed the truncated $Ca_V\beta_2$-N4 protein that missed the reported phosphorylation sites.
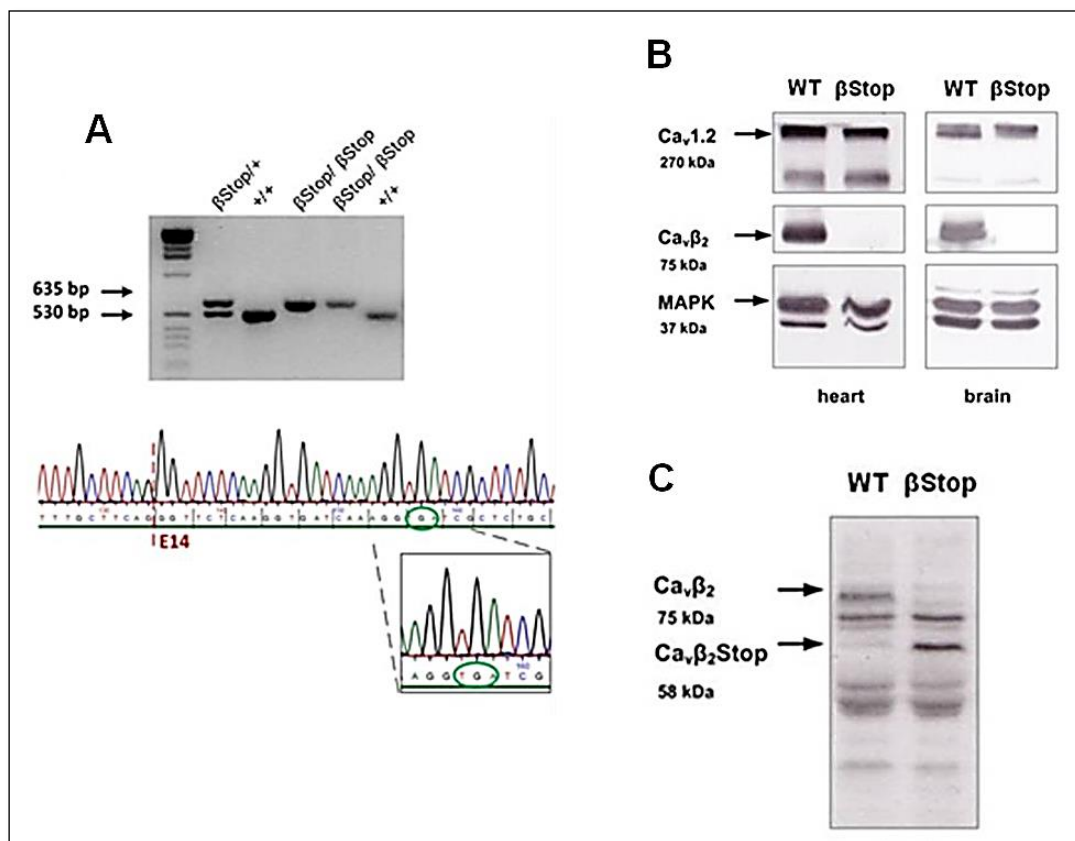
Figure 23. Generation analysis of βStop mice. A, genotyping of a $Ca_V\beta_2$Stop litter (635-bp βStop band, 530-bp WT band) and sequence analysis of the βStop knock-in mice. The sequence shows exon 14 of a homozygous βStop offspring. The stop mutation is in-frame within exon 14. PCR primers bind 5′ and 3′ of the loxP site remaining after Cre recombination. The primers amplify a 635-bp fragment in $Ca_V\beta$Stop DNA (including one loxP site after Cre recombination) or a 530-bp fragment in WT DNA (without loxP site). B and C, Western blot analysis of heart and brain membrane fractions. B, $Ca_V1.2$ and $Ca_V\beta_2$ protein expression. The truncated $Ca_V\beta_2$ protein is not detected by the common $Ca_V\beta_{2v2}$ antibody which binds C-terminal of the Stop mutation; loading control, MAPK. C, detection of the $Ca_V\beta_2$Stop protein with the N-terminal binding $Ca_V\beta_{2v2}$-N4/1195 antibody. These results were performed by Julia Brandmayr (modified from Brandmayr et al., 2012)

To study the effect of the $Ca_V\beta_2$-N4 truncation for cardiac β-adrenergic regulation, patch clamp experiments were carried out on isolated CMs. Isolated CMs of either genotype had normal size (CtrβStop, 170 ± 14 pF, n = 13; βStop, 149 ± 8 pF, n = 13) (Fig. 24A), normal IV relation (Fig. 24B) and normal I_{Ca} density at +10 mV (CtrβStop, 3.39 ± 0.2 pA/pF, n = 13; βStop, 3.01 ± 0.2 pA/pF, n = 13) (Fig. 24C)
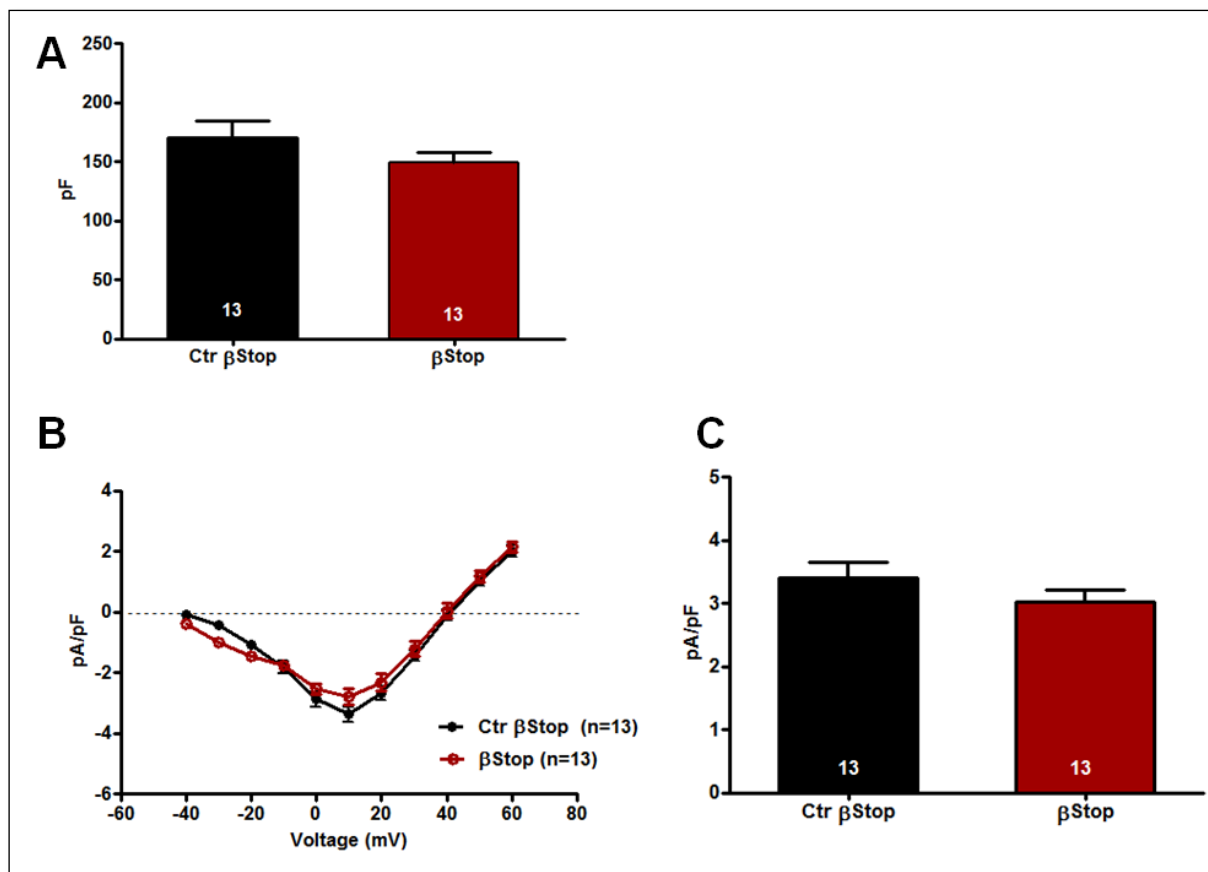
Figure 24. $I_{Ca,}$ in ventricular CMs from βStop mice. A, bar graph display cell capacitance. Electrical capacitance of the cell membrane was measured by patch-clamp techniques. The cell membrane capacitance is propotional to the surface area with a constant of 1 µF/cm^2 B, current-voltage relation of I_{Ca}. Peak current density is plotted against the voltage pulse. C, The bar graph summarizes current densities for CtrβStop and βStop. Data points represent means $\pm$ S.E.M. (modified from Brandmayr et al., 2012)

Basal properties of the $Ca_V1.2$ current were unaffected as expected from the report that deletion of the *CACNB2* gene in the adult heart has minimal effects on I_{Ca} (Meissner et al., 2011). Further analysis showed normal half-maximal activation constants (CtrβStop, -16.3 ± 1.7 mV, n = 8; βStop, -14.1 ± 0.9 mV, n=9) (Fig. 25A), normal half-maximal steady state inactivation ($V_{0.5}$: CtrβStop, -18.2 ± 1,6 mV, n = 3; βStop, -18.7 ± 1.2 mV, n = 5) (Fig. 25B), and normal half-maximal recovery time from inactivation ($\tau_{1/2}$: CtrβStop, 135.3 ms, n = 6; βStop, 147.6 ms, n = 6) (Fig. 25C)
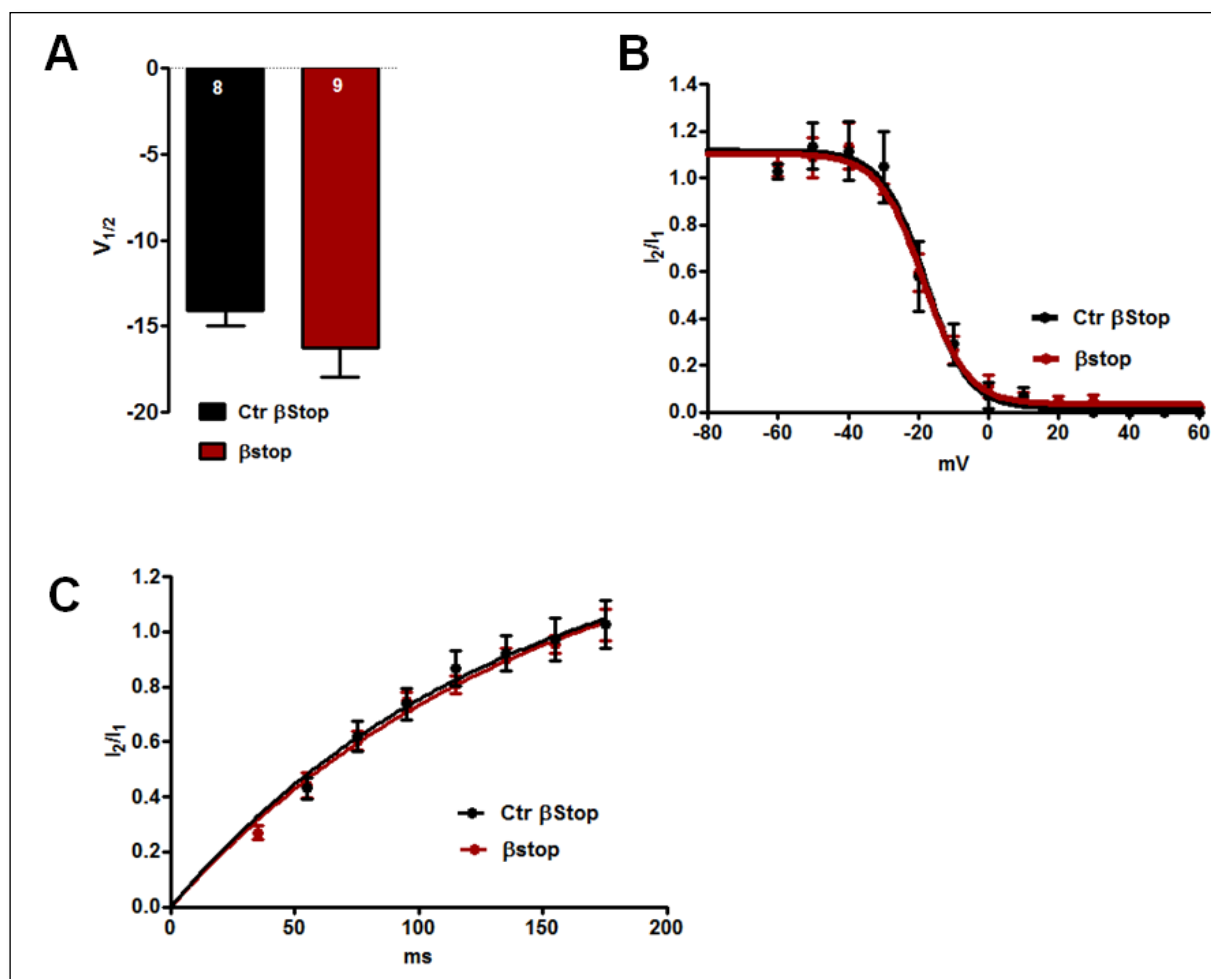
Figure 25. Analysis of I_{Ca} in ventricular CMs from βStop mice. A, bar graph of the mean time constant of current activation. B, steady-state inactivation of I_{Ca}. $E_{0.5}$ was calculated after fitting the data sets with a Boltzmann equation. C, recovery from inactivation of $I_{Ca.}$ Data points represent means ± S.E.M. (modified from Brandmayr et al., 2012)

It is widely accepted that CDF is caused by activation of CaMKII followed by phosphorylation of a component of the $Ca_V1.2$ channel complex. Recently, our group reported that CDF requires phosphorylation of $Ca_V1.2$ at $Ser^{1512/1570}$ (Blaich et al., 2012). In contrast, Colbran and co-worker (Grueter et al., 2006) reported that phosphorylation of $Ca_V\beta_2$-N4 by CaMKII at Thr^{500} modulated CDF. Because Thr^{500} was not present anymore in the βStop protein, we tested whether or not the truncation of the $Ca_V\beta_2$-N4 C terminus might affect I_{Ca} facilitation. CDF was not affected by the truncation of the $Ca_V\beta_2$-N4 protein (Fig. 26), suggesting that phosphorylation of the $Ca_V\beta_2$-N4 subunit is not a necessary prerequisite to induce CDF under basal conditions.
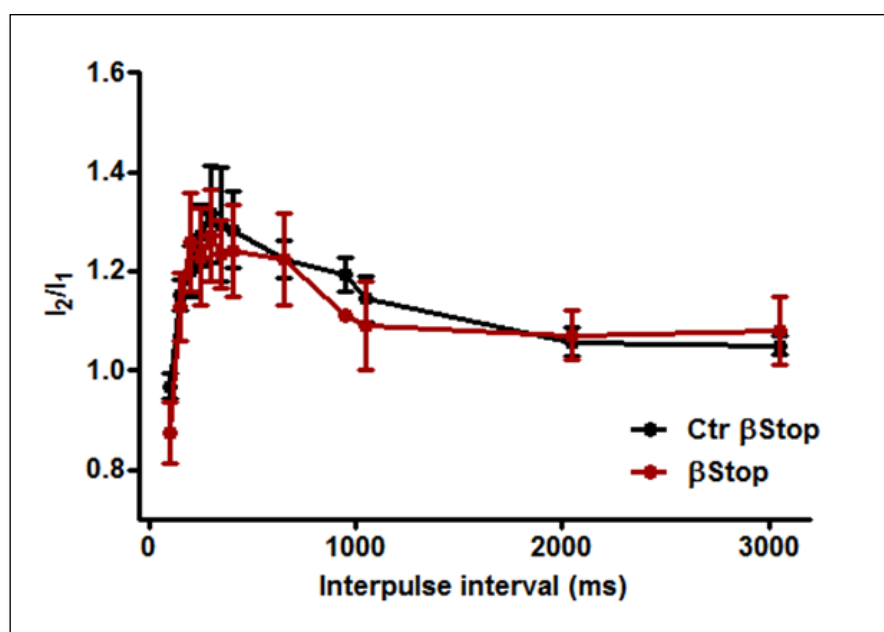
Figure 26. Facilitation of I_{Ca} in ventricular CMs from βStop mice. Facilitation of I_{Ca} unchanged CDF in Ctr βStop (n = 5) and βStop CMs (n = 8). (modified from Brandmayr et al. 2012)

It has been postulated that $Ca_V\beta_2$-N4 $Ser^{479/480}$ is PKA phosphorylated (Gerhardstein et al., 1999). Whether this site is required for β-adrenergic stimulation of $Ca_V1.2$ has been questioned. The effect of β-adrenergic agonist on the βStop mouse was further investigated.

Telemetric ECG measurement of heart rate (HR) and activity revealed no differences in CtrβStop and βStop mice (Fig. 27A). Both genotypes showed a typical cardiac response to isoproterenol and phenylephrine administration with an increase and a drop in HR, respectively (Fig. 27B). Fractional shortening (FS) was identical in CtrβStop and βStop. Isoproterenol doubled FS in both genotypes (Fig. 27C).
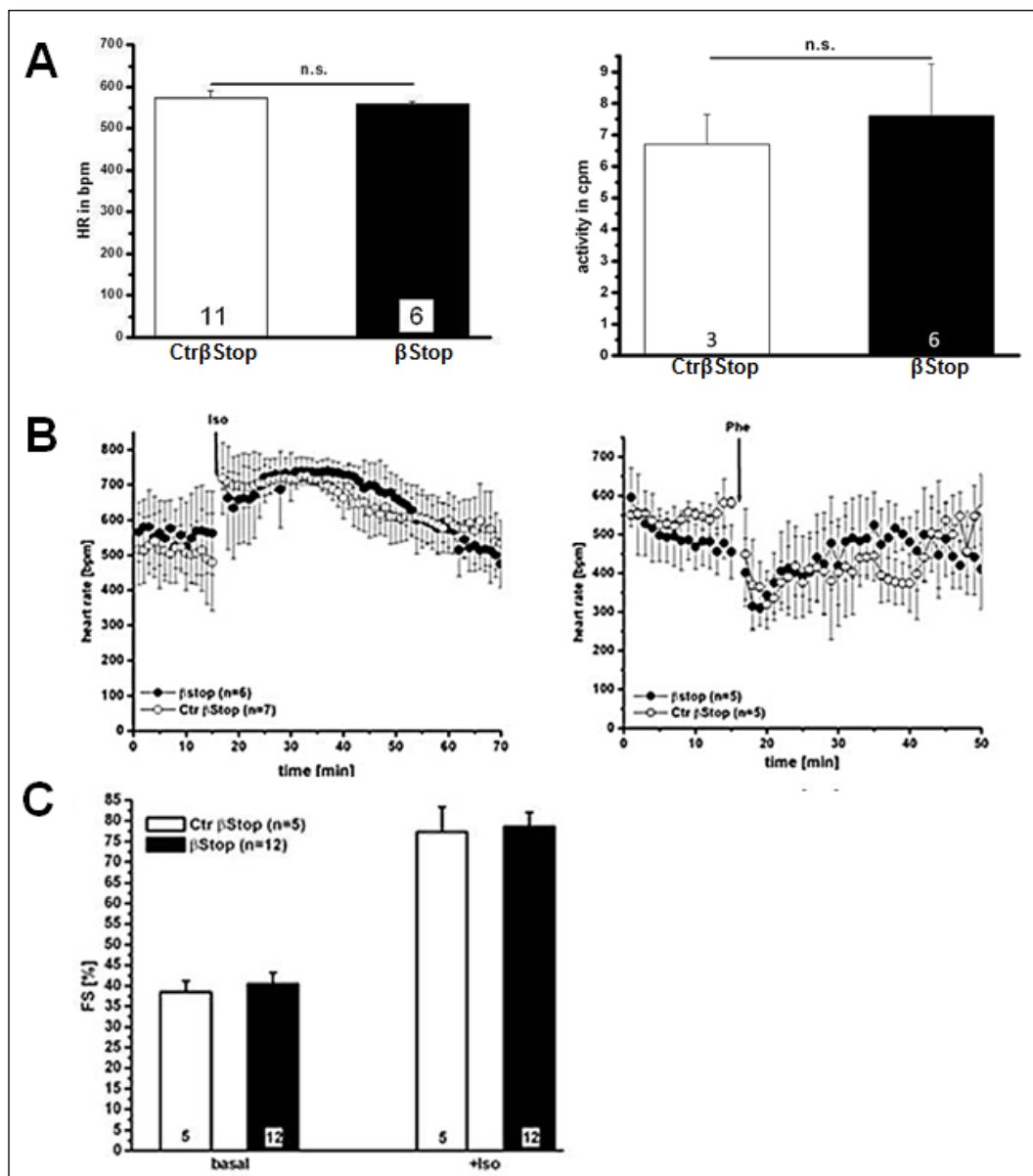
Figure 27. βStop mutation does not prevent positive inotropic heart regulation. A, heart rate is measured as beats per min (bpm) and activity as counts per min (cpm). Both values are obtained by ECG recording (DSI ETA-F20 transmitter) in awake, freely moving animals. B, normal regulation of beating frequency by isoproterenol (0.1 mg/kg of body weight intraperitoneally) and phenylephrine (0.3 mg/kg of body weight intraperitoneally). C, FS is unchanged in βStop mice before and after isoproterenol administration (0.1 mg/kg of body weight intraperitoneally). This experiment was performed by Anne Blaich (modified from Brandmayr et al., 2012)

In agreement with the ECG results, isoproterenol stimulated I_{Ca} of Ctr βStop and βStop CMs to the same level. Representative current traces for βStop CMs are shown in Fig. 28A and B. Isoproterenol treatment increased I_{Ca} in CtrβStop CMs by 193 ± 25% and in βStop CMs by 180 ± 24% (Fig. 28C). Furthermore, there was no change in the slow or fast component of inactivation either with or without isoproterenol stimulation (Fig. 28D). The fast component of inactivation describes Ca^{2+}-dependent inactivation (CDI), the slow component the voltage-dependent inactivation. Neither inactivation pathway is affected by the C-terminal truncation of the $Ca_V\beta_2$-N4 protein. These data indicate that the putative PKA phosphorylation sites $Ser^{479/480}$ of the $Ca_V\beta_2$-N4 subunit are not necessary to observe the positive inotropic β-adrenergic regulation of the heart muscle.
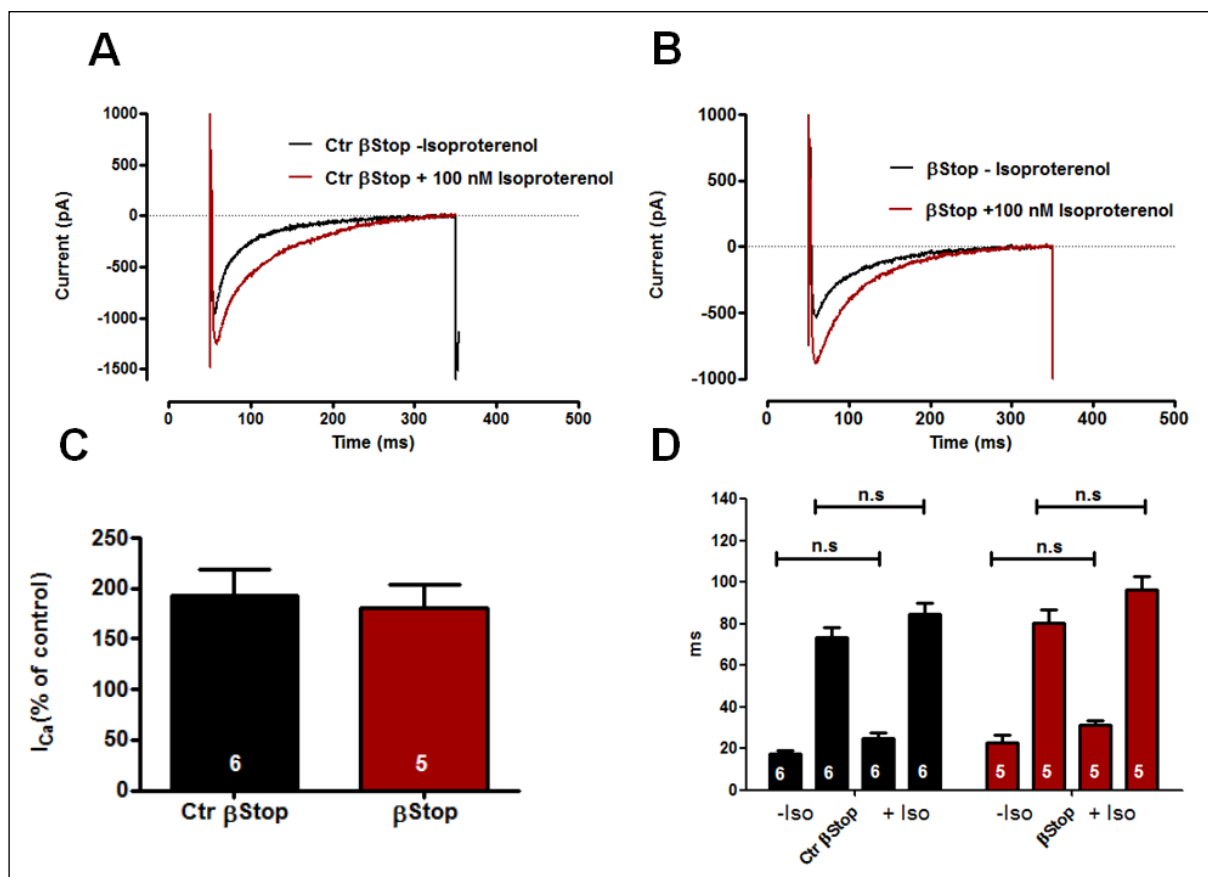
Figure 28. Analysis of I_{Ca} from CtrβStop and βStop CMs. A and B, representative current traces ± isoproterenol (100 nM) from CtrβStop (A) and βStop (B). C, statistics of isoproterenol (100 nM) stimulation of I_{Ca} in CtrβStop and βStop CMs. D, Bar graphs summarizing the comparisons of the time course of inactivation (modified from Brandmayr et al., 2012)

3.3. S1928 and $Ca_V\beta_2$-N4 mutation

The negative experiments from the βStop project raised the possibility that the positive inotropic effect was mediated by phosphorylation of both the $Ca_V1.2$ and $Ca_V\beta_2$-N4 subunit. We tested this hypothesis by cross-breeding the βStop line with the $Ca_V1.2^{SA}$ or the $Ca_V1.2^{SF}$ lines. The $Ca_V1.2^{SA}$ mouse line expresses a $Ca_V1.2$ channel containing the mutation S1928A. Mice homozygous for the double mutation $Ca_V1.2^{S1928A}/Cav1.2^{S1928A}$, $Ca_V\beta_2^{P501Stop}/Ca_V\beta_2^{P501Stop}$ (SAβStop) had the same size and weight as the heterozygous littermates. Circadian cardiac rhythm was not altered in these mice (Fig. 29A). The cell capacitance of Ctr SAβStop and double knock-in SAβStop CMs was the same (CtrSAβStop: 168.6 ± 12 pF (n=15); SAβStop: 163.0 ± 18 pF (n = 6) (Fig. 29B). We did not observe an effect of the double mutation on CDF (Fig. 29C).
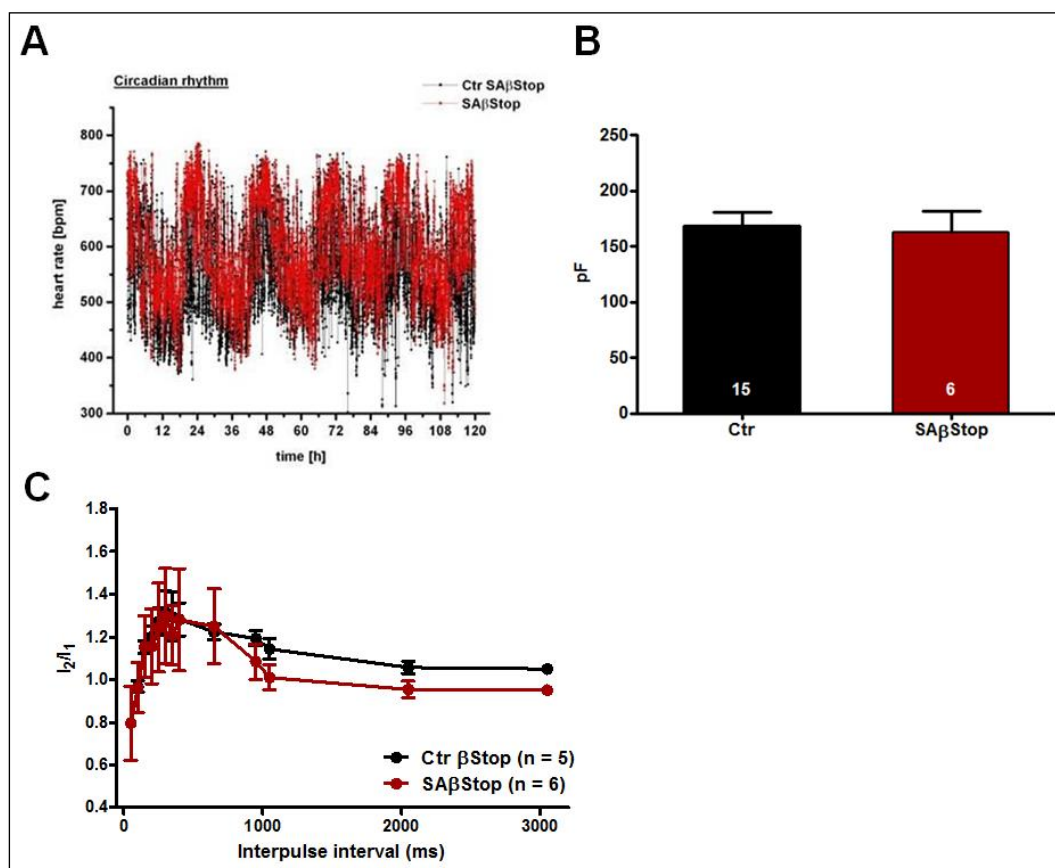
Figure 29. Heart rate and I_{Ca} analysis of SAβStop mice. A, circadian cardiac rhythm in heterozygous Ctr SAβStop and homozygous SAβStop mice (performed by Katrin Domes). B, bar graph of cell capacitance. C, unchanged CDF in Ctr SAβStop and SAβStop. (modified from Brandmayr et al., 2012)

β-adrenergic regulation was tested in the SAβStop mouse line. Isoproterenol stimulated HR (Fig. 30A) and FS (Fig. 30C) in both mouse lines to the same extent. Phenylephrine decreased the HR to the same extent in both genotypes (Fig.30B).
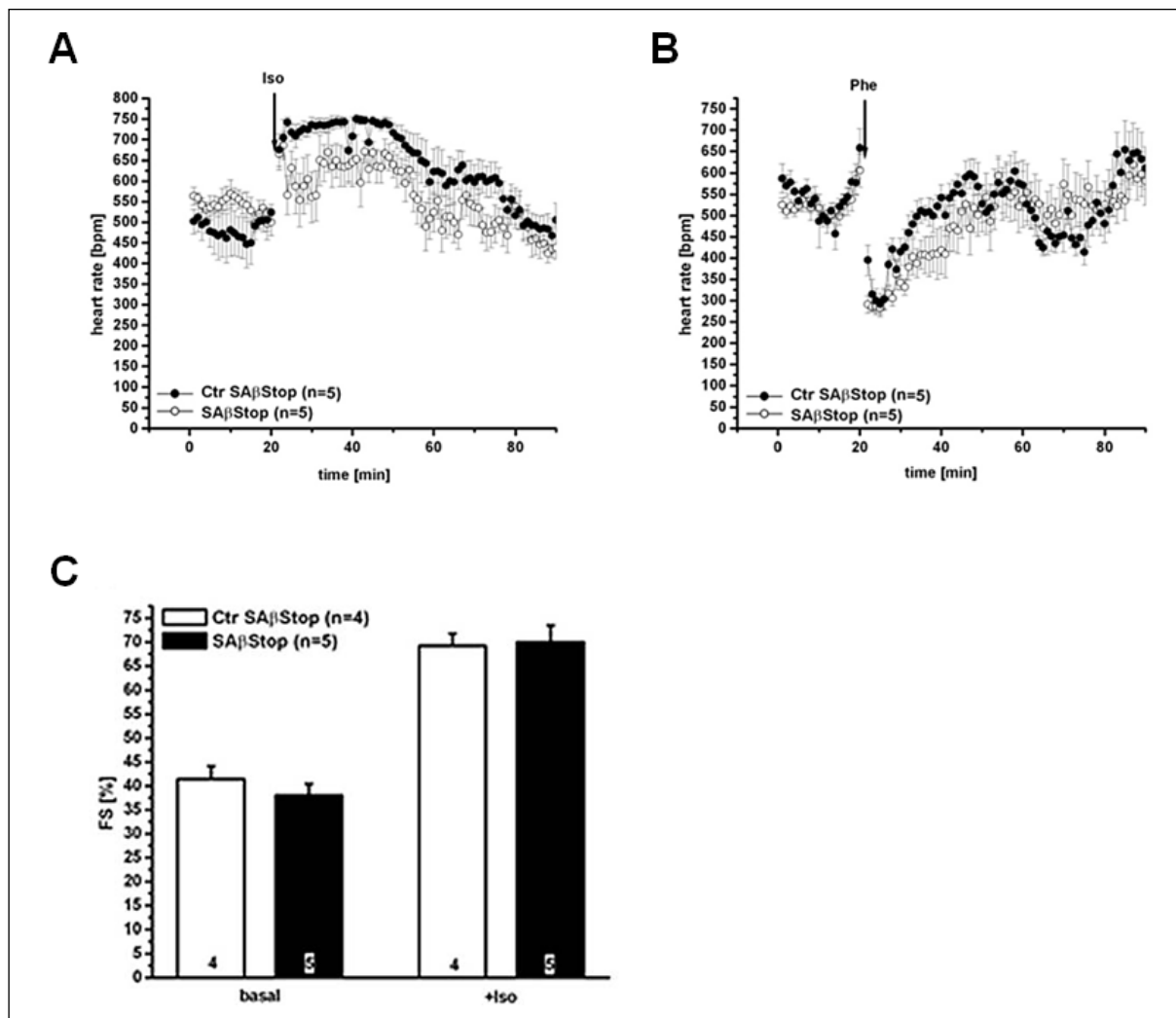
Figure 30. SAβStop mutation does not prevent positive inotropic heart regulation. A and B, stimulation of heart rate by intraperitoneal injection of isoproterenol (A) or phenylephrine (B) in Ctr SAβStop and SAβStop mice. C, FS unchanged in SAβStop before and after isoproterenol administration (0.1 mg/kg of body weight i.p.). Experiments were done by Katrin Domes. (modified from Brandmayr et al., 2012)

Stimulation of the corresponding CMs by 100 nM isoproterenol increased I_{Ca} by 194 ± 19.2% (n = 6) and 205.3 ± 14% (n = 6) in heterozygous CtrSAßStop and homozygous SAßStop, respectively (Fig. 31A and B) There was no significant difference in the slow or fast component of inactivation either with or without isoproterenol stimulation (Fig. 31C).
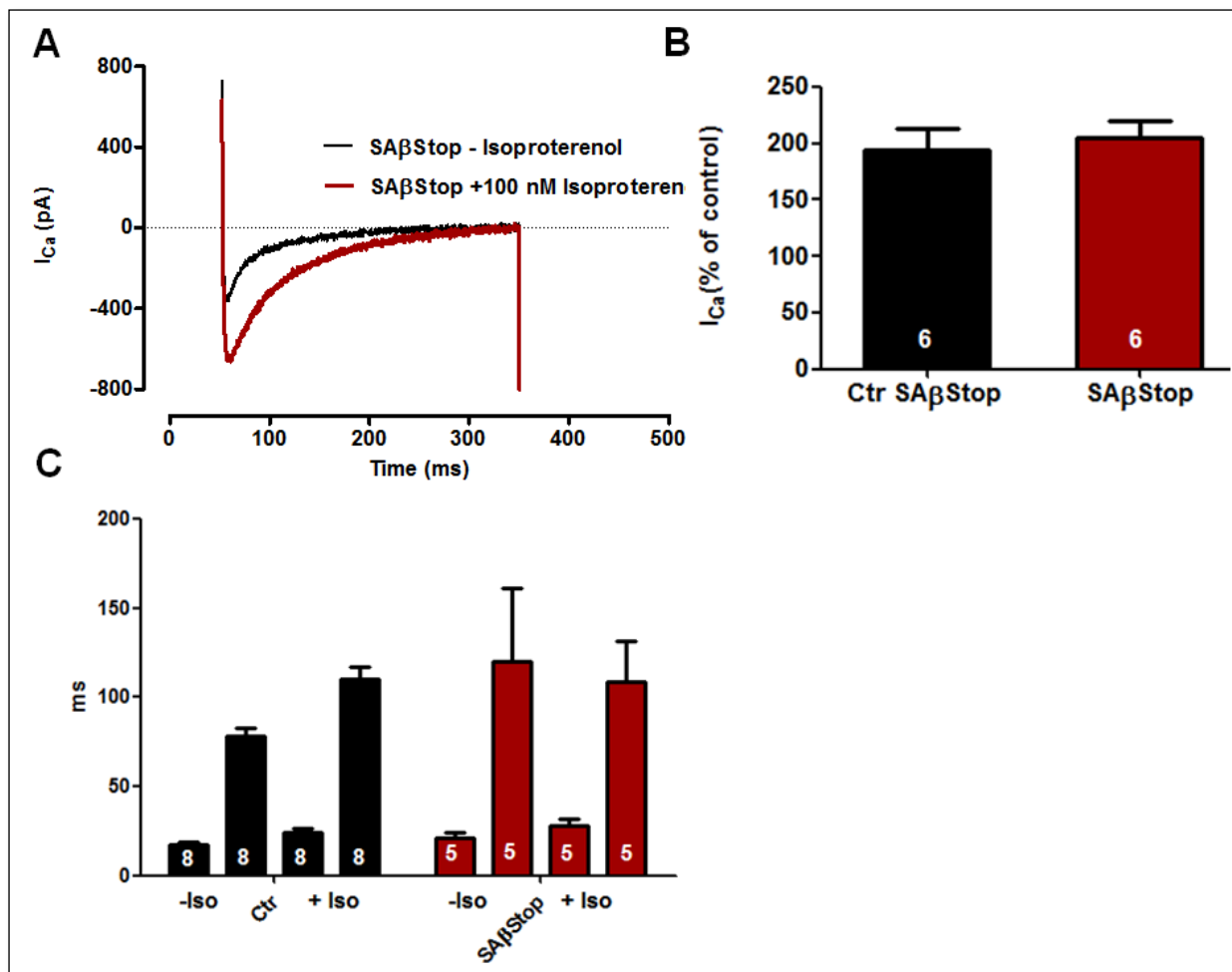
Figure 31. Analysis of I_{Ca} from CtrSAβStop and SAβStop CMs. A, I_{Ca} trace ± isoproterenol (100 nM) in SAβStop CMs. B, statistics of isoproterenol (100 nM) stimulation of I_{Ca} in Ctr SAβStop and SAβStop mice. C, unchanged in time course of inactivation before and after isoproterenol administration. (modified from Brandmayr et al., 2012)

3.4. S1512, S1570 and Ca$_V$β$_2$-N4 mutation

In the next series of experiments we tested the double mutation Ca$_V$1.2$^{S1512/1570A}$ /Ca$_V$1.2$^{S1512/1570A}$, Ca$_V$ß$_2$^{P501Stop}/Ca$_V$ß$_2$^{P501Stop} (SFßStop). Mice homozygous for the double mutation SFßStop had the same size and weight as the heterozygous litters. Circadian cardiac rhythm was not altered in these mice (Fig. 32A). The cell capacitance of Ctr SFßStop and double knock-in SFßStop CMs was the same (Ctr SFßStop: 213 ± 13 pF (n = 9); SFßStop: 195 ± 17 pF (n = 8) (Fig. 32B). As shown for the SF mice (Blaich et al., 2010), CDF was also significantly decreased in the SFßStop mice (Fig. 32C).
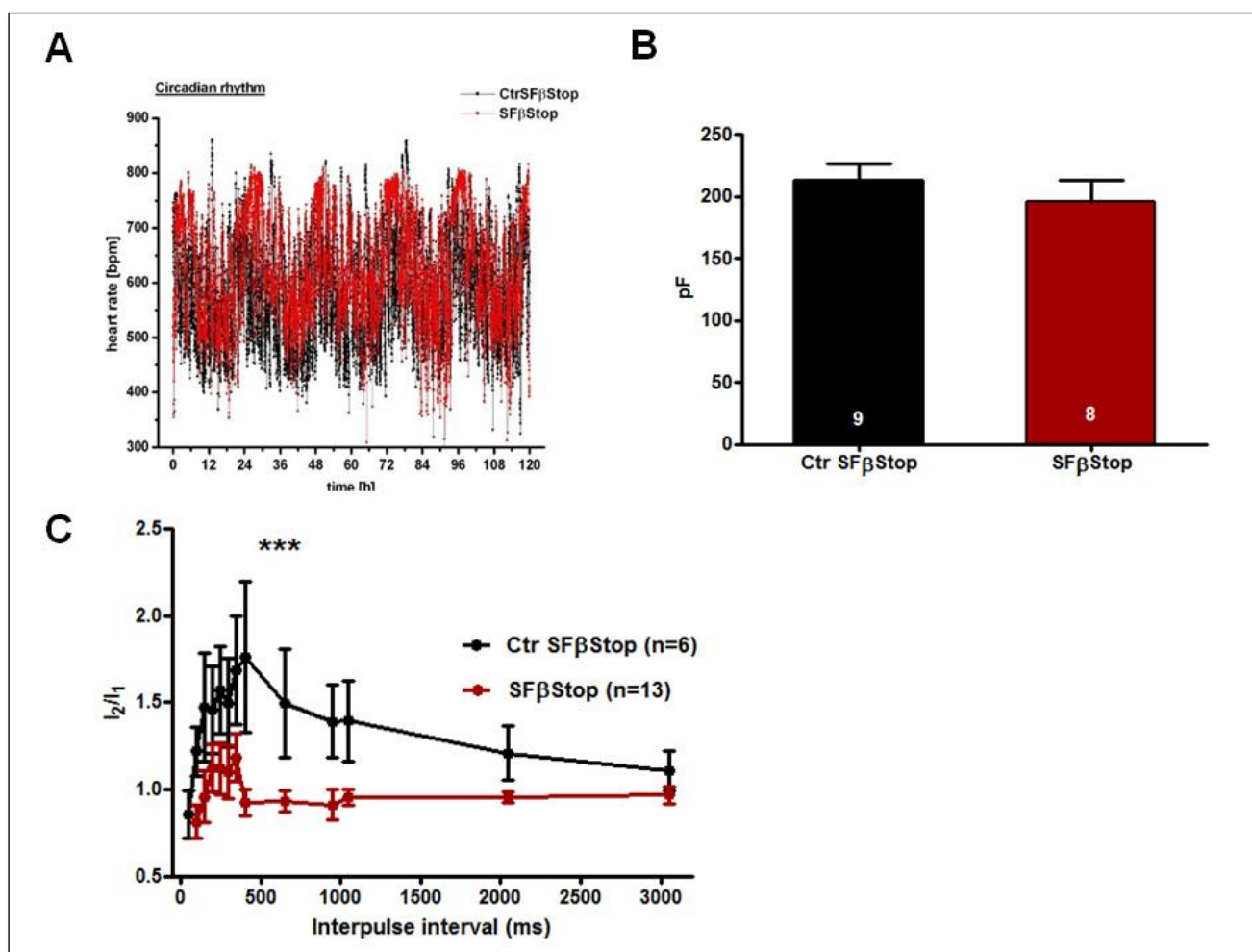
Figure 32. Heart rate and I_{Ca} analysis of SFβStop mice. A, circadian cardiac rhythm in heterozygous Ctr SFβStop and homozygous SFβStop mice (performed by Katrin Domes). B, bar graph of cell capacitance. C, unchanged CDF in Ctr SFβStop and SFβStop. ***, p < 0.001 (modified from Brandmayr et al., 2012)

Isoproterenol stimulated HR (Fig. 33A) and FS (Fig. 33C) in both mouse lines to the same extent. Phenylephrine decreased the HR to the same extent in both genotypes (Fig. 33B).
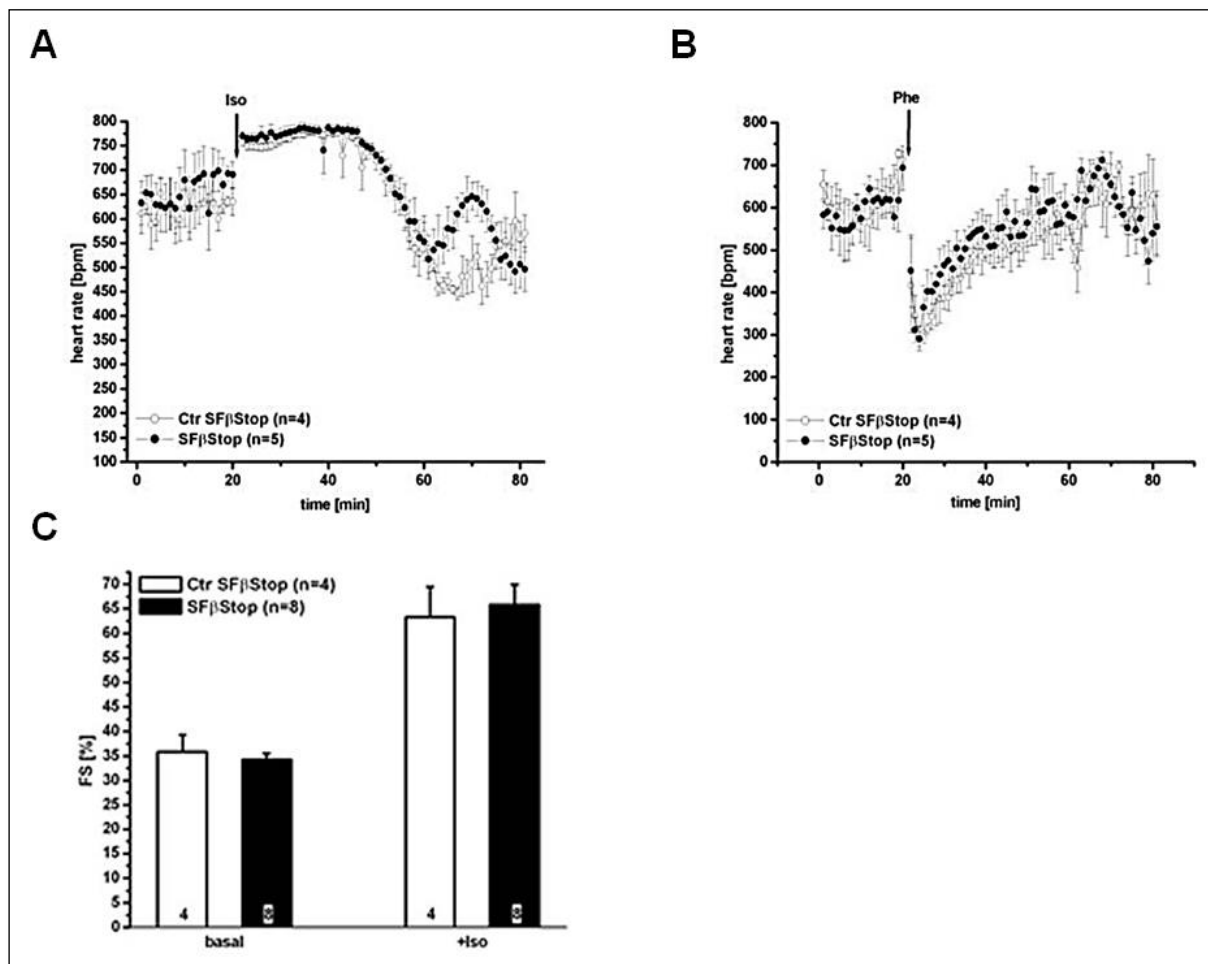
Figure 33. SFβStop mutation does not prevent positive inotropic heart regulation. A and B, stimulation of heart rate by intraperitoneal injection of isoproterenol (A) or phenylephrine (B) in Ctr SFβStop and SFβStop mice. C, FS unchanged in SFβStop before and after isoproterenol administration (0.1 mg/kg of body weight i.p.). Experiments were done by Katrin Domes (modified from Brandmayr et al., 2012).

Stimulation of these CMs by 100 nM isoproterenol increased I_{Ca} by 187 ± 17 (n = 10) and 196 ± 26 (n = 8) in the heterozygous Ctr SFβStop and homozygous SFβStop line, respectively (Fig. 34A and B). We concluded from this analysis that neither double mutation affected the β-adrenergic stimulation of FS in the intact mouse nor that of I_{Ca} in the CMs. There was no significant difference in the slow or fast component of inactivation either with or without isoproterenol stimulation (Fig. 34C).
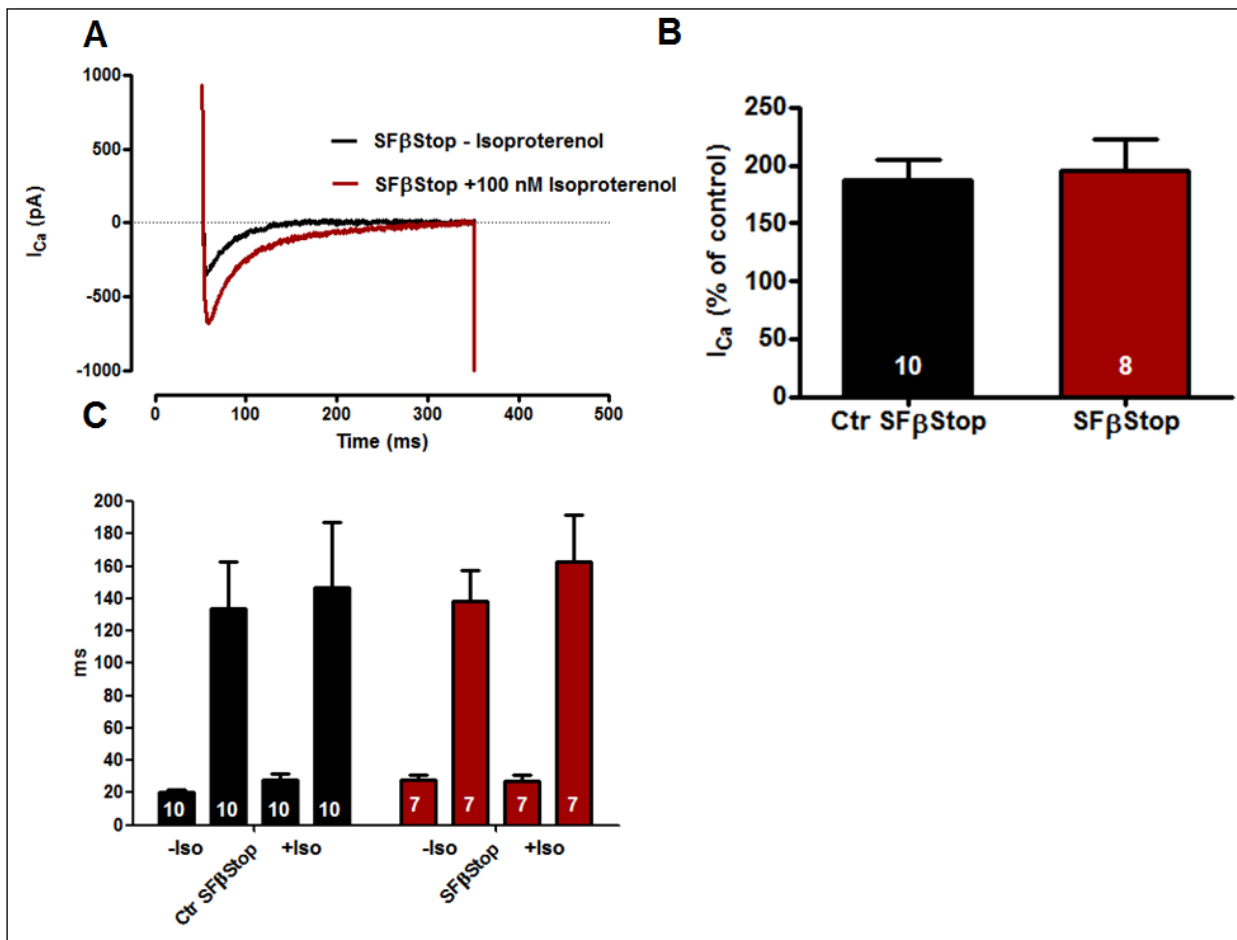
Figure 34. Analysis of I_{Ca} from Ctr SFβStop and SFβStop CMs. A, I_{Ca} trace ± isoproterenol (100 nM) in SFβStop CMs. B, statistics of isoproterenol (100 nM) stimulation of I_{Ca} in Ctr SFβStop and SFβStop mice. C, unchanged in time course of inactivation before and after isoproterenol administration. (modified from Brandmayr et al., 2012)

4. Discussion

4.1. I1624E mutation of the $Ca_V1.2$ channel transforms the channel to CDI phenotype

Calcium channels mediate the influx of calcium ions into the cell upon membrane polarization. Ca^{2+}calmodulin-dependent inactivation and facilitation exert two opposing effects of altering calcium influx through the L-type calcium channel. Activation of CaMKII can facilitate I_{Ca} by shifting channel gating to frequent long openings. The inhibitory form, Ca^{2+}-dependent inactivation, promotes the shutting off of channel conductance during a maintained depolarization. Both inhibitory and facilitatory forms of autoregulation appear to involve CaM. CaM interacts with distinct CaM-binding domains on the C terminus of the $Ca_V1.2$. The first CaM-binding region identified was an "IQ-like" domain on the carboxy tail of α_{1C}; a previously identified 'CBD' (Peterson et al., 1999). Point mutations within IQ result in marked and distinct effects on both forms of modulation of heterologously expressed $Ca_V1.2$ channels *in vitro*. Over the last decades, these types of regulation have been proven. However, many questions remain about the mechanisms underlying CaM modulation of L-type calcium channels especially in the complex *in vivo* environment.

In this study, we have shown that exchange of Ile with Glu in the CaM-binding motif (IQ) of the $Ca_V1.2$ channel gene is lethal to mice. Electrophysiological analysis of CMs from mice with a conditional heart-specific I/E mutation in the *CACNA1C* gene revealed that the mutation abolishes CaM/CaMKII-mediated regulation of the $Ca_V1.2$ channel. In addition, the mutation transforms the $Ca_V1.2$ channel to a phenotype that recapitulates the properties of a Ca^{2+}-inactivated channel.

In heart muscle, $Ca_V1.2$ is strongly associated with a number of regulatory proteins, building up a macromolecular signaling complex (Dai et al., 2009). Among the association partners, CaM is permanently bound to the channel and acts as a resident Ca^{2+} sensor (Mori et al., 2004). Ca^{2+}-bound CaM regulates both CDI and CDF of $Ca_V1.2$ (Halling et al., 2006), the latter by regulating the activity of CaMKII that is tethered to the $Ca_V1.2$ channel (Hudmon et al., 2005). The major binding site for CaM is the IQ motif (amino acids 1624 – 1635). Mutations in the IQ motif have been shown to inhibit CaM binding to the $Ca_V1.2$ channel, thus reducing facilitation and CDI (Zuhlke et al., 2000). Especially exchange of Ile1624 with Glu in the IQ motif of the $Ca_V1.2$ channel reduces CaM affinity by ∼100 fold and prohibits effectively facilitation and CDI of I_{Ca} in the *Xenopus oocyte* expression system (Zuhlke et al., 2000). This work clearly demonstrated that exchange of Ile1624 with Glu in the cardiac

murine *CACNA1C* gene likewise altered the electrophysiological properties of I_{Ca} in CMs and reduced the life span of the mutant mice.

Experiments using peptides containing either the entire IQ motif of $Ca_V1.2$ or the I/E mutation showed an ~100 fold decreased affinity of the I/E mutation peptide for CaM (Zuhlke et al., 2000). However, no *in vivo* quantitative measurements of affinity changes are available for the full-length channel with this mutation. Therefore, this number must be viewed with caution. The I/A mutant, which has equally strong effect on CDI as the I/E mutant but leaves CDF intact in heterologous expression studies, showed no measurable changes in its association with CaM, as shown by both biochemical studies (Zuhlke et al., 2000) and crystal structure investigations (Fallon et al., 2005). Therefore, one cannot rule out the possibility that the effects of the I/E mutation also result from some distortion in the structure and correspondingly in the function of the IQ domain and not only from a reduction in CaM binding.

CaMKII is a major modulator of I_{Ca} activity (Maier and Bers, 2002). Inhibition of CaMKII by inhibitory peptides or blockers such as KN-93 prolongs recovery from inactivation (Guo and Duff, 2006), shifts the steady-state inactivation curve to more negative voltages, and reduces facilitation of I_{Ca} (Blaich et al., 2010). In addition, knock-out of CaMKIIδ slows down recovery from inactivation and reduces facilitation of I_{Ca} (Xu et al., 2010). The I/E mutation of the $Ca_V1.2$ channel likewise prolonged recovery from inactivation, shifted the steady-state inactivation curve to more negative voltages, and reduced facilitation of I_{Ca}. Thus, we conclude that the I/E mutation abolishes the effects of CaMKII on the $Ca_V1.2$ channel because the I/E mutation shows a reduced affinity for CaM (Zuhlke et al., 2000), preventing activation of CaMKII. At present, we cannot rule out the possibility that the I/E mutation distorts the C terminus of $Ca_V1.2$ *in vivo* and thereby reduces the affinity for CaMKII.

The fundamental role of CaM in mediating CDI has been discussed in several excellent reviews (Bers and Grandi, 2009; Halling et al., 2006). Unfortunately, pharmacological inhibitors of CaM are not useful to characterize the role of CaM in regulating cardiac I_{Ca} (Klockner and Isenberg, 1987). Instead, the role of CaM in cardiac I_{Ca} is assessed mainly by reducing intracellular Ca^{2+}, namely by the use of Ba^{2+} as the charge carrier for currents through $Ca_V1.2$ channels, by the use of high concentrations of intracellular Ca^{2+} buffers, or the replacement of intracellular CaM with a CaM that does not bind Ca^{2+} (Peterson et al., 1999). Each experimental condition attenuates CDI, as has been observed in part in this study using CMs from Ctr mice. In contrast, CDI was no longer observed in CMs from I/E

mice. Instead, inactivation of I_{Ca} in I/E CMs was not different from that in Ctr CMs under all conditions tested. Thus, although the I/E mutation decreases significantly the affinity of the IQ motif for CaM, the mutant channel inactivates in a way that recapitulates the binding of a fully activated CaM.

More information about I/E hearts has been published by our group in 2012 (Blaich et al., 2012). Analysis of I/E hearts revealed severe apoptosis of cardiac myocytes and an increased fibrosis. The amount of phospho-CaM kinaseII and phospho-MAPK was increased. A recent publication suggested that activated CaMKII represses cardiac transcription of the $Ca_V1.2$ gene and prevents CM hypertrophy (Bers, 2008). CMs expressed reduced levels of $Ca_V1.2^{I1624E}$ channel protein as also observed in HEK293 expression system (Blaich et al., 2012). These mice developed dilated cardiomyopathy (DCM) within 10 days after the first tamoxifen injection. The DCM of the I/E mice was caused by an initially reduced influx of Ca^{2+} during depolarization. This reduction was caused not only by a change in channel kinetics but also by a reduced expression of the $Ca_V1.2^{I/E}$ protein leading to decreased peak I_{Ca}.

The hindered association of CaM with the $Ca_V1.2$ channel reduces trafficking of the channel to the membrane during biosynthesis (Blaich et al., 2012), which could account for the observed reduction in channel expression. An additional reason may be the missing facilitation due to the absence of CaMKII-mediated regulation of I_{Ca}, which may reduce the ability of heart muscle to adapt to exercise. Indeed, mice deficient in CaMKIIδ show a reduced heart rate in response to work load or β-adrenergic stimulation (Blaich et al., 2012; Xu et al., 2010). This phenotype caused most likely by a fully inactivated I_{Ca}, may limit Ca^{2+} entry and thus reduce Ca^{2+}-induced Ca^{2+} release, leading to an insufficient contraction and finally to death of the mice.

4.2. Stimulation of the β-adrenergic receptor was unaffected in βStop, SAβStop and SFβStop mice

β-adrenergic receptor signaling via cAMP/PKA pathway plays a critical role in physiological processes in the heart. One of the main targets for PKA modulation is the $Ca_V1.2$, which mediates Ca^{2+} entry into cardiomyocytes. Truncation of the $Ca_V\beta_2$-N4 subunit at P501 by site-directed mutagenesis removed the "classical" PKA phosphorylation sites and that for PKG, CaMKII, and PKB. Removing these reported phosphorylation sites had no

effect on the basic properties of the murine cardiac I_{Ca}. The $Ca_V\beta_2$Stop mice showed normal β-adrenergic regulation, CDI, CDF, and basic behavior.

The reported results do not rule out the possibility that PKA modified an additional site on the truncated $Ca_V\beta_2$-N4 subunit that was necessary for β-adrenergic regulation of the channel (Gerhardstein et al., 1999). This consideration appears unlikely in view of the report that deletion of the $Ca_V\beta_2$-N4 subunit in the adult heart does not result in a severe phenotype (Meissner et al., 2011). The negative results reported here are only relevant for the relative classical tests carried out in this study. It could be that removal of these phosphorylation sites may alter more subtle cardiac functions that have not been associated with a phosphorylation event at the $Ca_V\beta_2$-N4 subunit so far.

An alternative possibility is that PKA phosphorylates simultaneously sites at the $Ca_V\beta_2$-N4 and the $Ca_V1.2$ subunit. This possibility was tested with two additional mouse lines. However, the combination of the $Ca_V\beta_2$-N4 mutation with mutation at the C terminus of the $Ca_V1.2$ protein did not influence the cardiac response to β-adrenergic stimulation. The $Ca_V\beta_2$-N4 mutation did not affect the reduced CDF caused by the SF mutation (Blaich et al., 2010). Our results do not rule out the possibility that phosphorylation at these sites might affect parameters of the $Ca_V1.2$ channel that have not been studied under our condition. However, the physiological significance of these putative parameters appears to be restricted because deletion of the cardiac $Ca_V\beta_2$-N4 gene in the adult mouse caused only negligible changes in the cardiac performance (Meissner et al., 2011).

An alternative target for PKA and β-adrenergic regulation of the heart has been proposed recently. Expression studies implicated PKA-dependent phosphorylation of Ser[1700] and Thr[1704] in the C terminus of $Ca_V1.2$ to be important for the β-adrenergic regulation (Fuller et al., 2010). The phosphorylation needs to be combined with proteolytic cleavage of the mature $Ca_V1.2$ protein close to amino acid 1800. The cleaved distal C terminus has to stay with the truncated $Ca_V1.2$ channel to allow β-adrenergic regulation. The distal part inhibits I_{Ca} of the truncated $Ca_V1.2$ channel. The inhibition is then removed by β-adrenergic stimulation (Fuller et al., 2010). To further support the above concept, Fu and colleagues (Fu et al., 2013) from the same group reported the *in vivo* role of these phosphorylation sites. Mutation of both residues to Ala in STAA mice reduced basal L-type Ca^{2+} currents and markedly decreased β-adrenergic stimulation of Ca^{2+} currents and cell contraction. STAA ventricular myocytes exhibited arrhythmic contractionsm. Moreover, STAA mice have reduced exercise capacity, and cardiac hypertrophy is evident at 3 months. However, β-adrenergic regulation of the $Ca_V1.2$ was still present in the STAA mice. Yang and colleagues (Yang et al., 2013) have also

investigated the role of Ala^{1800}in the cleavage of α_{1C} and the role of Ser^{1700} and Thr^{1704} in mediating the adrenergic regulation of Ca$_V$1.2 in the heart using a transgenic approach. They reported that adrenergic regulation of I_{Ca} and fractional shortening of cardiomyocytes do not require phosphorylation of either Ser^{1700} or Thr^{1704} of the α_{1C} subunit. The further investigation may be needed to solve the controversy.

For β-adrenergic regulation of the expressed I_{Ca}, an additional domain of the distal part, its AKAP binding site, is required. AKAPs are components that target various proteins of the β-adrenergic signaling cascade to Ca$_V$1.2. The AKAP binding site allows the close positioning of PKA to the Ca$_V$1.2 channel. Partial verification of the AKAP concept has been given by Nichols and colleagues (Nichols et al., 2010), Fuller and colleagues (Fuller et al., 2010) and Brandmayr and colleagues (Brandmayr et al., 2012). Truncation of the murine Ca$_V$1.2 channel at Asp^{1904} resulted in death around birth (Domes et al., 2011) and the I_{Ca} of embryonic CMs expressing a truncated Ca$_V$1.2 channel was not stimulated by isoproterenol or forskolin. Similar results have been reported, when the Ca$_V$1.2 protein was truncated at Gly^{1796} (Fu et al., 2011) These negative results are most likely caused by the deletion of the AKAP binding sequence (McConnachie et al., 2006).

The reported results suggest that the C-terminal phosphorylation sites of the Ca$_V$β$_2$-N4 subunit are not used to regulate basic properties of the murine cardiac I_{Ca}. In contrast, CaMKII-dependent phosphorylation of the C terminus of Ca$_V$1.2 is necessary for CDF. The results support again the previous notion (Domes et al., 2011; Fu et al., 2011) that the distal C terminus of the Ca$_V$1.2 channel is necessary for β-adrenergic regulation of murine I_{Ca}.

5. Summary

The data presented in this dissertation provide supporting evidence of the hypothesis that Ile1624 in the IQ motif is a CaM binding site and necessary for CDF and CDI of $Ca_V1.2$. Several studies have been undertaken to evaluate the role of Ile1624 resisudaul using *in vitro* expression system however, there are no reports about in vivo studies using trangenic mice. This is the first report describing changes in biophysical properties of LTCC caused by Ile1624 mutation *in vivo*. Using gene knock-in mouse lines technique, I/E mice with mutation of Ile1624 to Glu were created. Homozygous I/E mice were not viable. Therefore, a cardio-specific $Ca_V1.2$ mutation was induced by crossing the heterozygous mice with mice expressing Cre under the control of the alpha-myosin heavy chain promoter and carrying a floxed allele for $Ca_V1.2$. These mice were treated with tamoxifen before the experiment. The major finding of this experiment are shown in table 1.

Another purpose of the dissertation is to determine the role of phosphorylation sites in exon 14 on β subunit of LTCC. We created a knock-in mouse line with targeted mutation of the *CACNB2* gene coding for $Ca_V\beta_2$-N4 by insertion of a stop codon after proline 501 in exon 14 (βStop mice). This mutation prevented translation of the $Ca_V\beta_2$-N4 C-terminus that contains the phosphorylation sites for the PKA, Akt/PKB and CaMKII. Electrophysiological experiments in βStop mice showed normal basal I_{Ca}. The regulation of the I_{Ca} by stimulation of the β-adrenergic receptor was unaffected. The major findings of this experiment are shown in table 2. Because of these negative experiments, it is possible that the positive inotropic effect was mediated by more than one phosphorylation site. Ser^{1928}, in the α_{1C} subunit, was previously identified as a α_{1C} PKA phosphorylation site. However, Lemke et al (2008) reported that S1928A point mutation did not significantly attenuate the β-adrenergic response. We then cross bred βStop mice with mice expressing the *CACNA1C* gene containing the mutation S1928A (SAβStop) or S1512A and S1570A (SFβStop) in the C terminus of the α_{1C} subunit. The β-adrenergic regulation of the cardiac I_{Ca} was unaltered in these mouse lines. We conclude that phosphorylation of the C-terminal sites in $Ca_V\beta_2$-N4 as well as Ser^{1928}, Ser^{1512}, and Ser^{1570} of the $Ca_V1.2$ protein are functionally not or only little involved in the adrenergic regulation of the murine cardiac $Ca_V1.2$ channel. The major findings of these experiments are shown in tables 3 and 4.

Table 10. Major findings from I/E mutation

Major findings	Supporting results
1. I/E mice had a reduced in $Ca_V1.2$ expression.	- $Ca_V1.2$ protein level in cardiac ventricular tissue was reduced. - I_{Ca} from CMs was reduced.
2. I/E mutation mimics the effect of CaMKII inhibitor on $Ca_V1.2$ channel properties.	- Recovery from inactivation of I_{Ca} was slowed down. - Steady-state inactivation curve of I_{Ca} was shifted to the left. - CaMKII inhibitor KN 93 did not influence recovery from inactivation and steady-state inactivation in CMs from I/E mice.
3. I/E mutation abolishes CaM/CaMKII-mediated effects on facilitation.	- Facilitation of I_{Ca} was almost gone.
4. I/E mutation transforms the LTCC to a phenotype mimicking CDI.	- The time course of I_{Ca} inactivation in I/E mice was not influenced by the use of Ba^{2+} as charge carrier. - Inactivation of I_{Ca} was not slowed down upon BAPTA dialyzed.
5. I1624E is a lethal mutation.	- Homozygous I/E mice were not viable. - Heart specific I/E mutation reduced life span and mice died within 3 weeks after treatment with tamoxifen. - I/E mutation leads to dilated cardiomyopathy and death (Blaich et al. 2012).

Table 11. Major findings from βStop mutation

Major findings	Supporting results
1. βStop mice have normal phenotype.	- βStop mice had a normal life expectancy. - ECG measurement of HR was normal. - no alterations in $Ca_V1.2$ expression in CMs. - normal LTCC function (no alterations in I_{Ca}, steady state inactivation, recovery time from inactivation).
2. PKA phosphorylation sites $Ser^{479/480}$ are not necessary for β-adrenergic regulation of the heart muscle.	- typical cardiac response (HR, FS) to isoproterenol and phenylephrine. - normal increased I_{Ca} response to isoproterenol. - no change in slow and fast component of inactivation either with or without isoproterenol stimulation.
3. Phosphorylation of the $Ca_V\beta_2$-N4 subunit is not a necessary prerequisite to induce CDF under basal condition.	- LTCC of βStop showed normal facilitation property.

Table 12. Major findings from SAβStop mutation

Major findings	Supporting results
1. SAβStop mice have normal phenotype.	- normal size and weight. - normal circadian cardiac rhythm.
2. PKA phosphorylation sites Ser^{1928} and Ser$^{479/480}$ are not necessary for β-adrenergic regulation of the heart muscle.	- typical cardiac response (HR, FS) to isoproterenol and phenylephrine. - normal increased I_{Ca} response to isoproterenol. - no change in slow and fast component of inactivation either with or without isoproterenol stimulation.
3. Phosphorylation of the Ca$_V$β$_2$-N4 subunit and PKA phosphorylation site Ser^{1928} are not a necessary prerequisite to induce CDF under basal condition.	- LTCC of SAβStop showed normal facilitation property.

Table 13. Major findings from SFβStop mutation

Major findings	Supporting results
1. SFβStop mice have normal phenotype.	- normal size and weight. - normal circadian cardiac rhythm.
2. PKA phosphorylation sites Ser^{1512}, Ser^{1570} and Ser$^{479/480}$ are not necessary for β-adrenergic regulation of the heart muscle.	- typical cardiac response (HR, FS) to isoproterenol and phenylephrine. - normal increased I_{Ca} response to isoproterenol. - no change in slow and fast component of inactivation either with or without isoproterenol stimulation.
3. SFβStop mice show facilitation property same as SF mice.	- as shown in SF mice, CDF was also significantly decreased in the SFβStop mice.

6. Reference

Abiria, S.A., and Colbran, R.J. (2010). CaMKII associates with CaV1.2 L-type calcium channels via selected beta subunits to enhance regulatory phosphorylation. J Neurochem *112*, 150-161.

Anderson, M.E., Braun, A.P., Schulman, H., and Premack, B.A. (1994). Multifunctional Ca2+/calmodulin-dependent protein kinase mediates Ca(2+)-induced enhancement of the L-type Ca2+ current in rabbit ventricular myocytes. Circ Res *75*, 854-861.

Antzelevitch, C. (2003). Molecular Genetics of Arrhythmias and Cardiovascular Conditions Associated with Arrhythmias. Pacing and Clinical Electrophysiology *26*, 2194–2208.

Bernatchez, G., Talwar, D., and Parent, L. (1998). Mutations in the EF-hand motif impair the inactivation of barium currents of the cardiac alpha1C channel. Biophys J *75*, 1727-1739.

Berrou, L., Bernatchez, G., and Parent, L. (2001). Molecular determinants of inactivation within the I-II linker of alpha1E (CaV2.3) calcium channels. Biophys J *80*, 215-228.

Bers, D.M. (2002). Cardiac excitation-contraction coupling. Nature *415*, 198-205.

Bers, D.M. (2008). Calcium cycling and signaling in cardiac myocytes. Annu Rev Physiol *70*, 23-49.

Bers, D.M., and Grandi, E. (2009). Calcium/calmodulin-dependent kinase II regulation of cardiac ion channels. J Cardiovasc Pharmacol *54*, 180-187.

Blaich, A., Pahlavan, S., Tian, Q., Oberhofer, M., Poomvanicha, M., Lenhardt, P., Domes, K., Wegener, J.W., Moosmang, S., Ruppenthal, S.*, et al.* (2012). Mutation of the calmodulin binding motif IQ of the L-type Ca(v)1.2 Ca2+ channel to EQ induces dilated cardiomyopathy and death. J Biol Chem *287*, 22616-22625.

Blaich, A., Welling, A., Fischer, S., Wegener, J.W., Kostner, K., Hofmann, F., and Moosmang, S. (2010). Facilitation of murine cardiac L-type Ca(v)1.2 channel is modulated by calmodulin kinase II-dependent phosphorylation of S1512 and S1570. Proc Natl Acad Sci U S A *107*, 10285-10289.

Bodi, I., Mikala, G., Koch, S.E., Akhter, S.A., and Schwartz, A. (2005). The L-type calcium channel in the heart: the beat goes on. J Clin Invest *115*, 3306-3317.

Bossuyt, J., Helmstadter, K., Wu, X., Clements-Jewery, H., Haworth, R.S., Avkiran, M., Martin, J.L., Pogwizd, S.M., and Bers, D.M. (2008). Ca2+/calmodulin-dependent protein kinase IIdelta and protein kinase D overexpression reinforce the histone deacetylase 5 redistribution in heart failure. Circ Res *102*, 695-702.

Brandmayr, J., Poomvanicha, M., Domes, K., Ding, J., Blaich, A., Wegener, J.W., Moosmang, S., and Hofmann, F. (2012). Deletion of the C-terminal phosphorylation sites in the cardiac beta-subunit does not affect the basic beta-adrenergic response of the heart and the Ca(v)1.2 channel. J Biol Chem *287*, 22584-22592.

Brodde, O.E. (1991). Beta 1- and beta 2-adrenoceptors in the human heart: properties, function, and alterations in chronic heart failure. Pharmacol Rev *43*, 203-242.

Budde, T., Meuth, S., and Pape, H.C. (2002). Calcium-dependent inactivation of neuronal calcium channels. Nat Rev Neurosci *3*, 873-883.

Bunemann, M., Gerhardstein, B.L., Gao, T., and Hosey, M.M. (1999). Functional regulation of L-type calcium channels via protein kinase A-mediated phosphorylation of the beta(2) subunit. J Biol Chem *274*, 33851-33854.

Buraei, Z., and Yang, J. (2010). The ss subunit of voltage-gated Ca2+ channels. Physiol Rev *90*, 1461-1506.

Catalucci, D., and Condorelli, G. (2006). Effects of Akt on cardiac myocytes: location counts. Circ Res *99*, 339-341.

Catalucci, D., Latronico, M.V., Ceci, M., Rusconi, F., Young, H.S., Gallo, P., Santonastasi, M., Bellacosa, A., Brown, J.H., and Condorelli, G. (2009). Akt increases sarcoplasmic reticulum Ca2+ cycling by direct phosphorylation of phospholamban at Thr17. J Biol Chem *284*, 28180-28187.

Catterall, W.A. (2000). Structure and regulation of voltage-gated Ca2+ channels. Annu Rev Cell Dev Biol *16*, 521-555.

Couchonnal, L.F., and Anderson, M.E. (2008). The role of calmodulin kinase II in myocardial physiology and disease. Physiology (Bethesda) *23*, 151-159.

Dai, S., Hall, D.D., and Hell, J.W. (2009). Supramolecular assemblies and localized regulation of voltage-gated ion channels. Physiol Rev *89*, 411-452.

Davare, M.A., Dong, F., Rubin, C.S., and Hell, J.W. (1999). The A-kinase anchor protein MAP2B and cAMP-dependent protein kinase are associated with class C L-type calcium channels in neurons. J Biol Chem *274*, 30280-30287.

Davies, A., Kadurin, I., Alvarez-Laviada, A., Douglas, L., Nieto-Rostro, M., Bauer, C.S., Pratt, W.S., and Dolphin, A.C. (2010). The alpha2delta subunits of voltage-gated calcium channels form GPI-anchored proteins, a posttranslational modification essential for function. Proc Natl Acad Sci U S A *107*, 1654-1659.

De Jongh, K.S., Murphy, B.J., Colvin, A.A., Hell, J.W., Takahashi, M., and Catterall, W.A. (1996). Specific phosphorylation of a site in the full-length form of the alpha 1 subunit of the cardiac L-type calcium channel by adenosine 3',5'-cyclic monophosphate-dependent protein kinase. Biochemistry *35*, 10392-10402.

Doering, C.J., Hamid, J., Simms, B., McRory, J.E., and Zamponi, G.W. (2005). Cav1.4 encodes a calcium channel with low open probability and unitary conductance. Biophys J *89*, 3042-3048.

Domes, K., Ding, J., Lemke, T., Blaich, A., Wegener, J.W., Brandmayr, J., Moosmang, S., and Hofmann, F. (2011). Truncation of murine CaV1.2 at Asp-1904 results in heart failure after birth. J Biol Chem *286*, 33863-33871.

Dzhura, I., Wu, Y., Colbran, R.J., Balser, J.R., and Anderson, M.E. (2000). Calmodulin kinase determines calcium-dependent facilitation of L-type calcium channels. Nat Cell Biol *2*, 173-177.

Fabiato, A. (1983). Calcium-induced release of calcium from the cardiac sarcoplasmic reticulum. Am J Physiol *245*, C1-14.

Fallon, J.L., Halling, D.B., Hamilton, S.L., and Quiocho, F.A. (2005). Structure of calmodulin bound to the hydrophobic IQ domain of the cardiac Ca(v)1.2 calcium channel. Structure *13*, 1881-1886.

Findeisen, F., and Minor, D.L., Jr. (2010). Structural basis for the differential effects of CaBP1 and calmodulin on Ca(V)1.2 calcium-dependent inactivation. Structure *18*, 1617-1631.

Fu, Y., Westenbroek, R.E., Scheuer, T., and Catterall, W.A. (2013). Phosphorylation sites required for regulation of cardiac calcium channels in the fight-or-flight response. Proc Natl Acad Sci U S A *110*, 19621-19626.

Fu, Y., Westenbroek, R.E., Yu, F.H., Clark, J.P., 3rd, Marshall, M.R., Scheuer, T., and Catterall, W.A. (2011). Deletion of the distal C terminus of CaV1.2 channels leads to loss of beta-adrenergic regulation and heart failure in vivo. J Biol Chem *286*, 12617-12626.

Fuller, M.D., Emrick, M.A., Sadilek, M., Scheuer, T., and Catterall, W.A. (2010). Molecular mechanism of calcium channel regulation in the fight-or-flight response. Sci Signal *3*, ra70.

Ganesan, A.N., Maack, C., Johns, D.C., Sidor, A., and O'Rourke, B. (2006). Beta-adrenergic stimulation of L-type Ca2+ channels in cardiac myocytes requires the distal carboxyl terminus of alpha1C but not serine 1928. Circ Res *98*, e11-18.

Gao, T., Yatani, A., Dell'Acqua, M.L., Sako, H., Green, S.A., Dascal, N., Scott, J.D., and Hosey, M.M. (1997). cAMP-dependent regulation of cardiac L-type Ca2+ channels requires membrane targeting of PKA and phosphorylation of channel subunits. Neuron *19*, 185-196.

Geib, S., Sandoz, G., Cornet, V., Mabrouk, K., Fund-Saunier, O., Bichet, D., Villaz, M., Hoshi, T., Sabatier, J.M., and De Waard, M. (2002). The interaction between the I-II loop and the III-IV loop of Cav2.1 contributes to voltage-dependent inactivation in a beta -dependent manner. J Biol Chem *277*, 10003-10013.

Gerhardstein, B.L., Puri, T.S., Chien, A.J., and Hosey, M.M. (1999). Identification of the sites phosphorylated by cyclic AMP-dependent protein kinase on the beta 2 subunit of L-type voltage-dependent calcium channels. Biochemistry *38*, 10361-10370.

Gifford, J.L., Walsh, M.P., and Vogel, H.J. (2007). Structures and metal-ion-binding properties of the Ca2+-binding helix-loop-helix EF-hand motifs. Biochem J *405*, 199-221.

Glossmann, H., Striessnig, J., Ferry, D.R., Goll, A., Moosburger, K., and Schirmer, M. (1987). Interaction between calcium channel ligands and calcium channels. Circ Res *61*, I30-36.

Grueter, C.E., Abiria, S.A., Dzhura, I., Wu, Y., Ham, A.J., Mohler, P.J., Anderson, M.E., and Colbran, R.J. (2006). L-type Ca2+ channel facilitation mediated by phosphorylation of the beta subunit by CaMKII. Mol Cell *23*, 641-650.

Guo, J., and Duff, H.J. (2003). Inactivation of ICa-L is the major determinant of use-dependent facilitation in rat cardiomyocytes. J Physiol *547*, 797-805.

Guo, J., and Duff, H.J. (2006). Calmodulin kinase II accelerates L-type Ca2+ current recovery from inactivation and compensates for the direct inhibitory effect of [Ca2+]i in rat ventricular myocytes. J Physiol *574*, 509-518.

Hagiwara, S., Ozawa, S., and Sand, O. (1975). Voltage clamp analysis of two inward current mechanisms in the egg cell membrane of a starfish. J Gen Physiol *65*, 617-644.

Halling, D.B., Aracena-Parks, P., and Hamilton, S.L. (2005). Regulation of voltage-gated Ca2+ channels by calmodulin. Sci STKE *2005*, re15.

Halling, D.B., Aracena-Parks, P., and Hamilton, S.L. (2006). Regulation of voltage-gated Ca2+ channels by calmodulin. Sci STKE *2006*, er1.

Hashambhoy, Y.L., Winslow, R.L., and Greenstein, J.L. (2009). CaMKII-induced shift in modal gating explains L-type Ca(2+) current facilitation: a modeling study. Biophys J *96*, 1770-1785.

Hell, J.W., Westenbroek, R.E., Warner, C., Ahlijanian, M.K., Prystay, W., Gilbert, M.M., Snutch, T.P., and Catterall, W.A. (1993). Identification and differential subcellular localization of the neuronal class C and class D L-type calcium channel alpha 1 subunits. J Cell Biol *123*, 949-962.

Hofmann, F., Biel, M., and Flockerzi, V. (1994). Molecular basis for Ca2+ channel diversity. Annu Rev Neurosci *17*, 399-418.

Hofmann, F., Flockerzi, V., Kahl, S., and Wegener, J.W. (2014). L-type CaV1.2 calcium channels: from in vitro findings to in vivo function. Physiol Rev *94*, 303-326.

Hudmon, A., Lebel, E., Roy, H., Sik, A., Schulman, H., Waxham, M.N., and De Koninck, P. (2005). A mechanism for Ca2+/calmodulin-dependent protein kinase II clustering at synaptic and nonsynaptic sites based on self-association. J Neurosci *25*, 6971-6983.

Hulme, J.T., Yarov-Yarovoy, V., Lin, T.W., Scheuer, T., and Catterall, W.A. (2006). Autoinhibitory control of the CaV1.2 channel by its proteolytically processed distal C-terminal domain. J Physiol *576*, 87-102.

Kamp, T.J., and Hell, J.W. (2000). Regulation of cardiac L-type calcium channels by protein kinase A and protein kinase C. Circ Res *87*, 1095-1102.

Kanevsky, N., and Dascal, N. (2006). Regulation of maximal open probability is a separable function of Ca(v)beta subunit in L-type Ca2+ channel, dependent on NH2 terminus of alpha1C (Ca(v)1.2alpha). J Gen Physiol *128*, 15-36.

Klockner, U., and Isenberg, G. (1987). Calmodulin antagonists depress calcium and potassium currents in ventricular and vascular myocytes. Am J Physiol *253*, H1601-1611.

Kobrinsky, E., Tiwari, S., Maltsev, V.A., Harry, J.B., Lakatta, E., Abernethy, D.R., and Soldatov, N.M. (2005). Differential role of the alpha1C subunit tails in regulation of the Cav1.2 channel by membrane potential, beta subunits, and Ca2+ ions. J Biol Chem *280*, 12474-12485.

Lee, J.H., Daud, A.N., Cribbs, L.L., Lacerda, A.E., Pereverzev, A., Klockner, U., Schneider, T., and Perez-Reyes, E. (1999). Cloning and expression of a novel member of the low voltage-activated T-type calcium channel family. J Neurosci *19*, 1912-1921.

Lee, T.S., Karl, R., Moosmang, S., Lenhardt, P., Klugbauer, N., Hofmann, F., Kleppisch, T., and Welling, A. (2006). Calmodulin kinase II is involved in voltage-dependent facilitation of the L-type Cav1.2 calcium channel: Identification of the phosphorylation sites. J Biol Chem *281*, 25560-25567.

Lemke, T., Welling, A., Christel, C.J., Blaich, A., Bernhard, D., Lenhardt, P., Hofmann, F., and Moosmang, S. (2008). Unchanged beta-adrenergic stimulation of cardiac L-type calcium channels in Ca v 1.2 phosphorylation site S1928A mutant mice. J Biol Chem *283*, 34738-34744.

Link, S., Meissner, M., Held, B., Beck, A., Weissgerber, P., Freichel, M., and Flockerzi, V. (2009). Diversity and developmental expression of L-type calcium channel beta2 proteins and their influence on calcium current in murine heart. J Biol Chem *284*, 30129-30137.

Llinas, R., and Yarom, Y. (1981). Electrophysiology of mammalian inferior olivary neurones in vitro. Different types of voltage-dependent ionic conductances. J Physiol *315*, 549-567.

Maier, L.S. (2009). Role of CaMKII for signaling and regulation in the heart. Front Biosci (Landmark Ed) *14*, 486-496.

Maier, L.S., and Bers, D.M. (2002). Calcium, calmodulin, and calcium-calmodulin kinase II: heartbeat to heartbeat and beyond. J Mol Cell Cardiol *34*, 919-939.

McConnachie, G., Langeberg, L.K., and Scott, J.D. (2006). AKAP signaling complexes: getting to the heart of the matter. Trends Mol Med *12*, 317-323.

McDevitt, D.G. (1989). In vivo studies on the function of cardiac beta-adrenoceptors in man. Eur Heart J *10 Suppl B*, 22-28.

McDonald, T.F., Pelzer, S., Trautwein, W., and Pelzer, D.J. (1994). Regulation and modulation of calcium channels in cardiac, skeletal, and smooth muscle cells. Physiol Rev *74*, 365-507.

McMullen, J.R., Shioi, T., Huang, W.Y., Zhang, L., Tarnavski, O., Bisping, E., Schinke, M., Kong, S., Sherwood, M.C., Brown, J.*, et al.* (2004). The insulin-like growth factor 1 receptor induces physiological heart growth via the phosphoinositide 3-kinase(p110alpha) pathway. J Biol Chem *279*, 4782-4793.

Meissner, M., Weissgerber, P., Londono, J.E., Prenen, J., Link, S., Ruppenthal, S., Molkentin, J.D., Lipp, P., Nilius, B., Freichel, M.*, et al.* (2011). Moderate calcium channel dysfunction in adult mice with inducible cardiomyocyte-specific excision of the cacnb2 gene. J Biol Chem *286*, 15875-15882.

Mikami, A., Imoto, K., Tanabe, T., Niidome, T., Mori, Y., Takeshima, H., Narumiya, S., and Numa, S. (1989). Primary structure and functional expression of the cardiac dihydropyridine-sensitive calcium channel. Nature *340*, 230-233.

Mitcheson, J.S., Hancox, J.C., and Levi, A.J. (1998). Cultured adult cardiac myocytes: future applications, culture methods, morphological and electrophysiological properties. Cardiovasc Res *39*, 280-300.

Mitterdorfer, J., Froschmayr, M., Grabner, M., Moebius, F.F., Glossmann, H., and Striessnig, J. (1996). Identification of PK-A phosphorylation sites in the carboxyl terminus of L-type calcium channel alpha 1 subunits. Biochemistry *35*, 9400-9406.

Moosmang, S., Kleppisch, T., Wegener, J., Welling, A., and Hofmann, F. (2007). Analysis of calcium channels by conditional mutagenesis. Handb Exp Pharmacol, 469-490.

Mori, M.X., Erickson, M.G., and Yue, D.T. (2004). Functional stoichiometry and local enrichment of calmodulin interacting with Ca2+ channels. Science *304*, 432-435.

Nagy, A., Rossant, J., Nagy, R., Abramow-Newerly, W., and Roder, J.C. (1993). Derivation of completely cell culture-derived mice from early-passage embryonic stem cells. Proc Natl Acad Sci U S A *90*, 8424-8428.

Nichols, C.B., Rossow, C.F., Navedo, M.F., Westenbroek, R.E., Catterall, W.A., Santana, L.F., and McKnight, G.S. (2010). Sympathetic stimulation of adult cardiomyocytes requires association of AKAP5 with a subpopulation of L-type calcium channels. Circ Res *107*, 747-756.

Nilius, B., Hess, P., Lansman, J.B., and Tsien, R.W. (1986). A novel type of cardiac calcium channel in ventricular cells. Biomed Biochim Acta *45*, S167-170.

Nowycky, M.C., Fox, A.P., and Tsien, R.W. (1985). Three types of neuronal calcium channel with different calcium agonist sensitivity. Nature *316*, 440-443.

Osterrieder, W., Brum, G., Hescheler, J., Trautwein, W., Flockerzi, V., and Hofmann, F. (1982). Injection of subunits of cyclic AMP-dependent protein kinase into cardiac myocytes modulates Ca2+ current. Nature *298*, 576-578.

Peterson, B.Z., DeMaria, C.D., Adelman, J.P., and Yue, D.T. (1999). Calmodulin is the Ca2+ sensor for Ca2+ -dependent inactivation of L-type calcium channels. Neuron *22*, 549-558.

Peterson, B.Z., Lee, J.S., Mulle, J.G., Wang, Y., de Leon, M., and Yue, D.T. (2000). Critical determinants of Ca(2+)-dependent inactivation within an EF-hand motif of L-type Ca(2+) channels. Biophys J *78*, 1906-1920.

Pietrobon, D., and Hess, P. (1990). Novel mechanism of voltage-dependent gating in L-type calcium channels. Nature *346*, 651-655.

Poomvanicha, M., Wegener, J.W., Blaich, A., Fischer, S., Domes, K., Moosmang, S., and Hofmann, F. (2011). Facilitation and Ca2+-dependent inactivation are modified by mutation of the Ca(v)1.2 channel IQ motif. J Biol Chem *286*, 26702-26707.

Qin, N., Platano, D., Olcese, R., Costantin, J.L., Stefani, E., and Birnbaumer, L. (1998). Unique regulatory properties of the type 2a Ca2+ channel beta subunit caused by palmitoylation. Proc Natl Acad Sci U S A *95*, 4690-4695.

Raybaud, A., Dodier, Y., Bissonnette, P., Simoes, M., Bichet, D.G., Sauve, R., and Parent, L. (2006). The role of the GX9GX3G motif in the gating of high voltage-activated Ca2+ channels. J Biol Chem *281*, 39424-39436.

Reuter, H. (1974). Localization of beta adrenergic receptors, and effects of noradrenaline and cyclic nucleotides on action potentials, ionic currents and tension in mammalian cardiac muscle. J Physiol *242*, 429-451.

Seisenberger, C., Specht, V., Welling, A., Platzer, J., Pfeifer, A., Kuhbandner, S., Striessnig, J., Klugbauer, N., Feil, R., and Hofmann, F. (2000). Functional embryonic cardiomyocytes after disruption of the L-type alpha1C (Cav1.2) calcium channel gene in the mouse. J Biol Chem *275*, 39193-39199.

Singer-Lahat, D., Gershon, E., Lotan, I., Hullin, R., Biel, M., Flockerzi, V., Hofmann, F., and Dascal, N. (1992). Modulation of cardiac Ca2+ channels in Xenopus oocytes by protein kinase C. FEBS Lett *306*, 113-118.

Splawski, I., Timothy, K.W., Sharpe, L.M., Decher, N., Kumar, P., Bloise, R., Napolitano, C., Schwartz, P.J., Joseph, R.M., Condouris, K.*, et al.* (2004). Ca(V)1.2 calcium channel dysfunction causes a multisystem disorder including arrhythmia and autism. Cell *119*, 19-31.

Stotz, S.C., and Zamponi, G.W. (2001). Structural determinants of fast inactivation of high voltage-activated Ca(2+) channels. Trends Neurosci *24*, 176-181.

Sun, H., Kerfant, B.G., Zhao, D., Trivieri, M.G., Oudit, G.Y., Penninger, J.M., and Backx, P.H. (2006). Insulin-like growth factor-1 and PTEN deletion enhance cardiac L-type Ca2+ currents via increased PI3Kalpha/PKB signaling. Circ Res *98*, 1390-1397.

Tanabe, T., Takeshima, H., Mikami, A., Flockerzi, V., Takahashi, H., Kangawa, K., Kojima, M., Matsuo, H., Hirose, T., and Numa, S. (1987). Primary structure of the receptor for calcium channel blockers from skeletal muscle. Nature *328*, 313-318.

Terrak, M., Wu, G., Stafford, W.F., Lu, R.C., and Dominguez, R. (2003). Two distinct myosin light chain structures are induced by specific variations within the bound IQ motifs-functional implications. EMBO J *22*, 362-371.

Treinys, R., and Jurevicius, J. (2008). L-type Ca2+ channels in the heart: structure and regulation. Medicina (Kaunas) *44*, 491-499.

Viard, P., Butcher, A.J., Halet, G., Davies, A., Nurnberg, B., Heblich, F., and Dolphin, A.C. (2004). PI3K promotes voltage-dependent calcium channel trafficking to the plasma membrane. Nat Neurosci *7*, 939-946.

Weissgerber, P., Held, B., Bloch, W., Kaestner, L., Chien, K.R., Fleischmann, B.K., Lipp, P., Flockerzi, V., and Freichel, M. (2006). Reduced cardiac L-type Ca2+ current in Ca(V)beta2-/- embryos impairs cardiac development and contraction with secondary defects in vascular maturation. Circ Res *99*, 749-757.

Williams, M.E., Feldman, D.H., McCue, A.F., Brenner, R., Velicelebi, G., Ellis, S.B., and Harpold, M.M. (1992). Structure and functional expression of alpha 1, alpha 2, and beta subunits of a novel human neuronal calcium channel subtype. Neuron *8*, 71-84.

Xiao, R.P., Cheng, H., Lederer, W.J., Suzuki, T., and Lakatta, E.G. (1994). Dual regulation of Ca2+/calmodulin-dependent kinase II activity by membrane voltage and by calcium influx. Proc Natl Acad Sci U S A *91*, 9659-9663.

Xu, L., Lai, D., Cheng, J., Lim, H.J., Keskanokwong, T., Backs, J., Olson, E.N., and Wang, Y. (2010). Alterations of L-type calcium current and cardiac function in CaMKII{delta} knockout mice. Circ Res *107*, 398-407.

Yang, L., Katchman, A., Samad, T., Morrow, J.P., Weinberg, R.L., and Marx, S.O. (2013). beta-adrenergic regulation of the L-type Ca2+ channel does not require phosphorylation of alpha1C Ser1700. Circ Res *113*, 871-880.

Yang, L., Liu, G., Zakharov, S.I., Bellinger, A.M., Mongillo, M., and Marx, S.O. (2007). Protein kinase G phosphorylates Cav1.2 alpha1c and beta2 subunits. Circ Res *101*, 465-474.

Yoshida, A., Takahashi, M., Nishimura, S., Takeshima, H., and Kokubun, S. (1992). Cyclic AMP-dependent phosphorylation and regulation of the cardiac dihydropyridine-sensitive Ca channel. FEBS Lett *309*, 343-349.

Yuan, W., and Bers, D.M. (1994). Ca-dependent facilitation of cardiac Ca current is due to Ca-calmodulin-dependent protein kinase. Am J Physiol *267*, H982-993.

Zamponi, M.T.A.a.G.W. (2005). Voltage-Dependent Inactivation of Voltage Gated Calcium Channels. In Voltage-Gated Calcium Channels, G.W. Zamponi, ed., p. 11.

Zhou, Z., and January, C.T. (1998). Both T- and L-type Ca2+ channels can contribute to excitation-contraction coupling in cardiac Purkinje cells. Biophys J *74*, 1830-1839.

Zuhlke, R.D., Pitt, G.S., Deisseroth, K., Tsien, R.W., and Reuter, H. (1999). Calmodulin supports both inactivation and facilitation of L-type calcium channels. Nature *399*, 159-162.

Zuhlke, R.D., Pitt, G.S., Tsien, R.W., and Reuter, H. (2000). Ca2+-sensitive inactivation and facilitation of L-type Ca2+ channels both depend on specific amino acid residues in a consensus calmodulin-binding motif in the(alpha)1C subunit. J Biol Chem *275*, 21121-21129.

Results of this dissertation have been partially published

1. **Poomvanicha, M**., Wegener, J.W., Blaich, A., Fischer, S., Domes, K., Moosmang, S., and Hofmann, F. (2011). Facilitation and Ca2+-dependent inactivation are modified by mutation of the Ca(v)1.2 channel IQ motif. J Biol Chem *286*, 26702-26707.

2. Blaich, A., Pahlavan, S., Tian, Q., Oberhofer, M., **Poomvanicha, M**., Lenhardt, P., Domes, K., Wegener, J.W., Moosmang, S., Ruppenthal, S.*, et al.* (2012). Mutation of the calmodulin binding motif IQ of the L-type Ca(v)1.2 Ca2+ channel to EQ induces dilated cardiomyopathy and death. J Biol Chem *287*, 22616-22625.

3. Brandmayr, J., **Poomvanicha, M**., Domes, K., Ding, J., Blaich, A., Wegener, J.W., Moosmang, S., and Hofmann, F. (2012). Deletion of the C-terminal phosphorylation sites in the cardiac beta-subunit does not affect the basic beta-adrenergic response of the heart and the Ca(v)1.2 channel. J Biol Chem *287*, 22584-22592.

Acknowledgments

This dissertation could not have been completed without the great support of many people.

Firstly, I would like to express my deep gratitude to Prof. Dr. Franz Hofmann (Carvas 923) for giving me the opportunity to be a member of his lab. He provided the vision, great ideas solution and motivational compliments. Without his guidance and constant feedback this PhD would not have been achievable.

I would like to say a very big thank you to Dr. Jörg Wegner for his insightful and helpful advice. Thanks to Dr. Anne Blaich for her support, guidance and helpful suggestions.

I would like to acknowledge Katrin Domes who have been very friendly, supportive and kindly helped facilitate every step of my project. She has been supportive since the days I began working on the first project.

My deep appreciation goes out to all current and previous lab members for their help and guidance during the pursuit of my graduate studies: Jie Ding, Florian Loga, Enrico Patrugo, Max Jelkmann, Elisabeth Angermeier, Beate Spießberger, Teodora Kennel, Mehmet Durmaz, Sahiner Selahattin. Their friendship and the warmth they extended to me during my time in Germany making me feel so welcome.

I am indebted to all my Thai friends in Munich who opened their homes to me and helping in whatever way they could. A big thank you to Thanak, who always staying by my side throughout this challenging period.

This PhD study would not have been possible without financial support by Thai government. I would also like to thank all staff at the Office of Educational Affairs in Germany and Office of the Civil Service Commission (OCSC) Thailand for providing all the required documents, taking good care and helping me out with any problems.

Finally, I would like to say a heartfelt thank you to my Mother, who has always been there for me. I would not be here without her love, moral support and understanding. I love you, Mom.

Curriculum Vitae

Personal Data

Name   Montatip   Poomvanicha

Date of birth   11 January 1980

Nationality   Thai

School education

05/1986 – 03/1992   Anuchon Watthana School, Thailand

05/1992 – 03/1995   La Salle Chotiravi Nakhonsawan, Thailand

05/1995 – 03/1998   Nakhonsawan School, Thailand

University education

Bachelor programm

06/1998 – 03/2003   Cardio-Thoracic Technology,

                                             Naresuan University, Thailand

Master programm

06/2003 – 03/2007   Physiolgy,

                                             Faculty of Medicine Siriraj Hospital,

                                             Mahidol University, Thailand

Doctoral programm

10/2009 – present   Institute of Pharmacology and Toxikology,

                                             Carvas923, Prof. Dr. F. Hofmann, TU München

Employment

04/2007.- present   Faculty of Allied Health Sciences,

                                             Naresuan University, Thailand

Dissertation   Modulation of cardiac L-type calcium channels

                                             by genetic modification